A MECHANISM FOR SELF EXCITATION IN HYDRAULIC CONTROL DEVICES

A MECHANISM FOR SELF EXCITATION
IN HYDRAULIC CONTROL DEVICES

by

Samir R. Ziada, B.Sc. (Mech. Eng.)

A Thesis
Submitted to the Faculty of Graduate Studies
in Partial Fulfillment of the Requirements
for the Degree
Master of Engineering

McMaster University

July 1977

TO MY PARENTS

MASTER OF ENGINEERING (1977)
(Mechanical Engineering)

McMaster University
Hamilton, Ontario

TITLE: A Mechanism for Self Excitation in Hydraulic Control Devices

AUTHOR: SAMIR REFAAT ZIADA
B.Sc. Mechanical Engineering,
Cairo University, Cairo, Egypt.

SUPERVISOR: Professor D. S. Weaver

NUMBER OF PAGES: ix, 182

ABSTRACT

Researchers in recent years have attributed the dynamic instability of certain hydraulic control devices (such as gates, valves, and seals) to a velocity dependent hydrodynamic load which is equivalent to a negative damping coefficient in the differential equation of motion. Such a model is not capable of predicting certain important features of observed check valve behaviour.

A semi-empirical model for check valve self-excited vibrations is derived. The results show that the gross behaviour of this model is qualitatively the same as the experimental observations. Hence, the existence of a hydrodynamic load component in phase with displacement appears essential for the hydrodynamic load modelling.

A general mathematical model is then derived from first principles. Closure of the hydraulic control device during vibrations and unsteady flow phenomenon including viscous losses are taken into account. The proposed model can be applied to any type of hydraulic control device with a jet-flow mechanism of excitation. Two applications for the model have been examined. Check valve and seal applications show that the model results are in reasonable agreement with the experimental observations.

ACKNOWLEDGEMENT

It is my pleasure to express my sincere gratitude to Dr. D. S. Weaver for his expert guidance, valuable advice and continuous encouragement throughout the duration of the present investigation.

The author also expresses his appreciation to Miss L. A. Oneschuk for typing the manuscript.

The financial support provided by the National Research Council of Canada and McMaster University is also acknowledged.

TABLE OF CONTENTS

LIST OF FIGURES

FIGURE	CAPTION	PAGE

CHAPTER 1

INTRODUCTION

Fluids may be classified as liquids, gases, or vapours. Each class presents its own handling problems. Moreover, it is sometimes required to transport solids in suspension. The problem of controlling fluid flows has always taxed man's ingenuity.

As operating conditions for different applications have become more arduous, the design of fluid flow control devices has changed, inevitably becoming more complex and sophisticated. Selection of any device for a particular application is determined by such factors as size of particulate matter in flow, viscosity, velocity, pressure, temperature and whether the fluid's state remains constant throughout the system. The type of service required of the device is also an important factor in its selection; for example, whether it is required for isolating or regulating service, and if shut-off service is needed, whether it be quick and bubble tight.

Today there are a great number of different types of fluid flow control devices. The applications to which each type of these devices can be used are beyond the scope of the present study. Only check valves, gates, and seals will be considered in this thesis.

1.1 Valves

1.1.1 Oscillation or "Hunting" of Valves

Under certain conditions of operation, almost all valves display a tendency to "chatter". Problems of this kind generally occur when the valve is operating partially closed and most frequently when just cracked open. They are caused by the slight but rapid movements of the valve element which change the flow area, giving rise to pressure fluctuations. For example, the spring type pressure relief valve is prone to chatter, and here oscillations can build up to such a degree as to cause mechanical failure of the seat (12). Sluice valves can also produce undesirable pressure fluctuations. In this case, the nature of the connection between valve spindle and wedge is generally such as to permit small movements of the wedge which result in changes in flow and pressure.

In the case of pressure-reducing valves, oscillations are sometimes inadvertently initiated. Normally, this valve is sensitive to changes in downstream pressure and by automatic adjustment, endeavours to maintain a reasonably constant outlet pressure. A change in the downstream conditions, due to reduced draw-off for example, causes the valve to move in the closing direction. If the valve over-corrects in its attempt to settle at the new required position, "hunting" may be initiated unless sufficient damping is incorporated in the servo-system.

These examples indicate that valve oscillation can be a very real problem and if engineers and manufacturers are conscious of this fact and understand the controlling mechanisms, they can design and specify the inclusion of appropriate preventive features.

1.1.2 Check Valves

Swing-check and lift-check valves act automatically and are used in systems where flow in one direction only is desired. Selection of the most suitable pattern and size is determined by parameters such as working temperature and pressure, flow velocity and allowable friction losses.

In the simplest form, a check valve (Figure 1.1) comprises a casing containing a hinged flap which is sensitive to small differences between upstream and downstream pressure. As long as the downstream pressure is less than the upstream pressure, the valve remains open, the degree of opening depending on the pressure difference. However, any drop in upstream pressure below downstream pressure will cause valve closure and hence prevent reverse flow.

Various forms of swing-check valves range from the single hinged pattern in pipelines a few inches in diameter, to the large multi-door patterns for large pipe systems several feet in diameter. Lift-check valves are normally

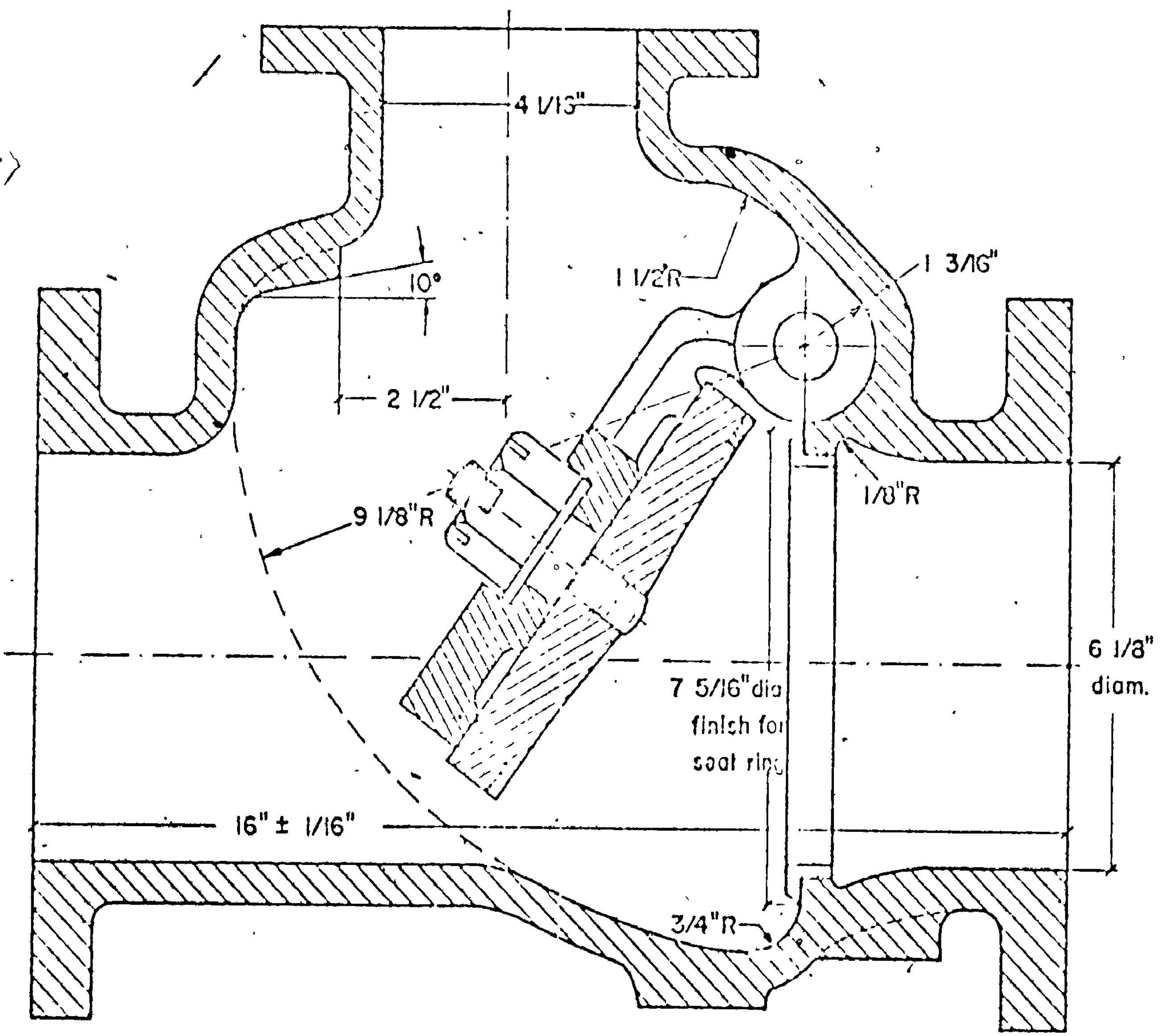

Figure 1.1. Inner Contours of Hydraulic Swing Check Valve, Ref. (11).

associated with smaller pipelines up to about twelve inches in diameter in high pressure systems.

The action of a simple check valve, installed in a centrifugal pumping installation, is basically as follows. The valve door is normally held open by impinging flow. If the reduction in flow velocity (following pump shut-down) is slow, as in the case of a centrifugal pump which continues to rotate for a short time after being shut down, the valve closes slowly.

When the pump is provided with a brake and therefore shuts down very rapidly, the pressure at the pump is suddenly reduced below that of the fluid downstream of the valve, and reverse flow may be established. The resulting pressure on the valve disc slams it heavily onto its seat. This leads to the generation of dangerous pressure surges which can cause damage to pipework and associated equipment or at the very least, cause a loud startling noise which may not be acceptable in commercial applications.

1.2 Hydraulic Gates

Today there are many different types of hydraulic gates. Gate selection for a particular application is determined by the operating conditions and the type of service required of the gate. The most common types are sluice, radial or tainter, submergible, drum, and vertical-lift with skimmer wall gates, (Figure 1.2).

Hydraulic control gates in open channels and closed conduits sometimes suffer from flow-induced vibrations, but the processes involved in the excitation are not completely understood. Nevertheless, analysis of the vibration observations and measurements (5), (7), (8), (9), and (10) leads to several general findings concerning the nature of vibrations. The major parameter of gate vibrations was found to be the gate lip and bottom seal design. The shape of this gate feature affected not only the magnitude of gate vibrations but also the operating zones where vibrations occurred and the vibration patterns assumed by the gates. Other factors which have some effects on gate vibration tendencies (7) include tailwater level, gate opening, gate rigidity, side seal adjustment, adjacent gate settings, and wind, particularly on the gate lifting cables.

1.3 Hydraulic Seals

All the well-known types of gate seals shown in Figure 1.3 are similar in operation. The elastic element is provided with a rubber detail. The displacement trajectories both of sealing element and mass centre of seal moving parts may be either curvilinear (Figure 1.3 (a), (b), and (c)) or rectangular (Figure 1.3 (d)) or a combination of both. The hydrodynamic load on a seal and the strained

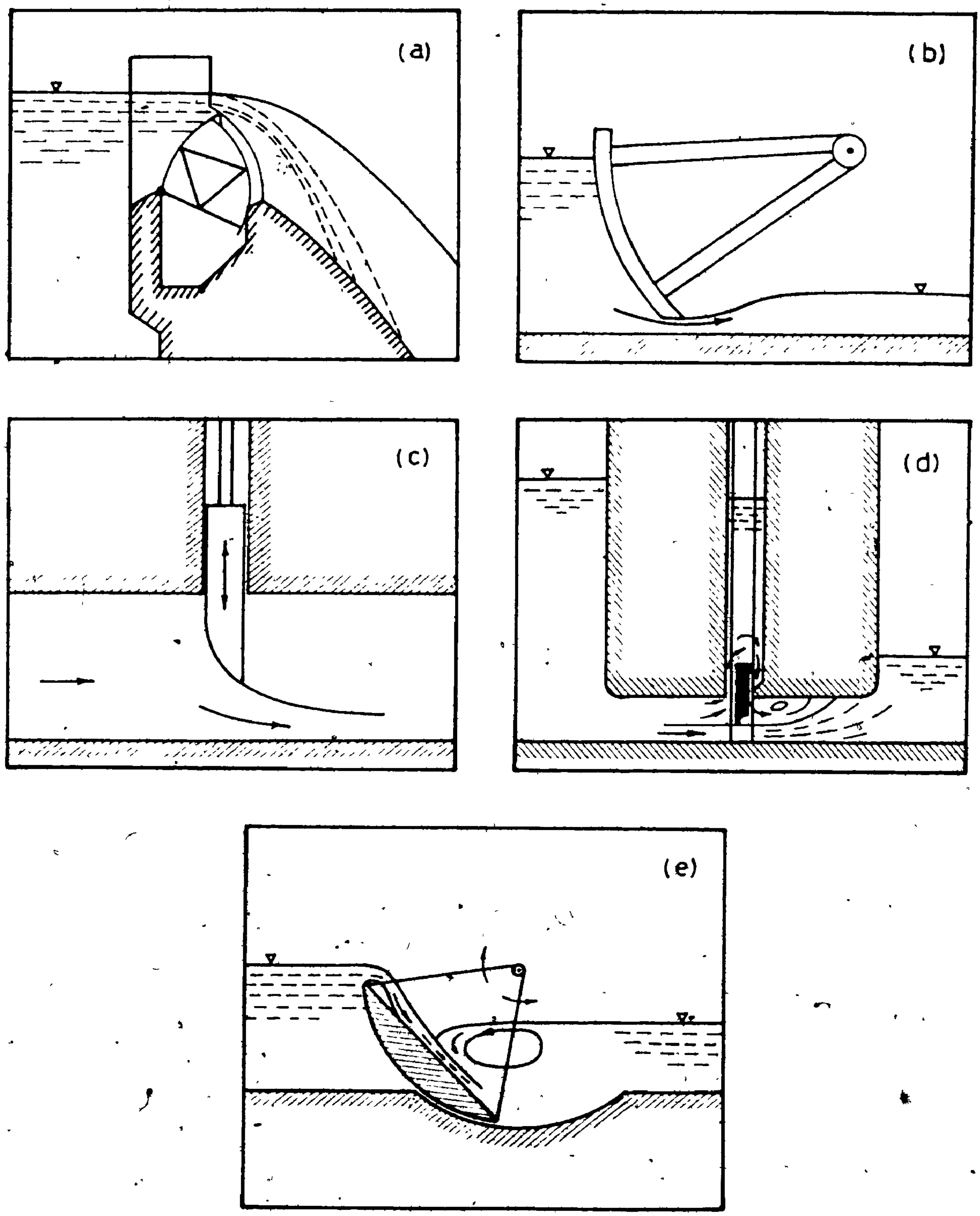

Fiqure 1.2. Hvdraulic Control Gates
(a) Drum Gate; (b) Radial or Tainter Gate; (c) Sluice Gate; (d) Vertical Gate with Skimmer Wall; and (e) Submergible Gate.

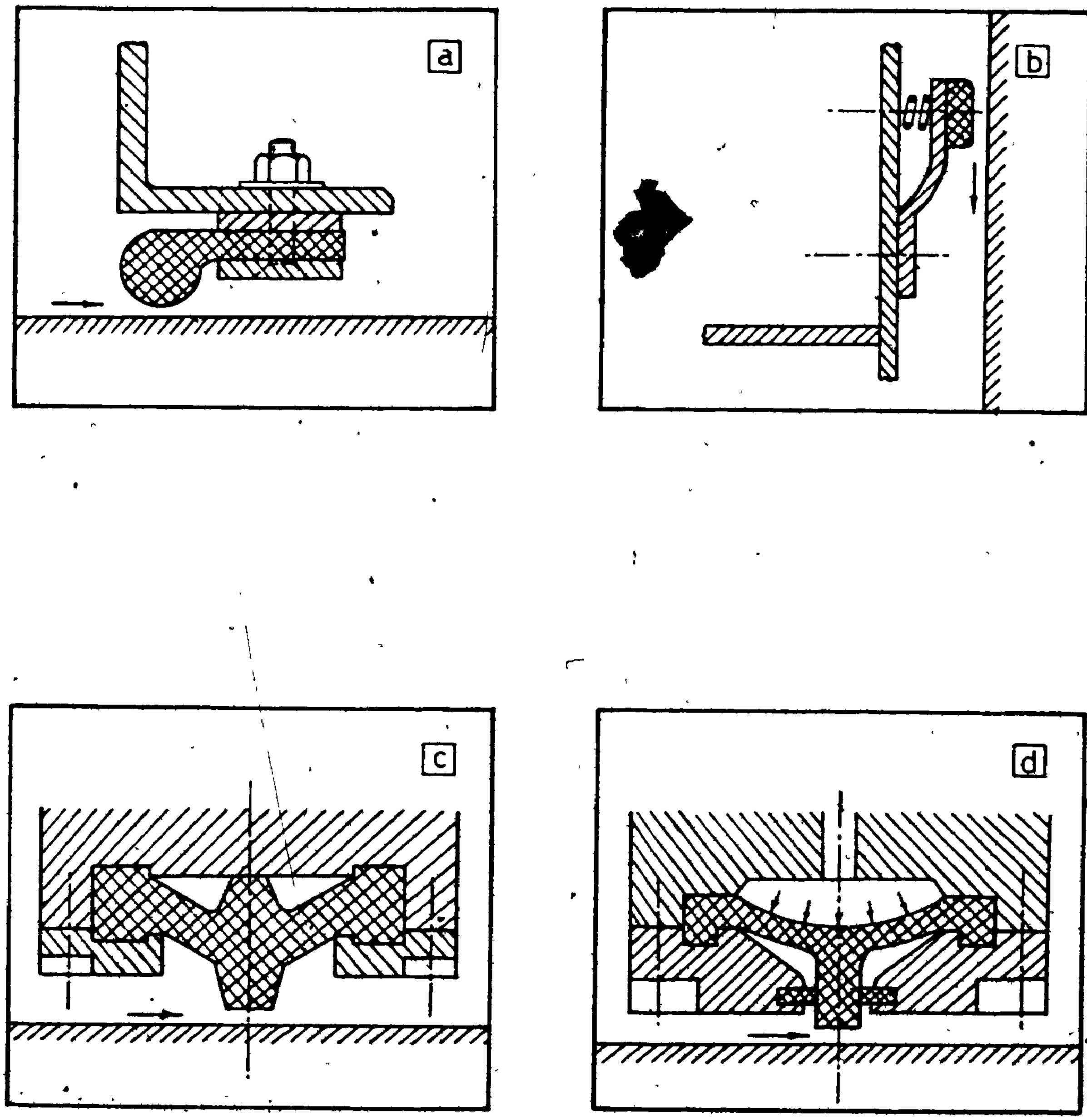

Figure 1.3. Hydraulic Seals.

state of the elastic element are also rather complicated.

It is evident that all types of seals of practical use may vibrate under certain conditions. Especially the seals of gates, dams, and navigation works are affected by oscillations as they are intended to operate within a wide range of hydrostatic heads and clearances. Conditions which are necessary for the vibration to occur seem to involve some factors which are difficult to determine by external analysis of gate and seal structure. To discover these factors very carefully controlled and ingenious experiments are required.

Sometimes the seal oscillations occur 'suddenly' in the course of operation, and the same type of seal will vibrate on one gate but not on another which is apparently operating under the same conditions. Lyssenko and Chepajkin (14) indicated experimentally that seal's oscillations have the following features:

a) For each type of seal, the oscillations were spontaneously initiated and disappeared at nearly definite heads.

b) The oscillations were found to be periodic and stable with evident dependence of their frequency on head.

Besides the unpleasant noise, the seal oscillation may cause intense and high-frequency vibration of gate components.

1.4 Purpose of Research

Since the mechanisms of many hydroelastic phenomena are not yet understood fully, it has not always been possible to model them satisfactorily. While the technical literature is expanding rapidly, the papers usually treat very specific problems. In addition, little effort has been directed to make much of the work done directly useful to the practicing engineer.

The purpose of this work is to derive a general mathematical model for self-excited vibrations which may fit most of fluid flow control devices. Unsteady flow and closure phenomena are essential features which should be included in the proposed model. The development of such a model would not only greatly assist in our understanding of the excitation mechanism but would also be of great importance for engineers whose task it is to design structures which are free from flow-induced vibrations.

CHAPTER 2

BASIC CONCEPTS OF

FLOW-INDUCED STRUCTURAL VIBRATIONS

2.1 Introduction

Vibrations are a natural phenomenon of elastic objects being acted upon by external dynamic forces. Control structures, for instance, are susceptible to vibrations induced by forces in flowing water. Usually vibration tendencies in control structures have been infrequent, minor in magnitude, and avoidable by special operation procedures. However, reports of recent vibrations experienced on structures in service (3), (6), (7), (9), (10), (11), (12), (13), and (23) have been of such magnitude that control structures have been severely damaged and structural alterations have been required to ensure satisfactory performance.

Although structural engineers have experienced these phenomena for hundreds of years and have come to recognize their general nature at least since the suspension bridge failures of the 1800's, the methods developed for their study are largely a contribution of aerodynamicists. The onset of powered flight early in this century brought the aerodynamicist an empirical familiarity with aeroelasticity.

Aeroelasticity is a branch of science concerned with the effects of aerodynamic forces on elastic structures (25). However, the material covered by aeroelasticity is essentially directed towards the performance of aircraft components. Frequent disastrous consequences of aeroelastic phenomena now known by such names as "flutter", and "divergence" stimulated their analytical study beginning in the 1920's.

Flutter is defined by the aerodynamicist (25) as the dynamic instability of an elastic body in a fluid stream, the only forces necessary to produce it being those caused by deflections of the elastic structure from its undeformed state. When the magnitude of the force increases with the amplitude of the motion it causes, the phenomena are called "self-excited".

Buffeting, as usually defined, represents the elastic response of a structure to forces which are little affected by the body motion. These forces may result from the presence of the body in a turbulent fluid flow. Resonant vibrations may be caused by periodic forces in the flow field such as the vortex street in the wake of a bluff body, but as long as the forces are not altered by the resulting elastic deflection, the phenomenon is considered as forced vibration.

In recent years, the term hydroelasticity has been introduced. It is concerned with the effects of hydrodynamic forces on elastic structures. This word was coined by analogy to aeroelasticity to denote its naval counterpart. Heller and

Abramson (26) proposed the following definition, "Hydroelasticity is concerned with phenomena involving mutual interactions among inertial, elastic and hydrodynamic forces". When the effects of inertial forces are so small that they may be neglected, the problem is one of "static hydroelasticity". "Dynamic hydroelasticity" is concerned with phenomena involving mutual interaction among inertial, elastic, and hydrodynamic forces, Figure 2.1.

While there are many similarities between aeroelasticity and hydroelasticity, a distinction between the two also exists, as their names suggest, on fluid properties. First, hydroelasticity may include the effect of a free surface, the interface between two fluid media. Such a surface is not present in aeroelastic phenomena. Secondly, the possibility of cavitation exists in hydroelasticity but not in aeroelasticity. Thirdly, the significance of the added mass which is usually negligible in aeroelasticity is of great importance in hydroelastic phenomena (22). Despite differences that are associated with the fluids involved, it is preferable to designate both fields by the term "fluid-elasticity", thus permitting the coherence sought in presenting the characteristics of flow-induced vibrations.

The basic definition and characteristic of fluid-elasticity (1) is shown in Figure 2.2. The symbols F and δ stand for generalized force and generalized structural deformation, respectively. Disregard for the moment, all solid lines

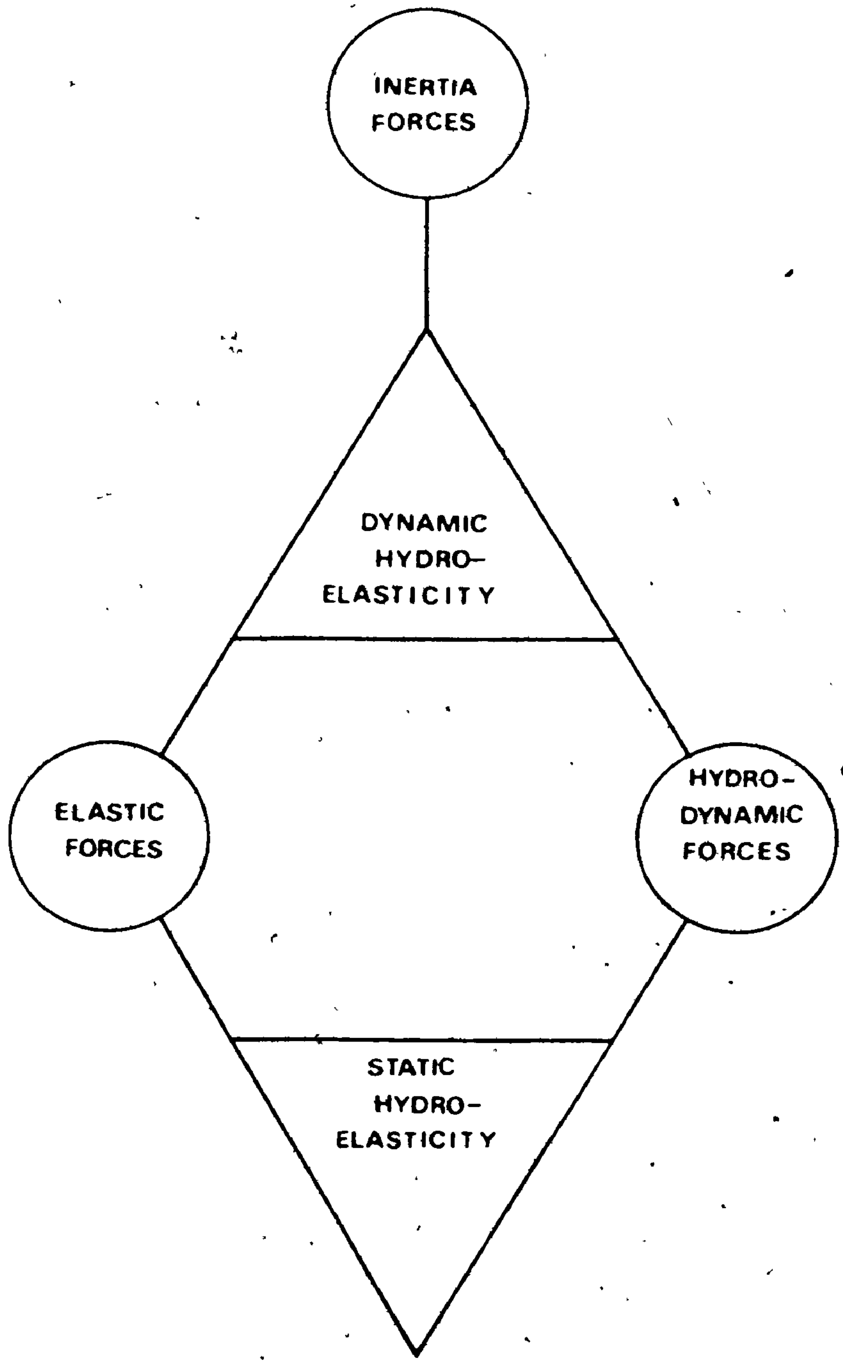

Figure 2.1. A Reduced Hydroelastic Triangle.

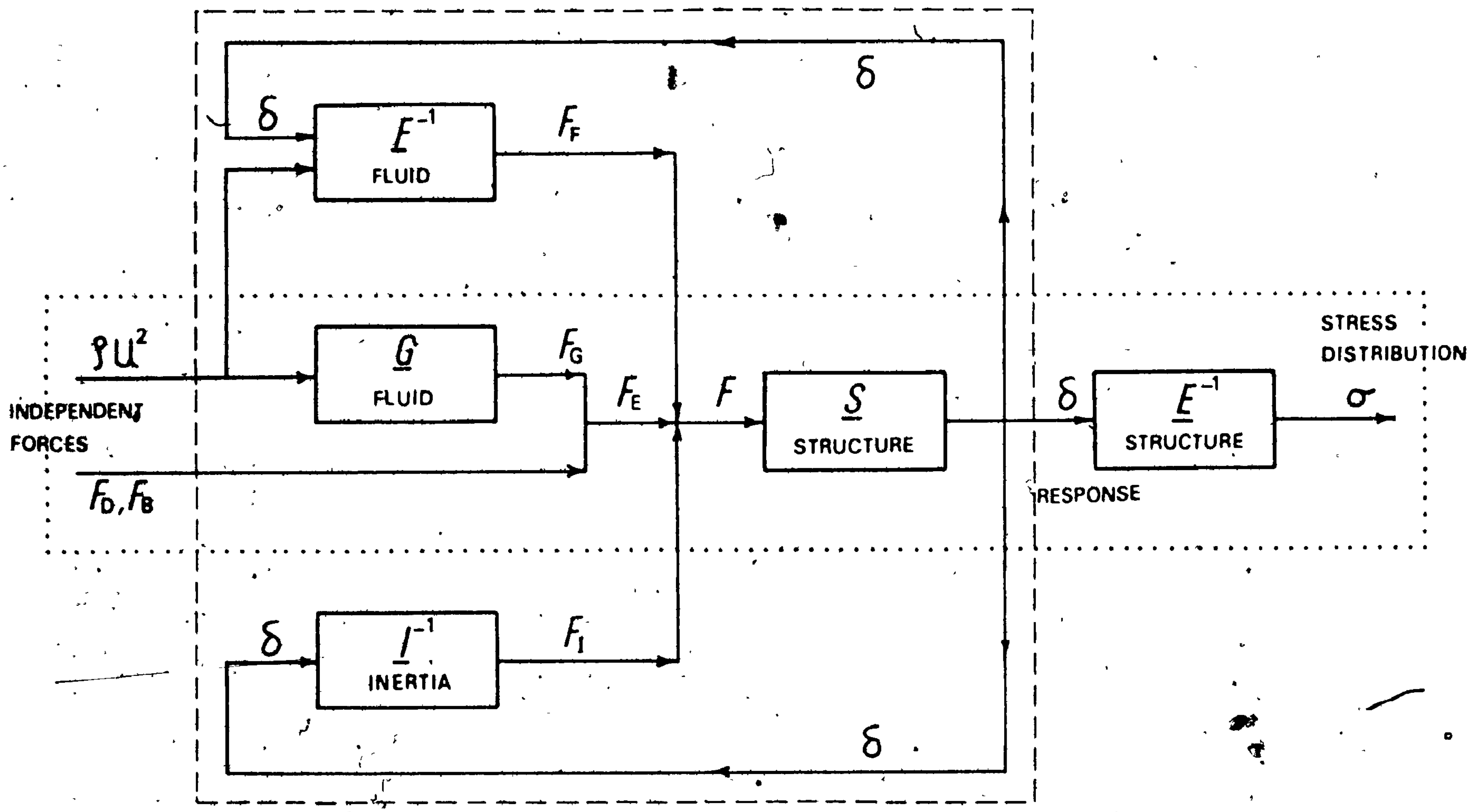

Figure 2.2. Fluidelastic System, Ref. (1).

crossing the dotted boundary so that $F = F_E$. It is then recognized that inside this boundary is the common problem of determining a structure's stress distribution, σ, caused by a loading, F_E. The underlined symbols, $\underline{S}$ and $\underline{E}$ are operators. They stand for the (sets of) equations which, for a given structure, relate loading and stresses to its deformation. The loading, F_E, is the sum of fluid-dynamic forces, F_G, the body forces, F_B, and other forces as disturbance forces, F_D. The symbol, $\underline{G}$, denotes a fluid-dynamic operator that relates F_G to a fluid flow characterized by a generalized stagnation pressure, ρU^2.

The dynamic fluidelastic problem is presented within the dashed boundary. The loading, F, now depends on the deformation, δ. This is shown by the additions of a deformation-dependent fluid-dynamic operator, $\underline{F}$, and an inertial operator, $\underline{I}$. By deleting $\underline{I}$, the static fluidelastic problem is retained within the dashed boundary.

2.2 Classification of Flow-Induced Vibrations

Whenever a structure is exposed to a high velocity fluid-flow, vibrations of the structure will be induced. These vibrations may be classified as one of three kinds (2):

(a) Forced vibrations induced by turbulence in the flow ;

(b) Self-controlled vibrations induced by flow periodicity; and

(c) Self-excited vibrations induced by a fluid-elastic phenomenon.

Structural motions of the first type are usually of a random nature and are called 'forced' since the motion of the structure has no appreciable affect on the fluid forces. This class of problems usually does not represent a source of great concern to designers since the analysis of these problems is relatively straight-forward as long as the fluid forces are known.

Self-controlled vibrations occur when some periodicity already exists in the flow field. If this periodicity coincides with one of the natural frequencies of the structure, the amplitude of vibration builds up to the point where the magnitude and frequency of the fluid forces are now controlled by the structural motion. In this type of vibration, an increase in stiffness or damping may prevent or limit the amplitude of motion. In some cases, it is also possible to modify the structural geometry and thus eliminate the periodicity in the flow.

In the case of self-excited vibrations, the oscillations of the structure creates the periodic forces which amplify the structures' motion. The difference between these vibrations and self-controlled vibrations is that in self-excited vibrations the periodic forces disappear in the absence of structural motion, and a change in geometry may be the only effective remedy.

Both self-controlled and self-excited vibrations are termed fluid-elastic vibrations since they involve mutual interactions of elastic, inertial and fluid-dynamic forces.

The physical situations in which flow induced vibrations arise are extremely diverse and, often, the mechanisms are not well understood. At least two recent symposia have dealt exclusively with flow-induced structural vibrations (23), (27), but no reference text on the subject exists. The study of fluidelasticity draws on five disciplines:

(1) Theory of elasticity
(2) Mechanical vibrations
(3) Fluid mechanics
(4) Theory of stability of non-conservative systems
(5) Stochastic processes.

2.3 Vibrations of Hydraulic Gates, Seals, and Valves

Vibration problems in flow control structures and devices are commonplace and have been the subject of many investigations. The purpose of this section is to attempt to review current knowledge related to vibrations of hydraulic gates, seals, and valves by critically evaluating the existing literature. The literature of flow-induced vibrations is so diverse that it is impossible to cover all known cases in the course of a brief survey.

Most of the reported papers on flow-induced vibration problems in service involve cut and try methods by which partial or complete solutions to these problems have been attained but little is learned which can be applied to other similar problems (3), (4), (5), (7), (10). Several other papers have given detailed treatment for very specific problems but the results may rarely be generalized. A few general papers on hydroelasticity have been written (1), (2) with an effort to put this relatively new field into the same conceptual framework as aeroelasticity. However, in the last few years some papers have appeared in the literature attempting to foster a reasonable understanding of the various phenomena.

Abelev and Dolnikov (9) classified the self-excited vibrations of hydraulic gates into two basic categories:

(1) eddy mechanism of excitation and

(2) the jet flow mechanism.

Before explaining these categories, flow separation and reattachment phenomenon must be reviewed briefly. When a high velocity flow passes an obstruction such as the gate bottoms (2), (28), the flow separates and produces a free shear layer. This unguided layer, which has a pronounced transverse velocity gradient, is unstable and eventually any lateral perturbation causes the layer to roll up into vortices which grow in size as they move downstream. When the lateral perturbations result from vibration of the solid boundary on which the separation point is located, a regular two-dimensional vortex train with a frequency of formation equal to that of the solid boundary is produced.

If the free shear layer develops from a sharp edge and does not reattach to the gate (2), (28), the frequency of vortex formation may become "locked in" with the frequency of the gate motion, thus reinforcing the excitation. Such vibrations are self-controlled and may occur over a wide range of gate openings. The addition of stiffness and damping will be the most effective remedies for this vibration type.

Unstable flow reattachment occurs in the case of intermediate gate widths. The result is a strong periodic excitation which may lead to destructive vibrations at certain heads and gate openings.

Stable flow reattachment will occur for large gate widths. This case is of little interest because the massiveness of such a structure will likely make it immune from fluctuating forces. All these cases can be put under the "eddy mechanism of excitation" as suggested by Abelev and Dolnikov (9).

The "jet flow mechanism" as defined by these writers was used to describe the effect of high velocity jets flowing over the top of vertical sluice gates and down between the downstream side of the gate and its skimmer wall. The high velocity jet reduces the pressure in the gap so that the gate is drawn towards the wall. This reduces the discharge through the gap, and may produce some inertia pressure which drives the gate back. The resulting horizontal gate vibrations are thus clearly self-excited.

The difference between these two categories of hydraulic gate flow-induced vibrations is that those due to eddies occur in the direction normal to the flow under the gate (vertical direction), while those due to the jet-flow mechanism are found to be normal to the flow along the downstream face of the gate, i.e. they occur in the direction of the minimum gate rigidity (horizontal direction).

In 1974, Hardwick (8), extending the ideas of Naudascher and Locher (28), explained the case of unstable reattachment very nicely. Based on his flow visualization experiments on a vertical-lift gate with a flat bottom which is free to vibrate vertically, Hardwick found that eddies which result from the breakdown of the free shear layer induce a temporary condition of reattachment of the main-stream to the gate bottom and so generate an exciting force. Oscillatory motion of the separation point amplifies the excitation and synchronizes it with the gate. Hardwick also gave a quantitative study of the gate vibrational response. He analyzed the pulsating hydrodynamic force into two components, one was in phase with the gate displacement and the other was in phase with its velocity. These forces were then combined in a differential equation of motion as a stiffness and a negative damping coefficient term respectively. His entire work was based on the critical assumption that the mean flow velocity under the gate during vibrations remains virtually unchanged and that the motion is simple harmonic. This may be true for large gate openings but for small openings the flow is very unsteady. If the vibrational response involves repeated opening and closing of the gate, the fluid velocity will be zero during a fraction of the cycle. In addition the negative damping coefficient term should be determined experimentally. Thus, Hardwick's explanation is not valid for the case where closure occurs during the cycle.

Abelev and Dolnikov (9) in their mathematical model for the jet-flow mechanism, assumed a simple linear variation in discharge coefficient which results in a negatively damped simple harmonic oscillator. The effect of fluid inertia will undoubtedly invalidate the assumed variation in discharge coefficient which has not been experimentally verified. At the very best, the proposed model will only be valid for very small oscillations where no appreciable variation in discharge occurs.

Violent chattering of household taps when nearly fully closed has been experienced occasionally by most people. Such self-excited vibrations have also been encountered with sink and bathtub plugs of particular designs when operating nearly fully closed. While the vibrations subside on full opening of these devices or closing them completely, and failure very rarely occurs, the unpleasant noise generated is a source of nuisance. The seal problems reported by Schmidgall (7) and by Chepajkin and Lyssenko (14) are discussed as a phenomenon related to the "jet-flow mechanism".

Schmidgall (7) explained the self-excited vibration of seals as follows: at static conditions, a gap forms between the seal and the seal plate when the upstream hydrostatic force acting against the seal js not great enough to deflect the seal to the seal plate. However, once a gap is formed between the seal and seal plate, water rushes through the gap reducing the pressure and causing the gap to close. Once closed, the flow stops, the static conditions is renewed, and the seal springs open again, thus setting up the vibration cycle.

Chepajkin and Lyssenko (14) analysed gate seal vibrations using a mathematical model very similar to that of Abelev and Dolnikov (9) for gates. Large variations do occur in the discharge coefficient as it becomes a non-linear function of the gap cross-section and frequency of oscillation. However, they neglected the large variations in mean fluid velocities in the gap between seal and sill during the vibration cycle and hence, the fluid inertial head has been neglected in comparison with the static head in their analysis. Finally, this model boils down again to a negatively damped simple harmonic oscillator as a result of a linear variation assumed for the discharge coefficient. Thus, Chepajkin and Lyssenko's theoretical model based on small simple harmonic motions and negative damping appears incapable of accounting for the flow phenomenon during a cycle which involves closure.

The only papers which give care to the importance of the large variation in discharge are these of Weaver, Kouwen and Mansour (13), and Weaver and Adubi (12). However, the first one gives a qualitative explanation only, being based on preliminary experiments on check valve to determine the static discharge characteristics. In the second paper, Weaver and Adubi deduced the self-excitation mechanism for swing check valve as a result of dynamic experiments and flow visualization during the vibration cycle. The results of this paper will be reviewed in the next chapter because of its importance for the present research.

2.4 Mathematical Models

Although it is well-known that most of structural vibrations induced by fluid flow are due to the mutual interactions among inertial, elastic, and hydrodynamic forces, it has not always been possible to model them satisfactorily, and the mechanisms of many hydroelastic phenomena are not yet fully understood. Toebes (1) has shown that the analysis of most fluidelastic phenomena may be viewed briefly and clearly by the determination of the so-called structural operators, inertial operators, and fluid-dynamic operators. Weaver (2) has reported that the energy transfer from the fluid to the structure is the result of nonconservative hydrodynamic forces which manifest themselves in the form of non-self-adjoint operators in the differential equation of motion. In particular, such equations admit complex eigenvalues or, in physical terms, oscillatory types of instability. In addition, the eigenvectors or unstable mode shapes are generally not the normal modes of free vibration but coupled modes which do not satisfy the usual orthogonality conditions. Thus, regardless of the specific mechanism involved, hydroelatic problems form a class which is distinct from free vibration, dynamic response and conservative stability problems.

2.5 Added Mass Theory

A structure submerged in water exhibits different dynamic characteristics than one which vibrates in the air. It is found that a system has a longer period of vibration and a higher damping when vibrating in water, compared to that in air. Since the stiffness does not change for small vibration, the increase in the natural period of vibration is only attributable to an increase in the apparent mass due to the surrounding water. The water surrounding the body is in continual motion as energy is imparted to the fluid and a pressure is exerted on the body. This apparent additional mass is termed "virtual", "added", or "hydrodynamic" mass (22).

$$F = (M + M_1) \frac{d^2x}{dt^2}$$

where M_1, the added mass, may sometimes be much greater than M, the actual mass of the body.

The ratio of the virtual mass to the actual mass of the structure is known as the "virtual mass factor". The virtual mass is also sometimes expressed as a coefficient times the mass of water enclosed in a right circular cylinder circumscribing the body. This coefficient is termed "virtual mass coefficient".

Weaver (2) has stated that if the fluid pressure on an accelerated body is determined from the appropriate boundary value problem, the added mass falls out of the analysis as an inertia term. However, many problems cannot be treated in this way and it may be useful to use an added mass term in a dynamic analysis of the structure.

The magnitude of the virtual mass depends upon the geometry and size of the structure, the level of submergence, amplitude and frequency of structural vibrations, and relative confinement (22).

When the confining surfaces are within about two characteristic dimensions of the vibrating body, the added mass coefficient increases considerably and values from five to ten or more are not unusual. For ship hull vibrations, the added mass is not dependent to any great extent on mode of vibration or frequency. This result appears to be generally applicable as long as the amplitudes are small, - up to five percent of a characteristic dimension of the structure. The added mass becomes both amplitude and frequency dependent at larger amplitude values. It is still not clear that added mass always increases with frequency at large amplitudes (2).

2.6 Unsteady Flow

The steady flow of fluids is now reasonably well understood and many references have appeared on this subject. However, the same cannot be said for unsteady flow. It is sometimes assumed that the flow rate under dynamic conditions can be predicted from the steady state characteristics of the system. For example, if the instantaneous pressure drop and flow area are known, then the flow rate at that instant is predicted as being the same as the steady flow rate that would exist at that steady pressure drop and flow area. However, some investigators (20), (21) have turned their attention to find the differences between these two flow rates.

McCloy (20) has reported three effects that can give rise to these differences which are as follows:

(1) Fluid inertia

(2) Dynamic discharge coefficient

(3) Friction losses.

For unsteady flow, a certain amount of the total pressure drop across the system is needed to accelerate and decelerate the fluid within the system. These inertia effects result in a delay in flow rate establishment. Since the densities of liquids are much greater than those of gases, it is clear that inertia effects are of more significance in liquid flows than in gas flows. Under periodically varied conditions, this time lag can result in attenuation of the flow rate amplitude as frequency increases.

The discharge coefficient may change under dynamic conditions. Daily, Hankey, and Olive (21) have taken into account the effects of fluid inertia, and have shown that, for water flow through square-edged orifices in pipes, the discharge coefficient increases when the flow accelerates and decreases when the flow decelerates. Also McCloy (20) has shown that the discharge must be frequency dependent.

Friction losses may be different under unsteady conditions. Since even the "steady state" analysis of turbulent losses is extremely complex, it is not surprising that there is little information concerning them under unsteady conditions. Daily, Hankey, and Olive (21) have shown that turbulent losses are affected by the rate of change of flow rate. Unfortunately their experimental results concern only transient conditions and do not deal with oscillatory flows.

CHAPTER 3

A MECHANISM FOR SELF EXCITATION IN HYDRAULIC CONTROL ELEMENTS

3.1 Introduction

Research efforts in the field of flow-induced structural vibrations have resulted in very diverse data on specific practical or highly idealized vibration problems. However, little has been done to synthesize such information. The great number of geometric and dynamic parameters as well as the complexity of the phenomena involved seem to have discouraged the search for a common conceptual framework. A detailed knowledge of specific or idealized vibration problems, without proper insight into the basic flow features and mechanisms of excitation will be of little use to an engineer whose task it is to design a structure that will safely withstand flow-induced forces.

The main object of this research is to derive a general model for self-excited vibrations which may be applicable to most hydraulic control elements. Such a model, based on first principles, would be of great importance for design engineers, especially if unsteady flow and closure occur during operation.

Before proceeding with the derivation of the theoretical model, experimental observations of hydraulic swing-check valve vibrations (11),(12) will be reviewed briefly. This will illustrate the most significant flow features, and provide data for an acceptance test for any proposed model, as will be explained later. Mathematical models of gate and seal vibrations which appeared in the literature (9),-(14) are discussed and compared with these experimental observations. Since these models do not match the experimental results, a semi-empirical model is derived from the previous dynamic experiments. The object of the preliminary semi-empirical model is to study the nature of the hydrodynamic load (whether it is velocity and/or displacement dependent) and to consider what flow features should be taken into account in order to model the hydrodynamic load mathematically.

3,2 Experimental Observations of Check Valve Vibrations(11)

3.2.1 Dynamic Behaviour of the Valve

Figure 3.1 shows both a static and dynamic stability map of the valve (11). The static system characteristic can be determined by the curve along which the available hydrostatic pressure difference just overcomes the elastic restraining spring force and thus, just holds the valve plate against its seat. The region of dynamic instability, as obtained experimentally, is divided by the static system characteristic

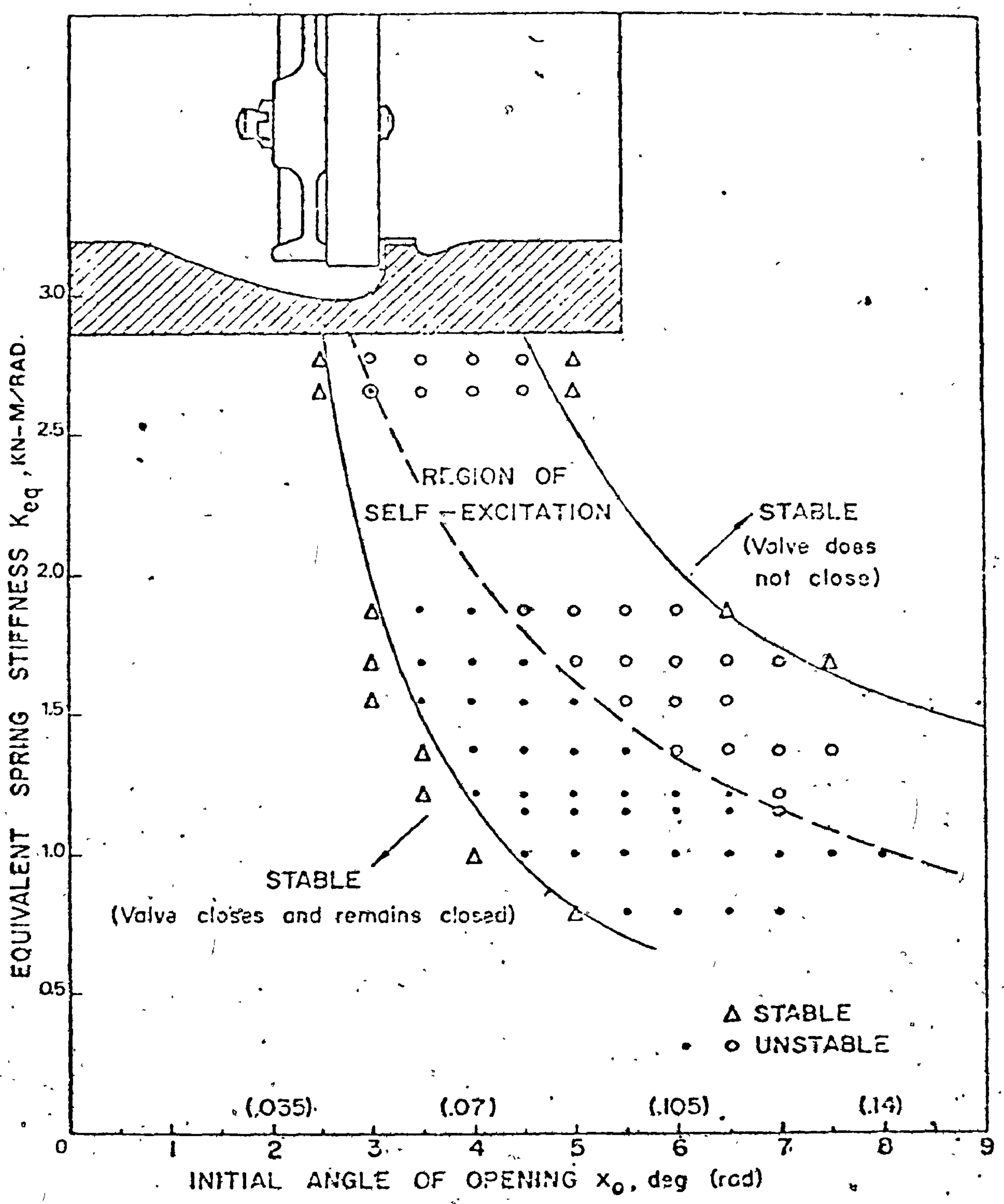

Figure 3.1. Stability Map of the Valve's Dynamic Behaviour, Ref. (11).

into two sub-regions. In the lower sub-region, the valve is expected to close and remain closed statically since the available hydrostatic pressure difference is large enough to overcome the restoring spring force. In the upper sub-region the valve is expected to remain open statically since the available hydrostatic pressure difference is not sufficient to close it. The occurrence of limit cycle oscillations in the area above the dashed line indicates that closure must be caused by dynamic pressures in excess of the available hydrostatic head. Once the dynamic pressure has attenuated, the spring will pull the valve open again. For the region below the dashed line, opening must be caused by some dynamic effect such as the reflection of a pressure wave or the mechanical bouncing of the valve off its seat. To the left of the lower sub-region of instability is a stable region where the valve always closes and remains closed. To the right of the upper sub-region of instability is another stable area where the valve does not close.

The influence of different parameters on the frequency and amplitude of vibration at constant upstream pressure is of great importance in characterizing the behaviour of the system. Figure 3.2 (a) shows that for a constant available hydrostatic head and initial angle of opening (x_0), the amplitude of vibration of the valve increases while the frequency decreases as the equivalent spring stiffness (Keq) increases.

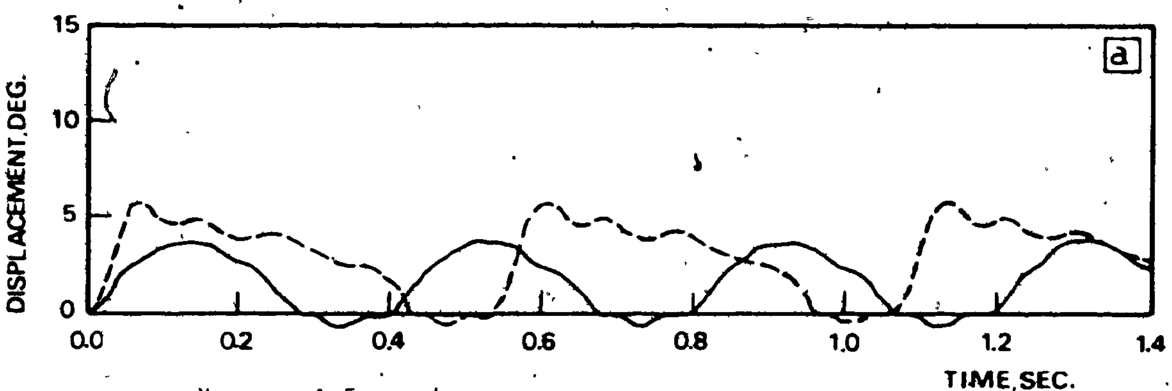

X_o = 4.5 deg.

– – – – Keq = 2.69 KN-m/rad

———— Keq = 0.96 KN-m/rad

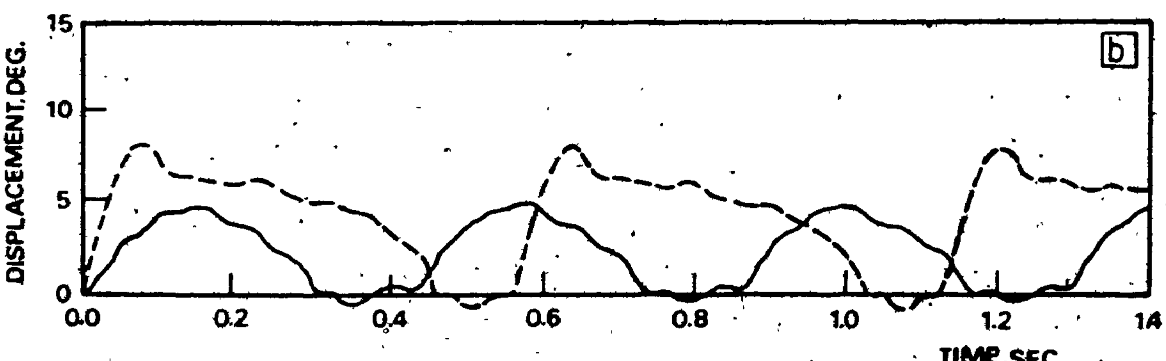

Keq = 1.32 KN-m/rad

– – – – X_o = 7 deg.

———— X_o = 4 deg.

Figure 3.2. Dynamic Measurements of the Valve's Vibrational Response, Ref. (11): (a) Effect of Stiffness; and (b) Effect of Initial Setting.

This is, of course, contrary to the effect of increased stiffness on free vibrations. In addition, the ratio of closing time to opening time during the cycle of vibration increases with an increase in equivalent spring stiffness.

Figure 3.2 (b) shows that the effect of increasing the initial angle of opening on the frequency and amplitude of vibration is qualitatively the same as increasing spring stiffness; both increase the violence of vibrations.

3.2.2 Mechanism of Self-Excitation

The mechanism of valve instability as reported by Weaver and Adubi (11) can be explained as follows:

At the maximum angle of opening, the valve begins to drift close under the influence of the hydrodynamic pressure difference, which is sufficient to just overcome the spring force. As the disc nears the seat, it begins to accelerate as the pressure difference begins to rise. This process is an interactive one. A small increase in the pressure difference advances the disc a small distance towards the seat. This reduces the flow area, leading to an increase in head loss and reduction in discharge, and hence a further rise in pressure difference. For rather small angles the pressure difference is relatively large due to the high rate of change of discharge which creates a significant inertial pressure difference. Hence, the disc accelerates rapidly towards the seat.

As the valve slams onto its seat, waterhammer pressure waves are generated on both upstream and downstream sides. The valve, responding only to the pressure difference, remains on its seat until this pressure difference is reduced to a point where it either forces the valve open, or allows the spring-restoring forces to initiate opening. It should be noted here that waterhammer wave reflection may initiate opening of the valve when it otherwise would have remained shut (that is, in the unstable region below the static system characteristic). Once the valve opens, the flow begins reestablishing itself and the pressure difference drops sufficiently to allow opening to continue under the influence of the spring. The cycle of events is then repeated.

3.2.3 Features of Check Valve Vibration

The significant conclusions drawn from the experimental observations are:

a) Fluid inertia produces a much greater flow velocity during the closing portion of the cycle than at the same angle during the opening part, Figure 3.3 (a). This hysteretic effect is also seen in the pressure difference records, Figure 3.3 (b); it leads to a net energy transfer from the fluid to the structure during each cycle.

b) A vortex is shed from the lower edge of the valve plate at the maximum angle of opening but it has no important

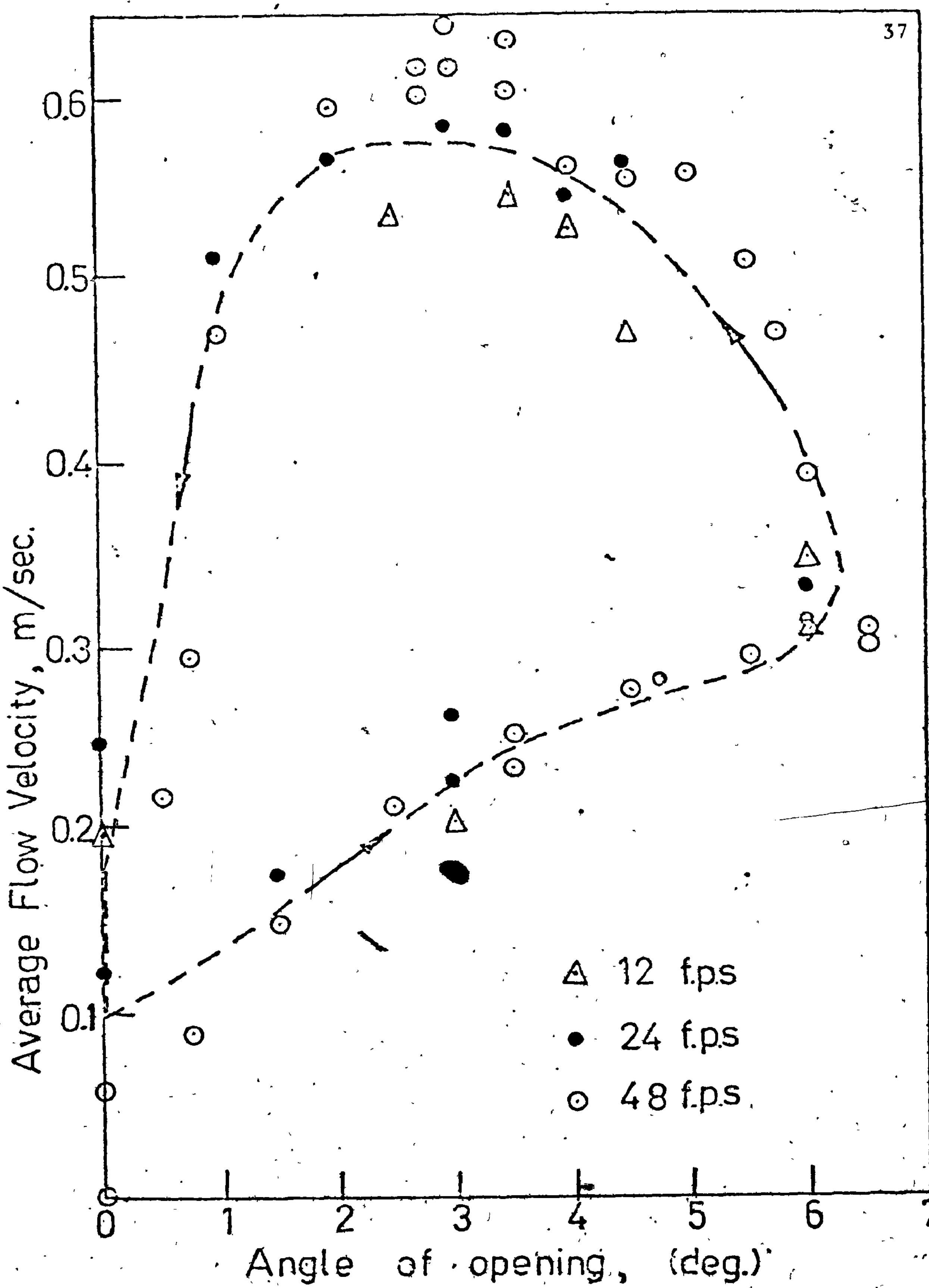

Figure 3.3(a). Velocity Measurements Across a Section of the Valve Apron During a Typical Cycle of Vibration. Ref. (11).

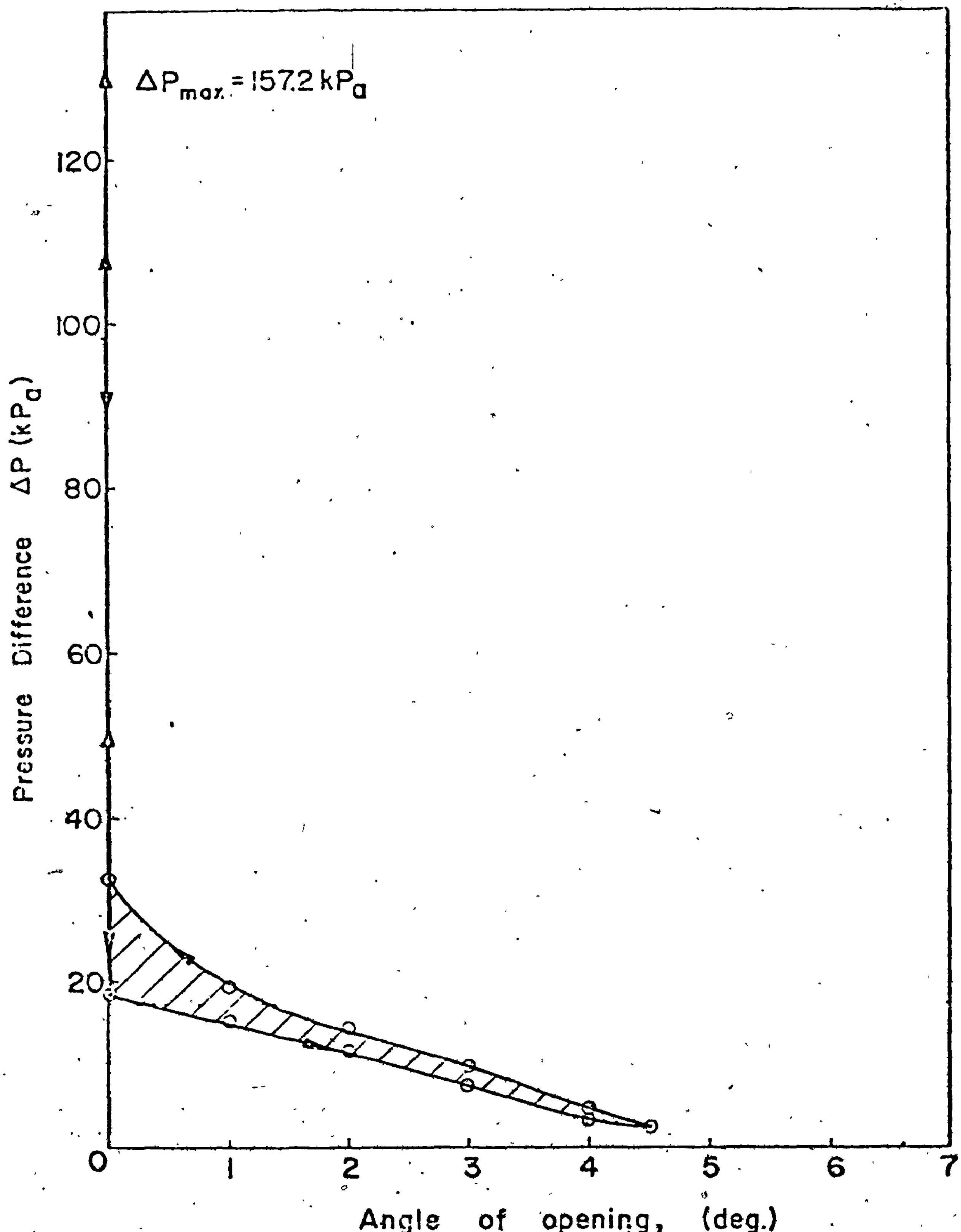

Figure 3.3(b). Pressure Difference vs Angle of Opening, Ref. (11).
K_{oq} = 1.32 KN-m/rad ; X_o = 4 1/2°

effect in the excitation mechanism.

c) The valve geometry controls the fluid flow behaviour, which in turn controls the closing portion of the vibration cycle.

d) Local flow effects are not significant.

e) The waterhammer waves produced at closure have almost completely attenuated before the next closure occurs.

f) The valve motion is not of a simple harmonic nature; the opening portion of each cycle being much more rapid than the closing portion.

g) The self-excited vibration frequencies are well below the natural frequencies, indicating no obvious dependence between natural frequencies and limit cycle frequencies.

i) The effect of an increase in stiffness is contrary to that normally expected. Increasing the initial angle of opening (no load setting) has the same effect as increasing stiffness, Figures 3.4.

3.3 Discussion of Negative Damping Model

Consider a linear system of the simplest form, where x stands for the displacement, and F for the exciting force. In the case of a simple harmonic oscillator, the forcing function can be written in the form

$$F = F_o \sin \omega t,$$

and the displacement as

$$x = X_o \sin (\omega t - \phi)$$

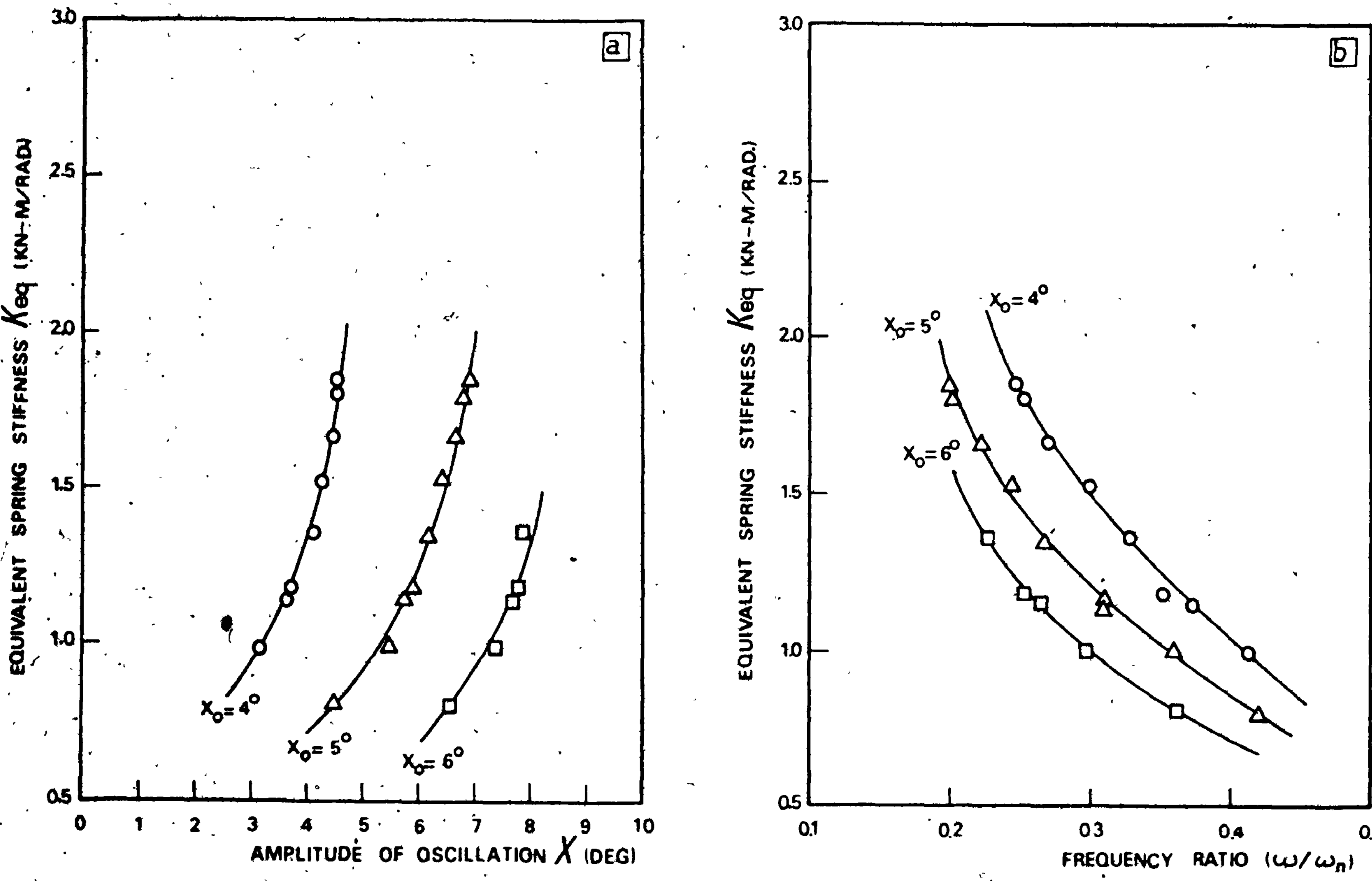

Figure 3.4. Results of Parametric Tests, Ref. (11):(a) Equivalent Spring Stiffness vs Amplitude of Oscillation; and (b) Equivalent Spring Stiffness vs Frequency Ratio.

where

F_o and X_o are amplitudes of the forcing function and displacement respectively;

ω is the frequency of the exciting force;

t stands for the time; and

ϕ represents the phase angle between the forcing function and displacement.

Figure 3.5 shows the exciting force plotted against the displacement for different values of the phase angle. The area bounded by each curve is proportional to the net energy transferred to the system per cycle. When the exciting force is in phase with the displacement, $\phi = 0$, the net energy transferred per cycle is equal to zero, the exciting force may be named as a displacement dependent force. The net energy transference per cycle is maximized when the exciting force is in phase with velocity, $\phi = \pi/2$, and it can be expressed as a velocity dependent force. Once again, the net energy transferred per cycle becomes zero when the exciting force is 180^o out of phase with the displacement, $\phi = \pi$.

Flow-induced vibrations are associated with the transfer of energy from the fluid to the structure; this has led some researchers in recent years to direct their efforts toward modelling the hydrodynamic load by a velocity dependent component. This velocity dependent component is equivalent to a negative damping force, as it causes a transference of energy to the system which perpetuates the motion.

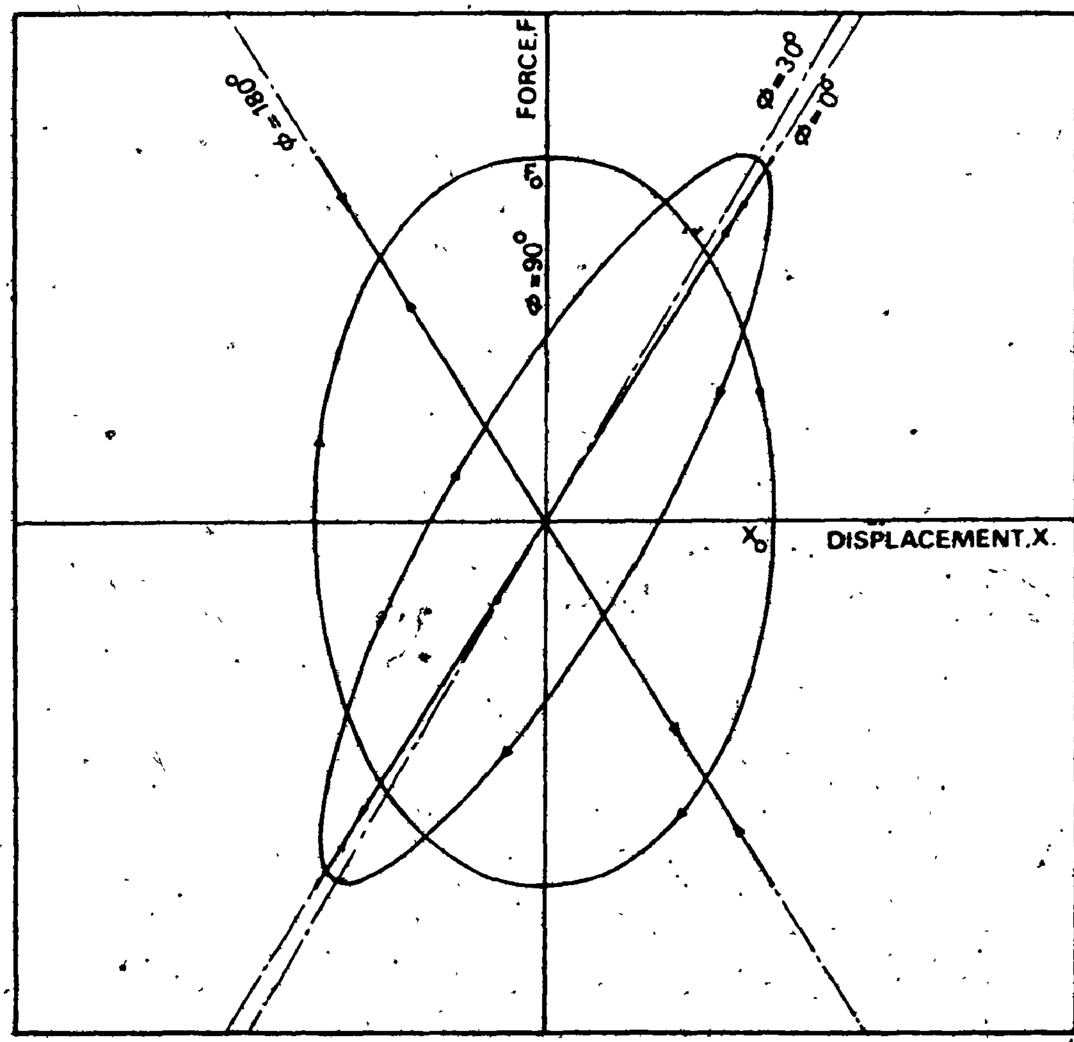

Figure 3.5. Plot of $F = F_0 \sin \omega t$ vs $x = X_0 \sin(\omega t - \phi)$ for Different Values of Phase Angle ϕ.

The linear variation in the dynamic discharge coefficient which has been assumed by Abelev and Dolnikov (9) and Lyssenko and Chepajkin (14) reduces their models, for gate and seal vibrations respectively, to a negatively damped simple harmonic oscillator. Such an oscillator exhibits limit cycle oscillations but an increase in stiffness causes the frequency of oscillations to increase (30). The reverse is true for the valve vibrations. Therefore, modelling of the hydrodynamic load in the form of a velocity dependent term (or negative damping coefficient) must be ruled out as a possible mechanism.

Further insight is gained from the unusual features of valve behaviour; the self-excited vibration frequencies are well below the natural frequencies and the effect of an increase in stiffness is the opposite of that normally expected. Hence, the hydrodynamic load may have a displacement dependent component which would play a significant part in changing the system stiffness from that of a simple elastic structure. This phenomenon can be examined clearly by studying a semi-empirical model of the valve.

3.4 Semi-empirical Model of Valve Vibration

3.4.1 Mathematical Formulation of the Hydrodynamic Load

Further careful examination of the experimental results is carried out in order to find a mathematical expression for the hydrodynamic load in terms of valve displacement. Figure 3.3 (b) shows the pressure difference across the valve disc plotted against angle of opening. It is clear that for the same angle the hydrodynamic load is greater during closing than during opening. The enclosed area in the diagram is proportional to the net energy added to the system per cycle of vibration. The limit cycle oscillation indicates that this net energy addition per cycle is balanced by the energy dissipated by the damping forces in the system plus the kinetic energy lost due to the velocity of the valve disc slamming onto its seat. Were this not the case, it would have resulted in oscillations of continuously increasing or decreasing amplitude depending on whether the net energy added is greater or smaller than the energy dissipated during the cycle.

The hydrodynamic load acting upon valve disc, F_H, is the result of two components, which are:

a) the added mass and hydrodynamic damping load F_A. This component is due to the participation of the surrounding water in the motion; it can be expressed mathematically by the form

$$F_A = J_H \ddot{x} + C_H \dot{x} \qquad 3.1.a$$

where

x is the valve angle of opening;

J_H is the effective moment of inertia of water, i.e. virtual mass effects;

C_H is the hydrodynamic damping coefficient.

b) the hydrodynamic load F, not including the added mass and damping effects. This is given by the integral of the pressure difference across the valve over its area.

$$F = \int_S \Delta p \; r_s \, ds \qquad 3.1.b$$

where

Δp is the pressure difference across the valve disc acting upon an infinitesimal area, ds, excluding added mass and damping effects

r_s is the effective moment arm of the infinitesimal area, ds, about the centre of rotation of the valve disc.

Thus, the total hydrodynamic load F_H is

$$F_H = F_A + F \qquad 3.1.c$$

The pressure difference, Δp, is proportional to four significant components, these are:

a) the static pressure drop across the valve, H_S,
b) the inertia pressure of the fluid in the upstream and downstream pipes, H_i;

$$H_i = \sum_{n=1}^{2} I_n \frac{dq}{dt} = \sum_{n=1}^{2} \frac{\sigma L n}{g} \frac{dv_n}{dt} \qquad 3.2$$

where

I is the fluid inertance, $\frac{\sigma L}{gA}$;

σ is the fluid specific weight;

L_1 is the length of upstream pipe;

L_2 is the length of downstream pipe;

v_n is the mean flow velocity in pipe n.

c) the effects of local high velocity flows parallel to or impinging against downstream side of valve disc. This component is clearly dependent on the total pressure drop across the valve, H.

d) system losses due to friction, entrance, sudden flow area changes and other minor losses.

Moreover, there are some other flow features which have smaller effects on the pressure difference, Δp, such as waterhammer pressure waves, cavitation, and vortex formation. The fluid velocity head is converted into a pressure head due to the sudden valve closure at the last few degrees. The resulting waterhammer waves and cavitation are attenuated, as observed experimentally (11), before the next cycle of valve oscillation and they do not have any dominant effect on the valve instability. However, the dynamic pressure wave action and the elastic strain energy associated with the valve bouncing are responsible for initiating valve opening when the spring force is not great enough to overcome the hydrostatic load on the valve disc.

Careful examination of the experimental records indicates that the cycle of valve vibration can be divided into three distinct phases. These are: the closing time from the maximum angle of opening until relatively small angles; closing time over the last few degrees; and the opening time. Within each phase, the rate of change of the hydrodynamic load with valve displacement is virtually constant.

In the first phase which includes valve closing over large angles, the hydrodynamic load increases slowly with decreasing closure angle. This increase is simply the result of decreasing the flow area and hence increasing pressure drop across the valve. Experimental observations show that the valve motion is relatively slow during this period of time.

During the second phase, for smaller opening angles, there is an increase in the rate at which the hydrodynamic load increases with decreasing closure angle. This can be explained by the large reduction in discharge over the last few degrees of closure. Static experiments conducted on the valve for various fixed angles of closure (13) indicated that for small angles, the local flow velocities through the gap between the disc and its seat increase dramatically as the angle decreases, even though the net discharge is dropping. This leads to a rapid increase in head loss across the valve as well as a significant inertial pressure difference owing to the rate of change of discharge. The rate of change of both the static head loss across the valve and dynamic pressure due to fluid inertia will accelerate the valve disc until it slams hard onto the seat.

Once the valve is closed, the flow is suddenly stopped.

Waterhammer pressure waves are generated both upstream and downstream of the valve. The valve remains on its seat until the pressure difference reduces to a point where it either forces the valve open, or allows the spring-restoring forces to initiate opening. The hydrodynamic load during opening decreases at a rate which is smaller than that found for larger angles during closing. The fact that the rate of hydrodynamic load decrease with increasing angle during opening is smaller than that during closing can be attributed to the fluid inertia effect which delays the reestablishment of flow. As a result, the pressure difference across the valve is smaller, the spring stiffness dominates, and the valve displays its natural response in quiescent fluid which is to open quickly.

Thus, the mean hydrodynamic pressure difference during each phase of the cycle can be depicted by a straight line approximation if care is taken to include only the same area. This piece-wise linear approximation is indicated in Figure 3.6;

where:

α_1, α_2, and α_3 are the rates of change of the hydrodynamic pressure with valve opening, i.e. the slopes of the straight line approximations within the three subdivisions of the cycle;

p_1 is the pressure difference across the valve

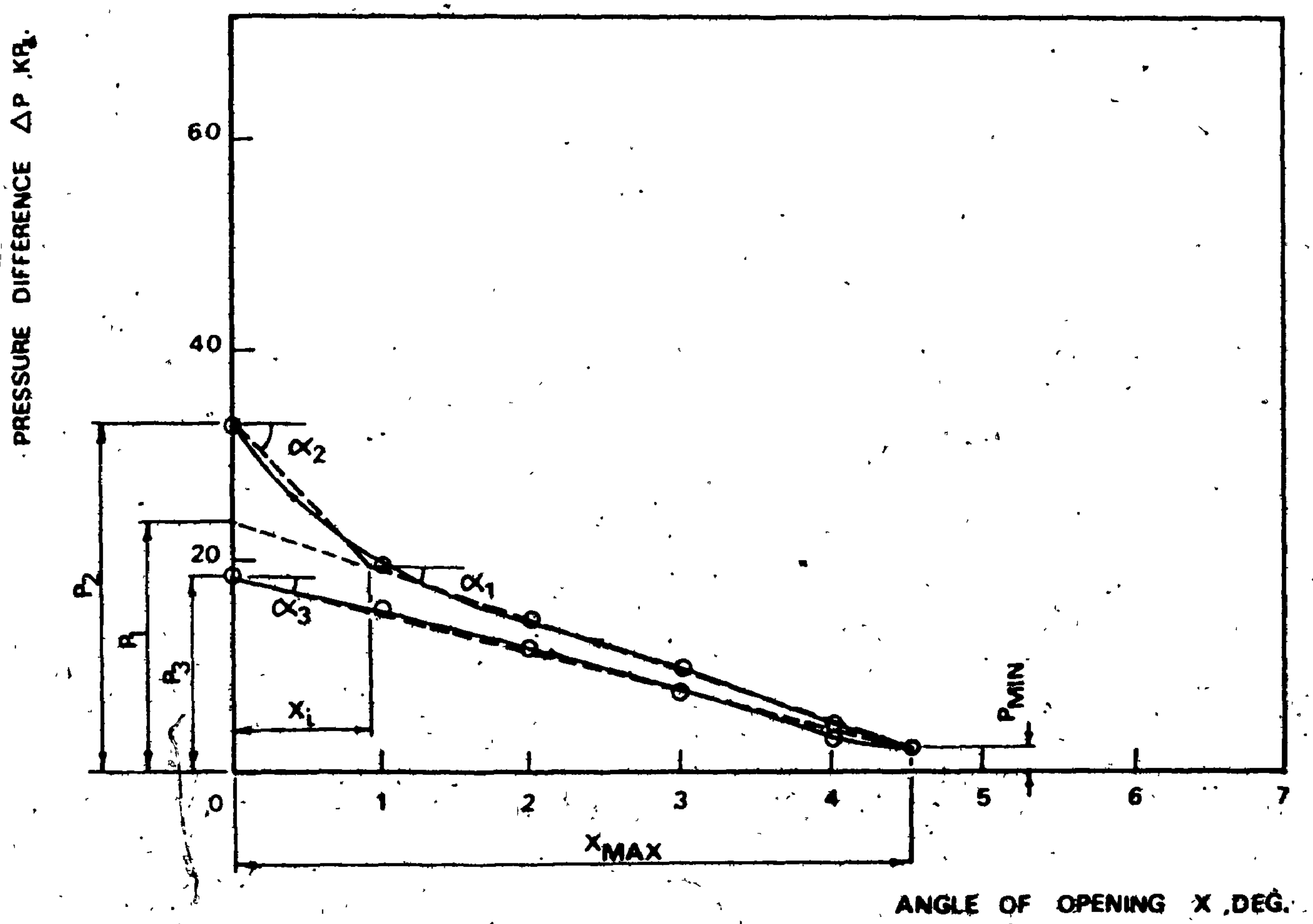

Figure 3.6. Bilinear Approximation for Pressure Difference vs the Valve's Angle of Opening.

at the instant of closing, if the fluid inertia and high flow velocity effects are neglected;

P_2 is the pressure difference across the valve at the instant of closing;

P_3 is the pressure difference across the valve at the instant of opening;

P_{min} is the minimum pressure difference during the cycle;

x_{max} is the maximum angle of opening; and

x_i is the angle at which the fluid inertia and local flow velocity effects become dominant.

It remains to determine these parameter values for different valve characteristics, i.e. for each combination of equivalent spring stiffness, initial angle of opening, and hydrostatic pressure drop across the valve.

In the first subdivision of the cycle (valve closing over larger angles) the hydrodynamic load is the driving force. Examination of the experimental results taken for five points from the instability region indicates that the pressure difference at the instant of closing (P_1), neglecting fluid inertia and local high flow velocity effects, is linearly dependent on the elastic strain energy stored in the valve spring, as shown in Figure 3.7 (a). This suggests that the hydrodynamic work done during closing is related to the elastic strain energy stored in the valve system.

For smaller opening angles during closing, when the fluid inertia head and local high flow velocity effects become significant, Figure 3.7 (a) shows the linear relationship between the elastic strain energy stored in the valve system and pressure difference at instant of closing (P_2). Increasing the elastic strain energy, by increasing K_{eq} and/or x_o, results in a larger amplitude and period of vibration. Hence, the fluid has longer to re-establish itself and higher discharges occur. The result is higher fluid inertia and local flow velocity effects. This is shown by an increase in the pressure difference across the valve at the instant of closing (P_2), Figure 3.7 (a). In addition, the fluid inertial head controls the valve movement over larger angles (x_i) as shown in Figure 3.8.

For small amplitudes of oscillation and hence small values of elastic strain energy stored, the effects of fluid inertia and local high flow velocity are small (see Figure 3.8 in which the angle x_i goes to zero for small amplitude of oscillations). This may be explained by the convergence of pressure differences P_1 and P_2 with decreasing elastic strain energy as shown in Figure 3.7 (a). Thus, for small amplitudes of oscillation the pressure difference across the valve during closing is approximated by one straight line instead of a bilinear approximation.

Once the valve is closed, the pressure difference

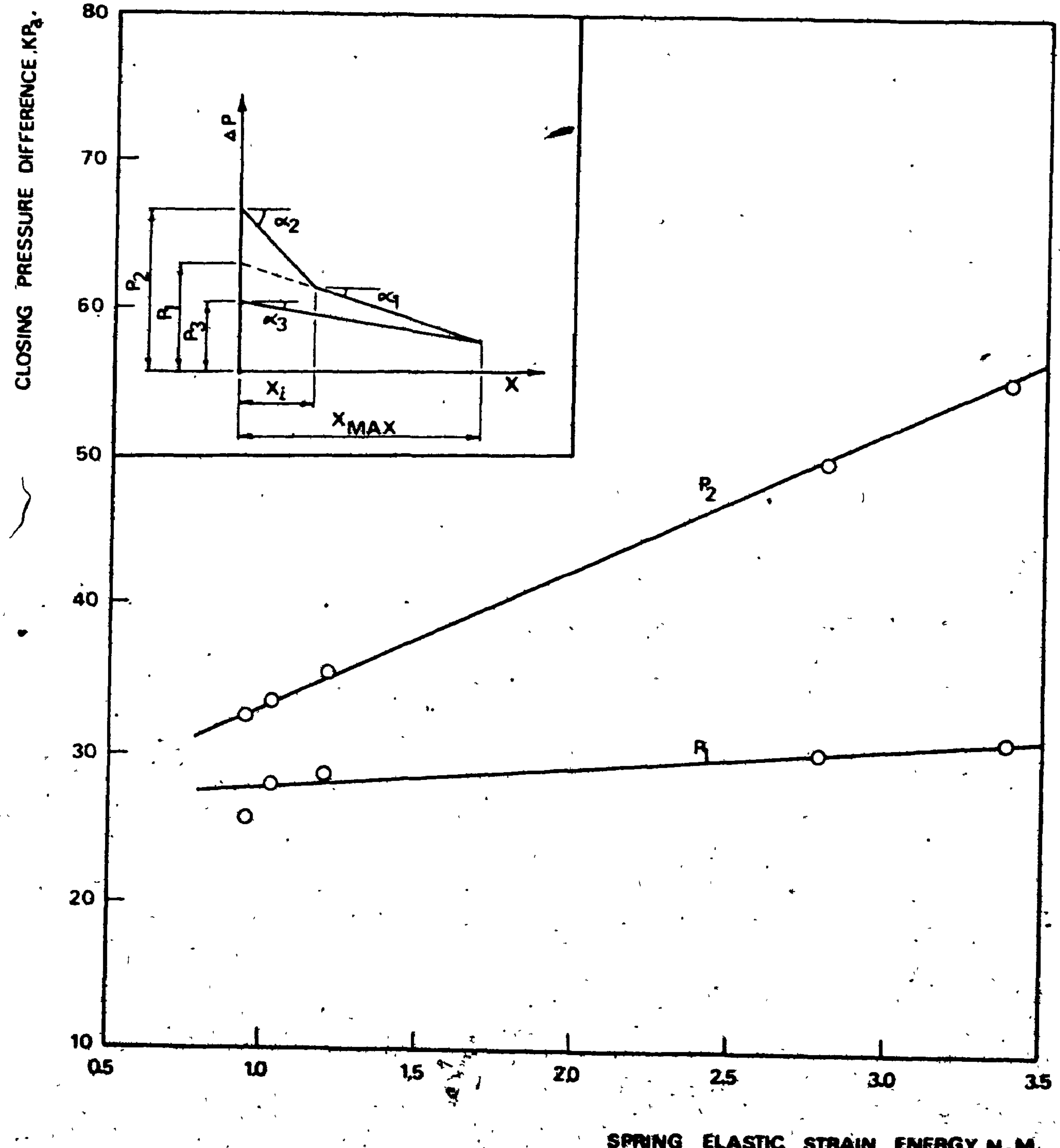

Figure 3.7(a). Pressure Difference at Instant of Closing vs the Elastic Strain Energy Stored in the Spring.

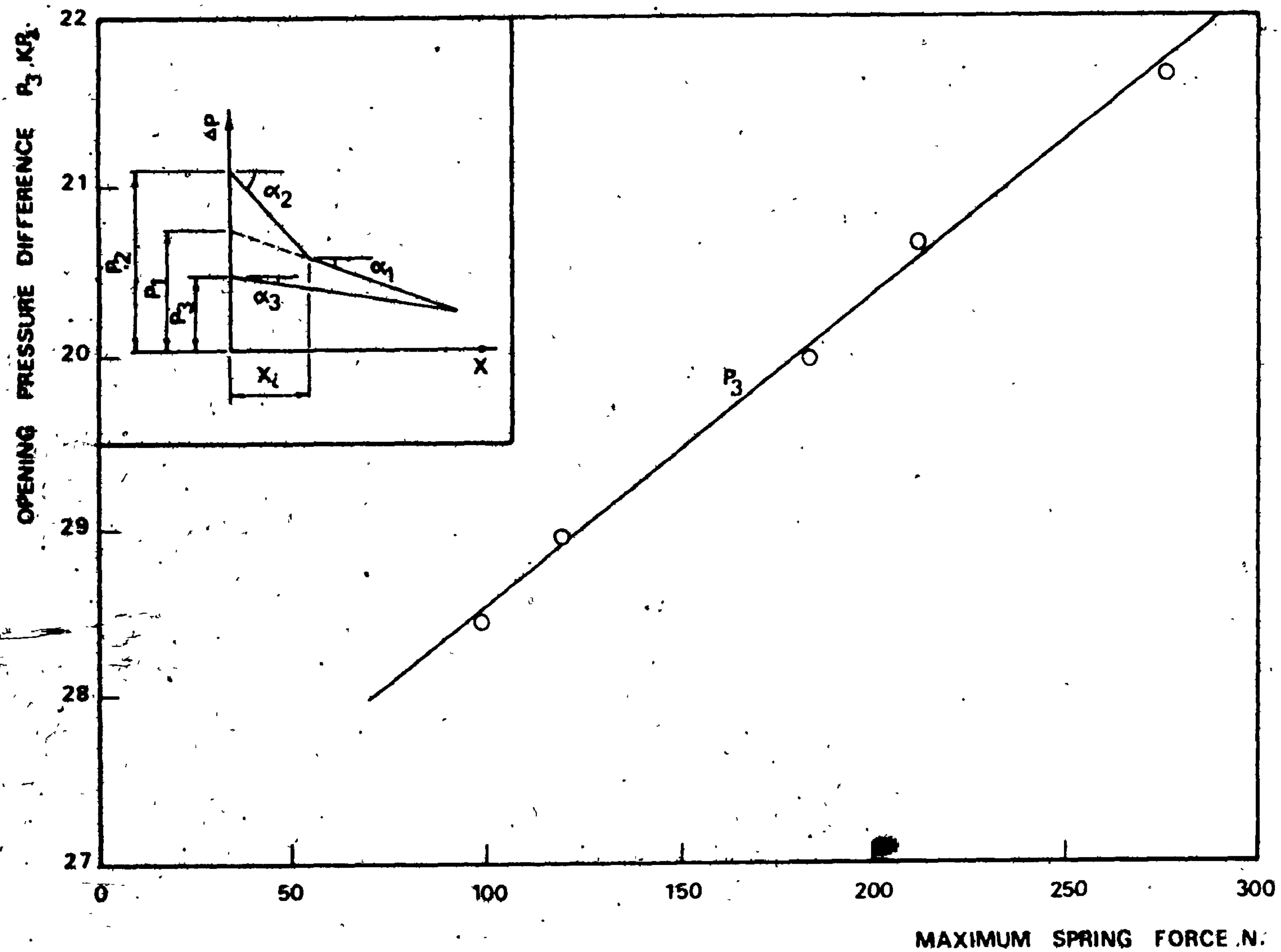

Figure 3.7(h). Pressure Difference at Instant of Opening vs Maximum Spring Force.

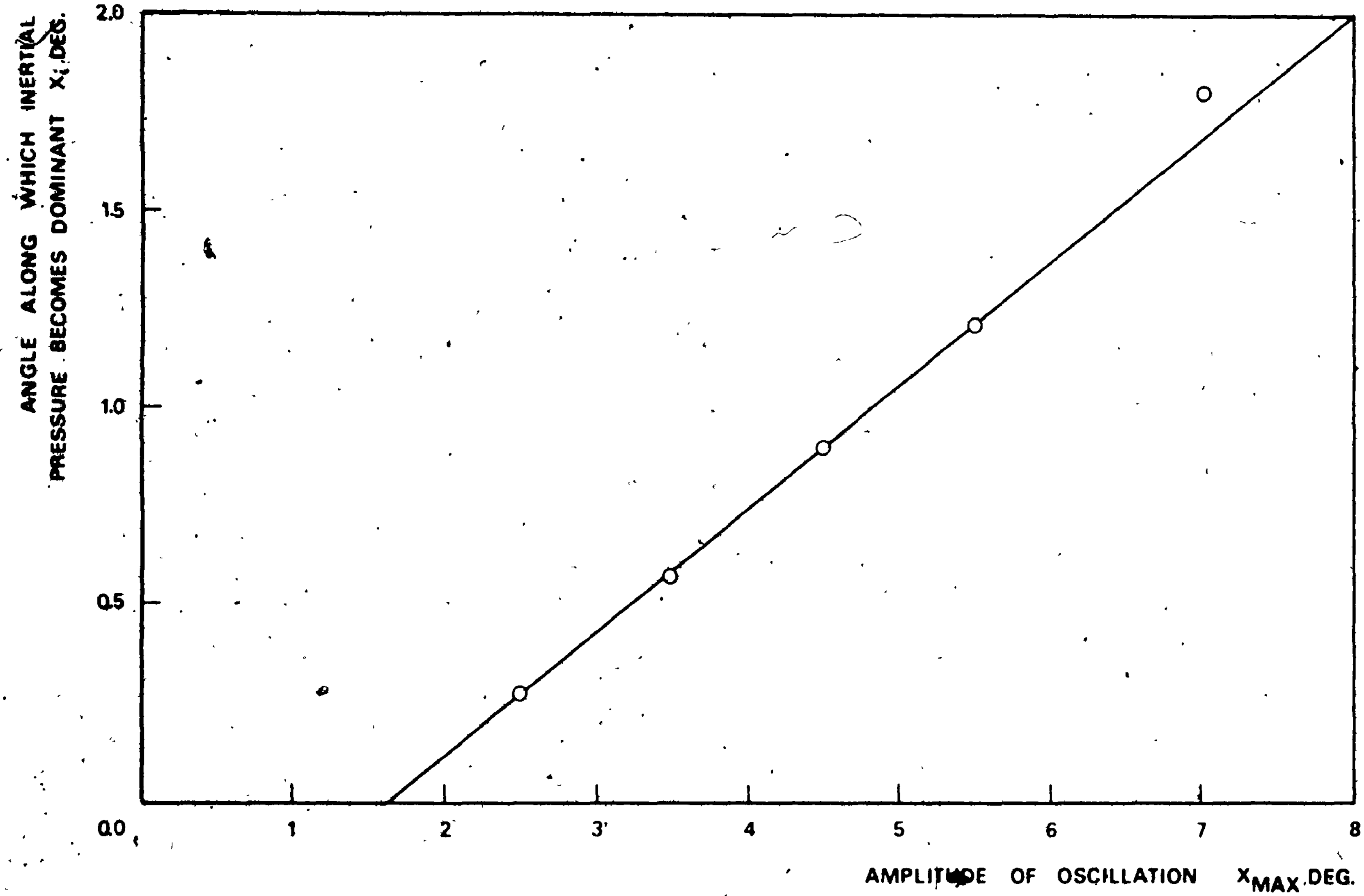

Figure 3.8. Angle Along Which Inertial Pressure Dominates Against Amplitude of Oscillation.

increases rapidly due to waterhammer waves both upstream and downstream of the valve. A short time later, the reflected waves reduce the pressure to a point where opening can occur, either initiated by the reflected waves or the spring. The pressure difference at which opening occurs, P_3, is plotted against the spring force at the instant of opening in Figure 3.7 (b). This shows that the pressure difference at the opening instant is proportional to the maximum spring force.

Finally, the minimum pressure difference attained during the cycle, at maximum angle of opening, is found to be independent of valve characteristics and hence, is taken as a constant.

In this subsection, a mathematical expression of the hydrodynamic load has been developed to represent the exciting force acting upon the valve disc. In order to derive the differential equation of motion of the valve system it is necessary to model the elastic structure.

3.4.2 Valve Modelling

The valve is modelled as a single degree of freedom system as shown schemetically in Figure 3.9, where:

J_d is the valve disc moment of inertia about its centre of rotation;

C_d is the damping coefficient of the valve system;

K_{eq} is the equivalent spring stiffness of the valve

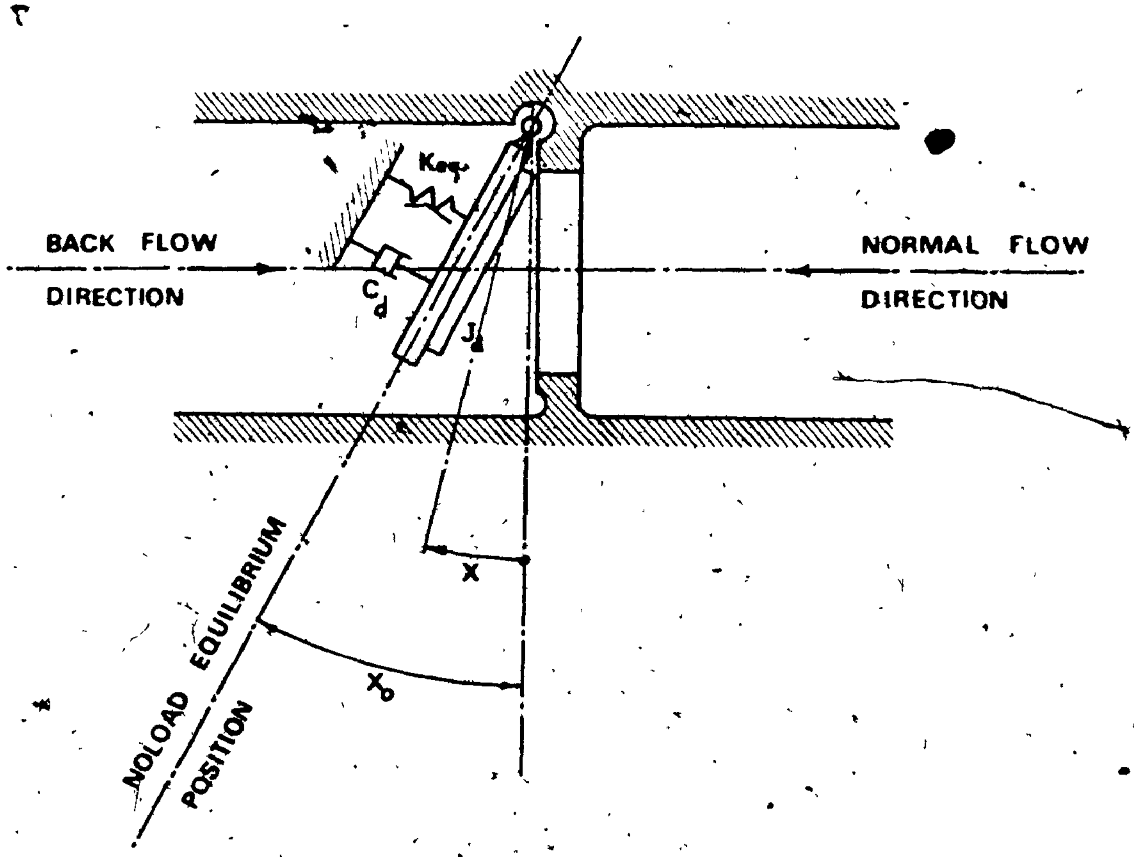

Figure 3.9. Schematic Representation of the Valve's Model.

system;

x_o is the initial setting angle of the valve in quiescent fluid; and

x is the valve angle of opening measured from the valve seat.

The differential equation of motion for the valve disc is:

$$J_d\ddot{x} + C_d\dot{x} + K_{eq}(x - x_o) + F_H = o \qquad 3.3$$

The hydrodynamic load F_H includes added mass and damping effects. This is given by the integral of the total pressure difference across the valve over its area, i.e.

$$F_H = \int_S \Delta p_t \, r_s \, ds$$
$$= C_i \, P_{av} R_o S \qquad 3.4$$

where:

Δp_t is the pressure difference across the valve disc acting upon an infinitesimal area, ds, which has an effective moment arm, r_s, about the centre of rotation. Since this pressure difference was measured experimentally, it represents the load felt by the valve disc and must include the added mass as well as the hydrodynamic damping effects;

P_{av} is the average pressure difference across the valve;

S is the valve disc area; and

C_i is an integration coefficient to reduce the elementary forces $\Delta p_t ds$ to a selected centre with effective moment arm R_o.

As illustrated in the previous subsection, the average hydrodynamic pressure difference can be replaced by a piece-wise linear approximation of the form:

$$P_{av} = P_j - \alpha_j x \qquad 3.5$$

where:

$$\begin{aligned} j &= 1 \ \ldots\ldots \text{ for } \dot{x} \leq 0 \ \ldots\ldots \text{and } x \geq x_i; \\ j &= 2 \ \ldots\ldots \text{ for } \dot{x} < 0 \ \ldots\ldots \text{and } x \leq x_i; \text{ and} \\ j &= 3 \ \ldots\ldots \text{ for } \dot{x} \geq 0 \ \ldots\ldots \text{and } x \geq 0 \end{aligned} \qquad 3.6$$

Using equations 3.3, 3.4, and 3.5, the equation of motion for the valve disc becomes:

$$J_d \ddot{x} + C_d \dot{x} + (K_{eq} - C_i R_o S \alpha_j) x = K_{eq} x_o - C_i R_o S P_j \qquad 3.7$$

where the value of j can be determined according to equation 3.6.

The valve vibrations are governed by equation 3.7. This piece-wise linear differential equation with constant coefficients can be analysed using the method of piece-wise matching as described by Butenin (29).

3.4.3 Semi-Empirical Model Results and Discussions

In this section, the equation governing the valve vibration is studied in more detail by means of the phase plane technique (30). The differential equation of motion has been solved numerically by computer using Runge-Kutta Method (26).

The phase plane simply represents a graph of displacement against velocity. For this particular problem, the phase plane is divided into three regions in each of which the trajectories* are described by a linear differential equation. For this equation stable foci occur at:

$$x_j = \frac{K_{eq}x_o - C_iR_oSP_j}{K_{eq} - C_iR_oS\alpha_j} \quad \text{and} \quad \dot{x}_j = 0$$

The foci location for different valve characteristics is of great importance in determining the system's behaviour.

First, when the maximum elastic strain energy stored is small, i.e. K_{eq} and x_o are small, the hydrodynamic load during closing has been approximated by one straight line instead of the bilinear approximation and hence, there is only one focus during the closing part of the cycle. Figure 3.10 (a) shows a schematic phase plane of the system in which the valve slams shut, bounces weakly several times and remains shut. A typical computer output** for this case is shown in Figures 3.11.

Increasing the equivalent spring stiffness or initial setting angle results in shifting the stable foci to the right in the phase plane; the valve suddenly begins to execute limit cycle oscillations, Figure 3.10 (b). Further increase in the maximum elastic strain energy stored, Figure 3.10 (c),

---

* The curve described by the representative point in the phase plane is called a trajectory.

** The computer programme list is given in Appendix A.

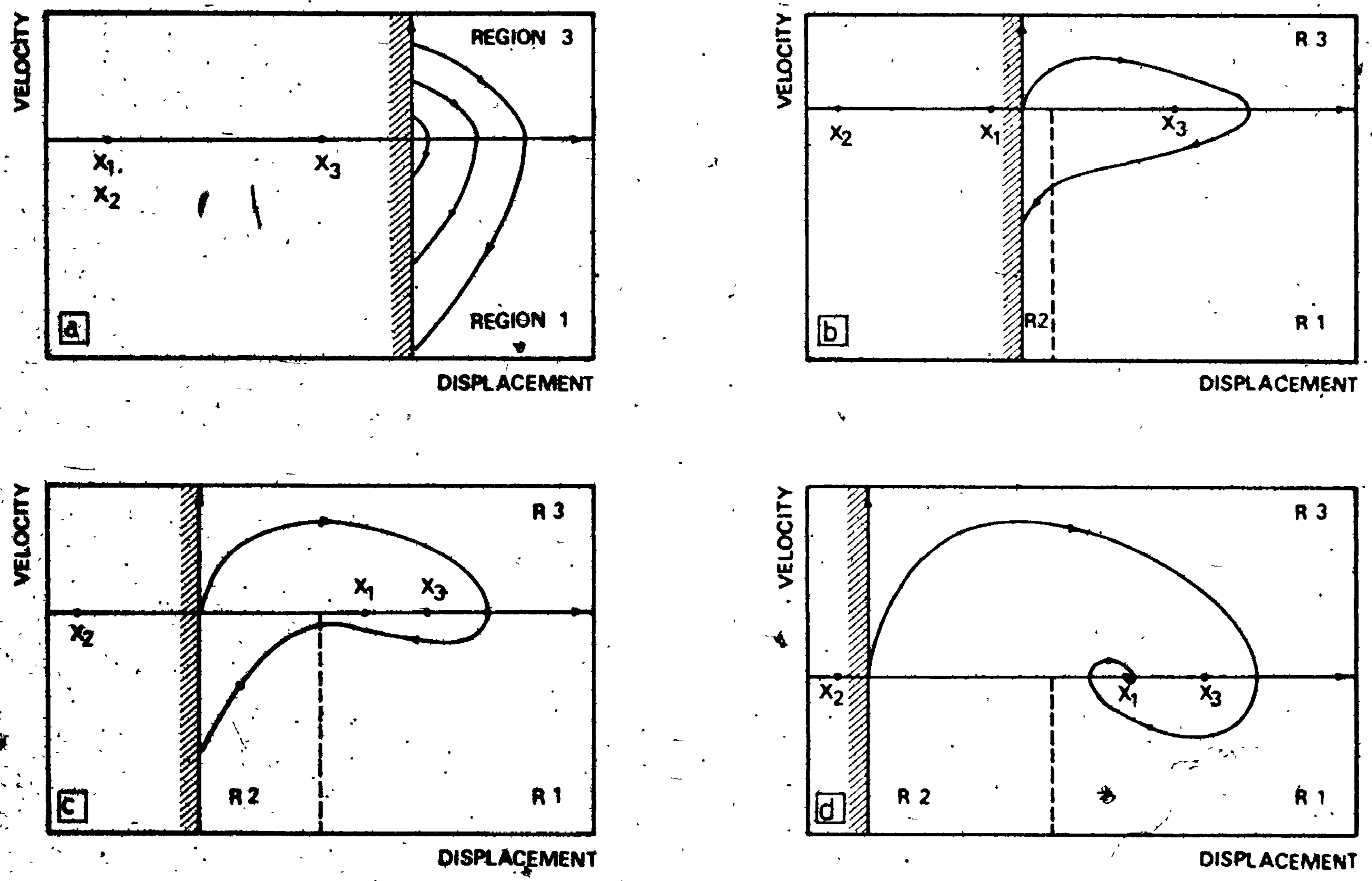

Figure 3.10. Schematic Phase Plane Representation of the Valve's Dynamic Behaviour.

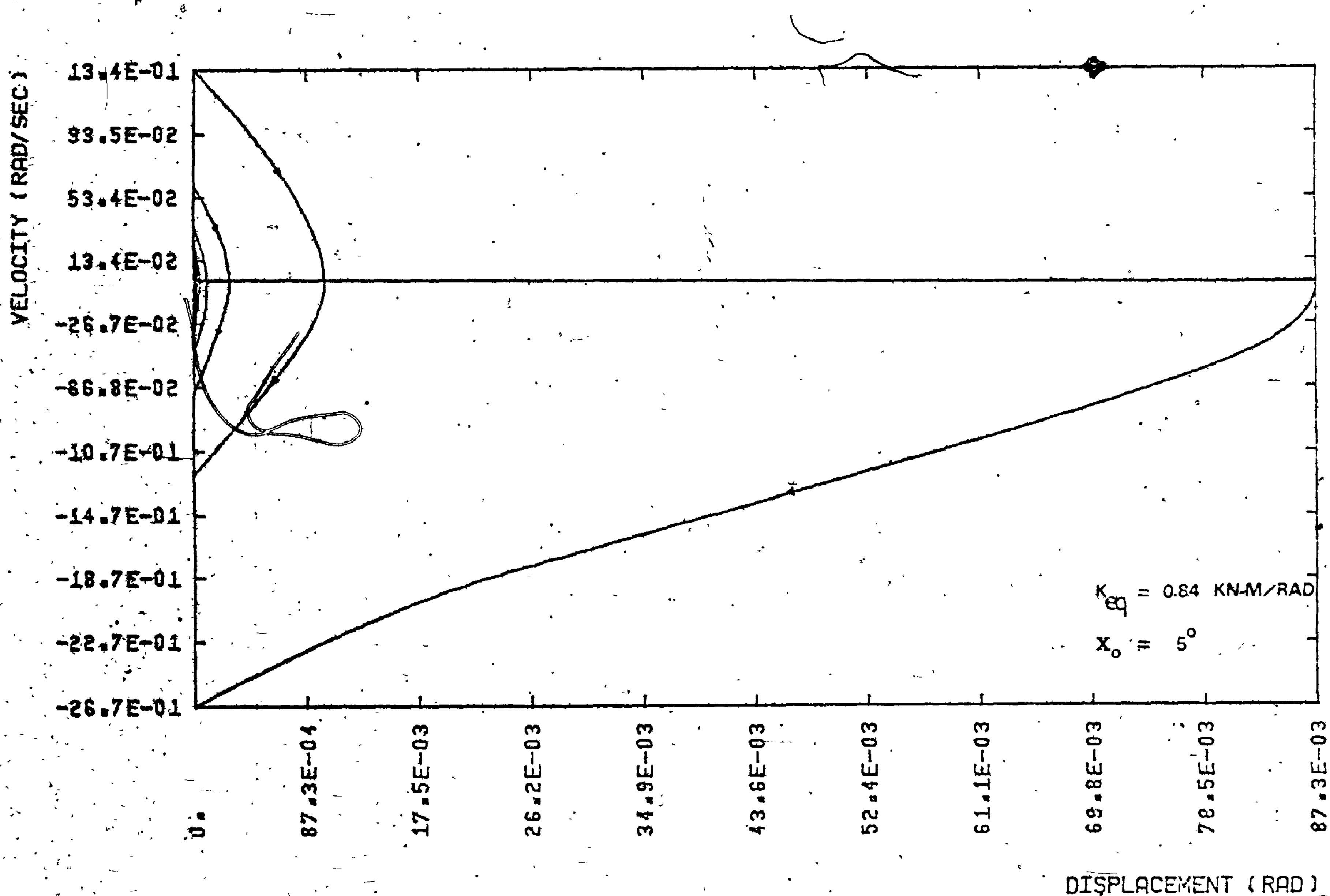

Figure 3.11 (a). Phase Plane Plot ; the Valve Closes and Stays Closed.

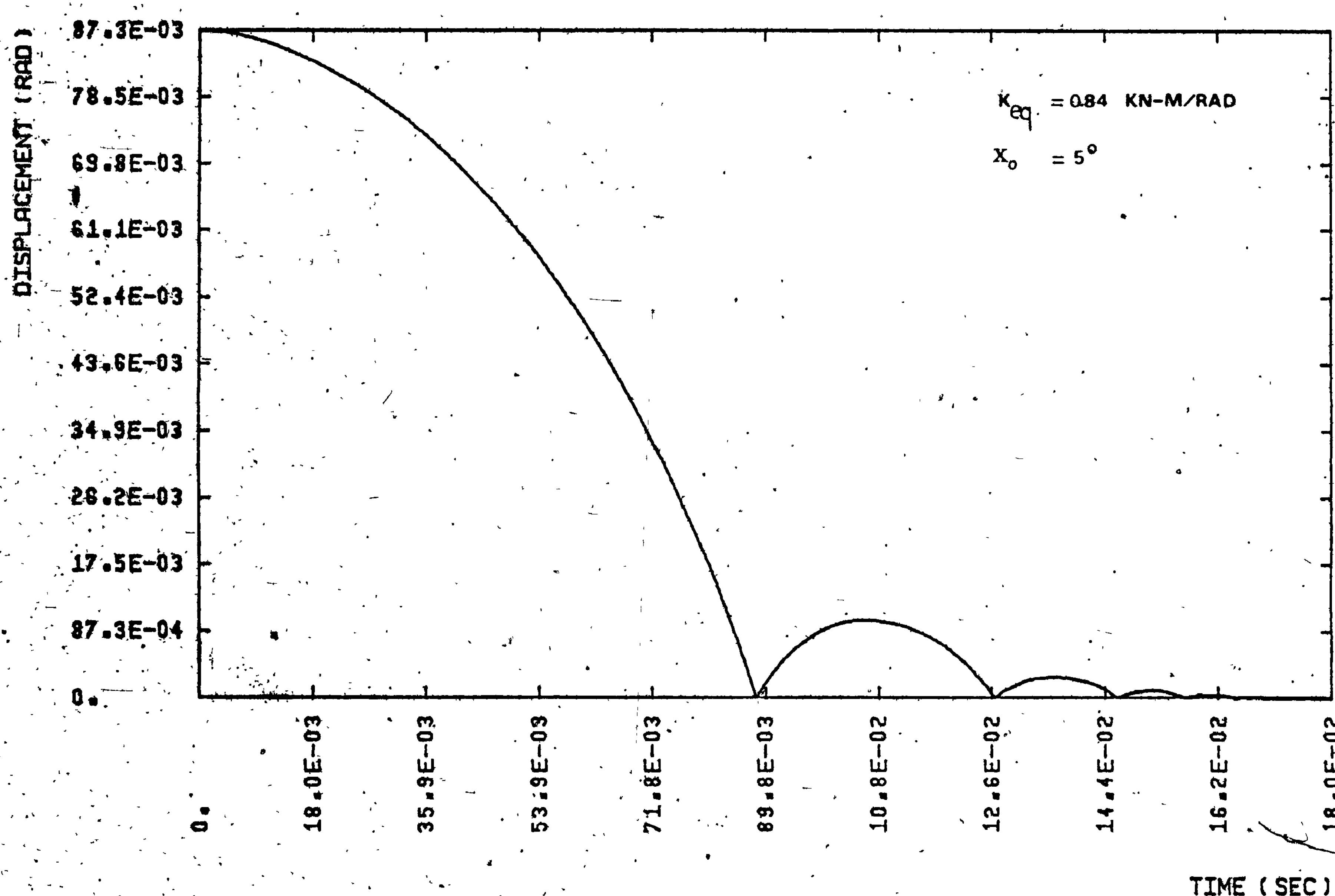

Figure 3.11(b). Transient Response; the Valve Closes and Stays Closed.

leads to larger amplitude, lower frequency, limit cycle oscillations. The effect of such an increase in stiffness or initial setting angle on the frequency and amplitude of vibration is shown in Figure 3.12.

For sufficiently large stiffness or initial angle, the valve slams shut then bounces back once and remains open at a small angle. Any further increase in equivalent spring stiffness or initial angle beyond this point simply results in increasing the angle at which the valve finally stays open. The schematic phase plane representation, Figure 3.10 (d), shows that if the closing hydrodynamic load over large angles does not bring the valve disc into the second region of the phase plane, the valve will not close. Once the valve disc crosses the separation line during closing, it must reach the seat. Figure 3.13 shows a typical computer output for the transient response in this case.

The influence of changing parameters (stiffness and initial angle of valve setting) on the frequency and amplitude of vibration for constant hydrostatic pressure difference is shown in Figures 3.14 and 3.15. In Figure 3.14 the amplitude of vibration is plotted against the equivalent spring stiffness. Each curve represents a different initial setting angle. In Figure 3.15 the frequency ratio* is plotted against the equivalent spring stiffness. The above figures show that

* The ratio of frequency of vibration to the fundamental frequency of the valve in the quiescent water for each spring combination.

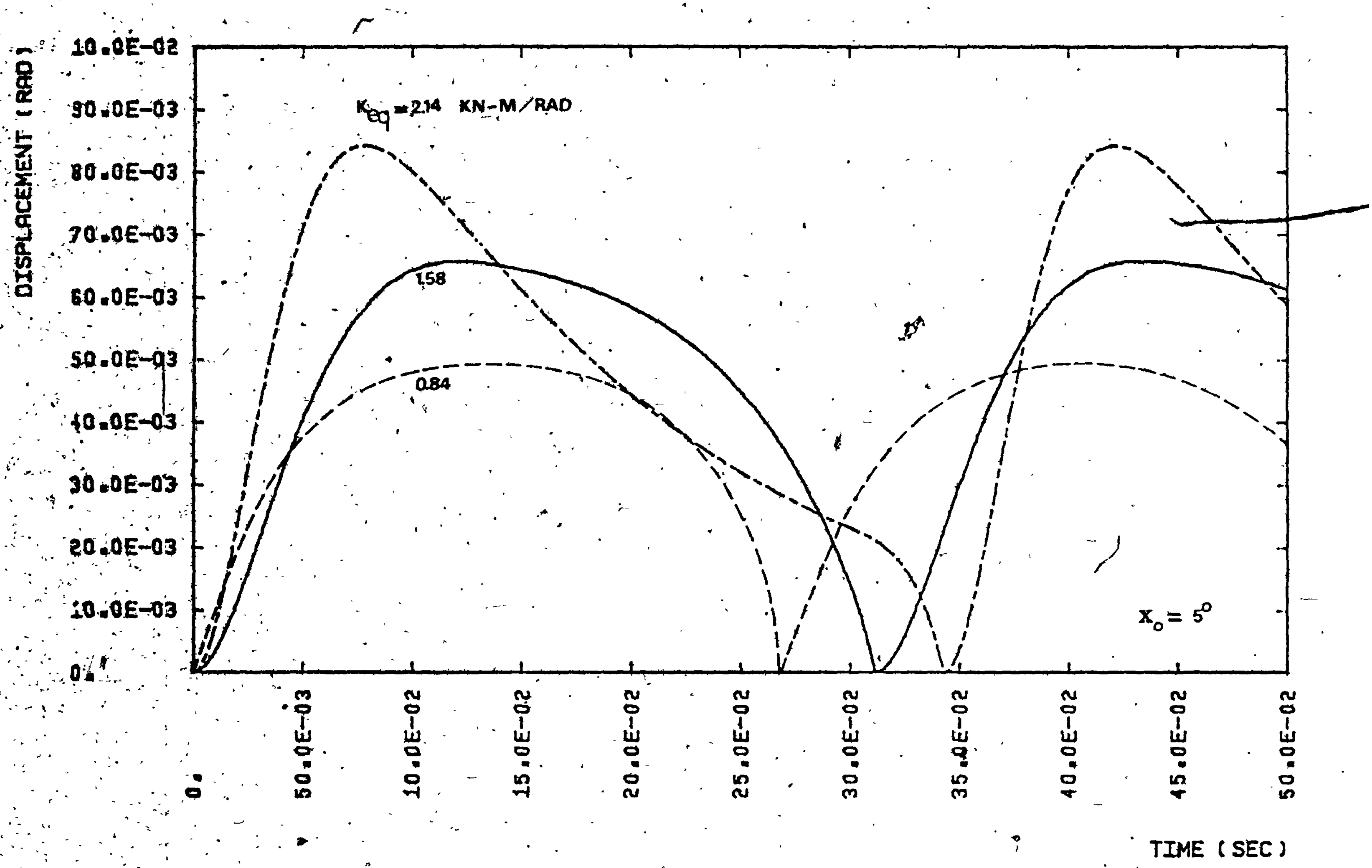

Figure 3.12(a) Effect of Stiffness on the Valve's Dynamic Behaviour.

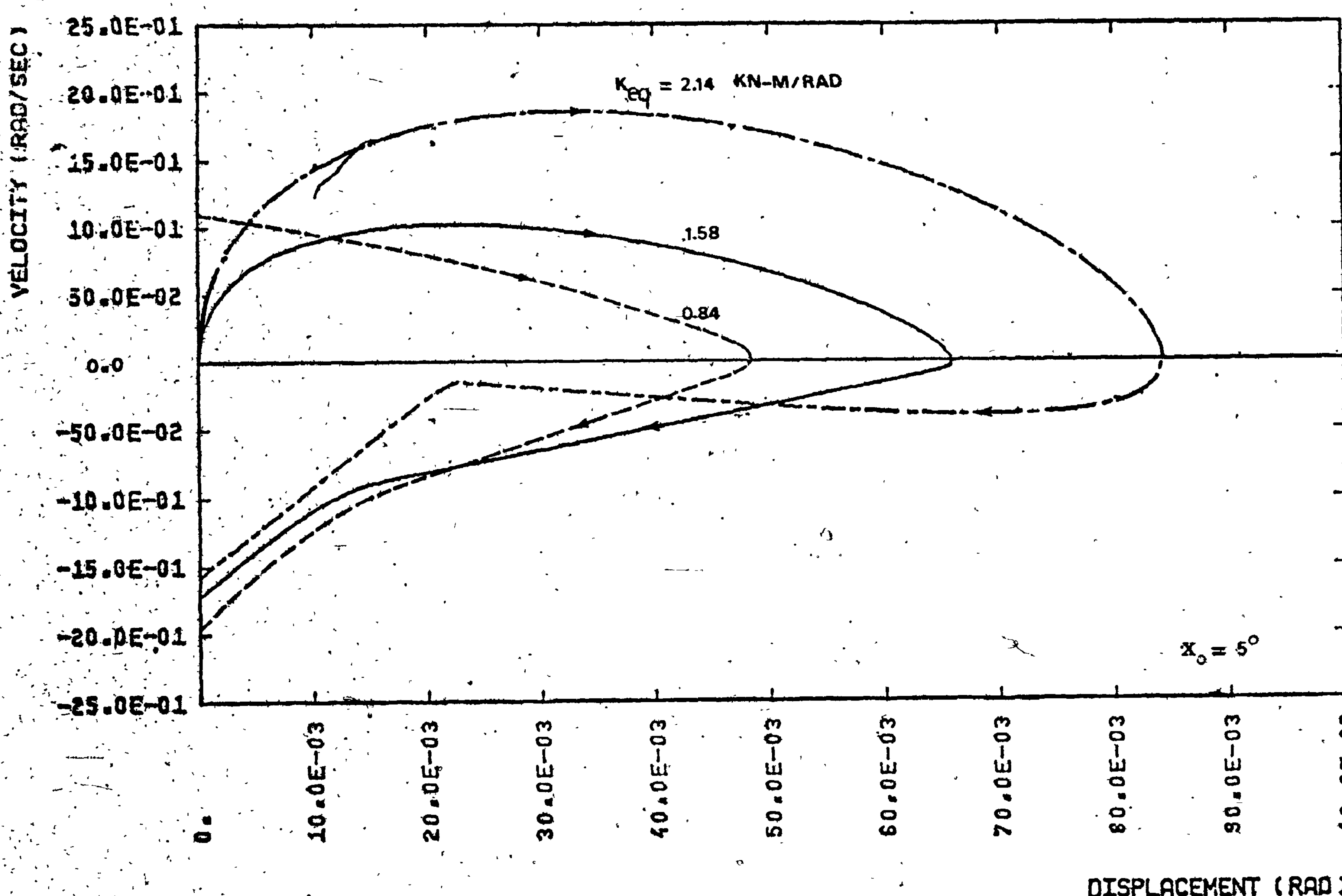

Figure 3.12(b). Phase Plane Plot of the Valve for Different Values of Spring Stiffness.

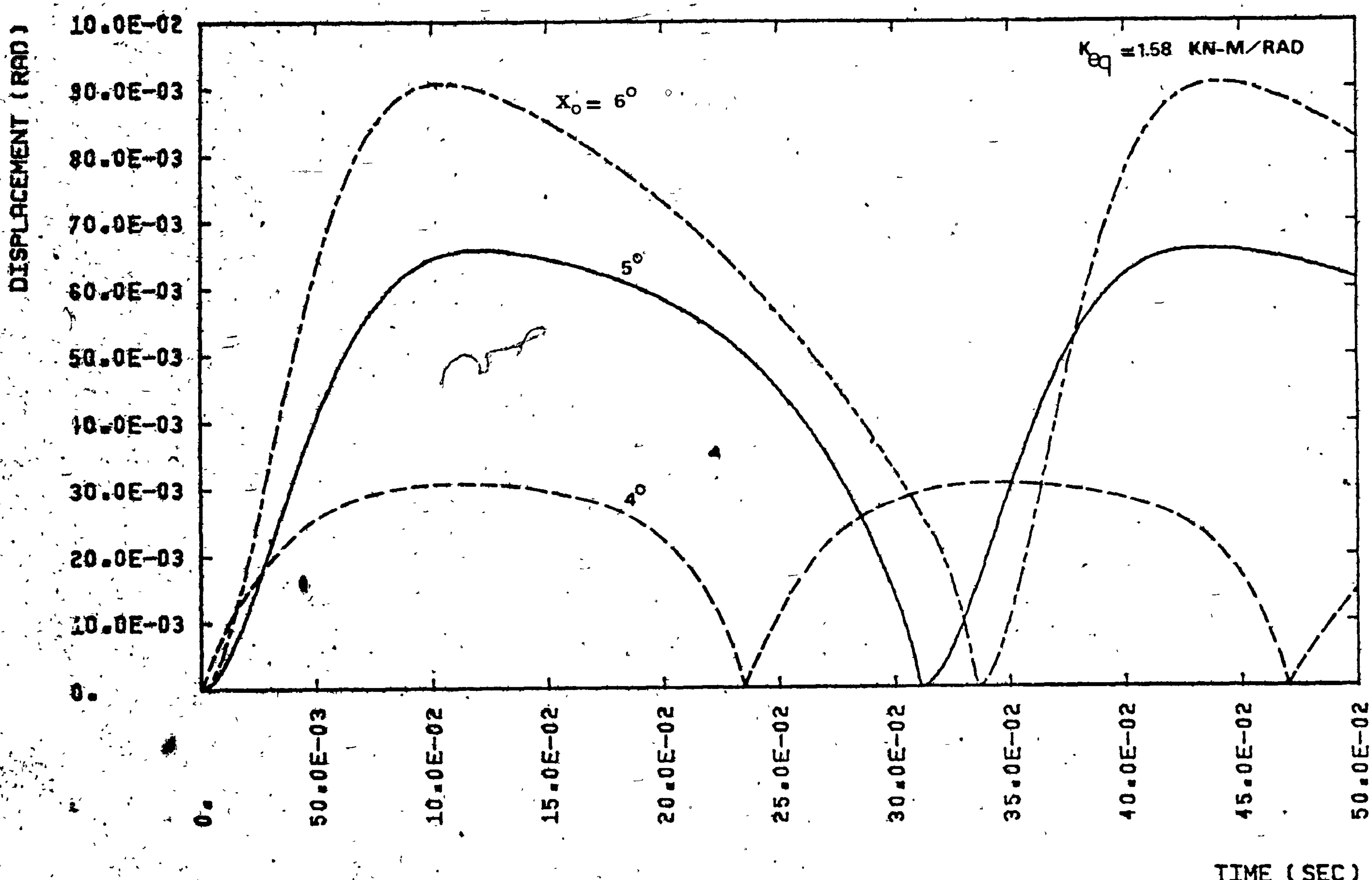

Figure 3.12(c) Effect of Initial Setting Angle on the Valve's Dynamic Behaviour.

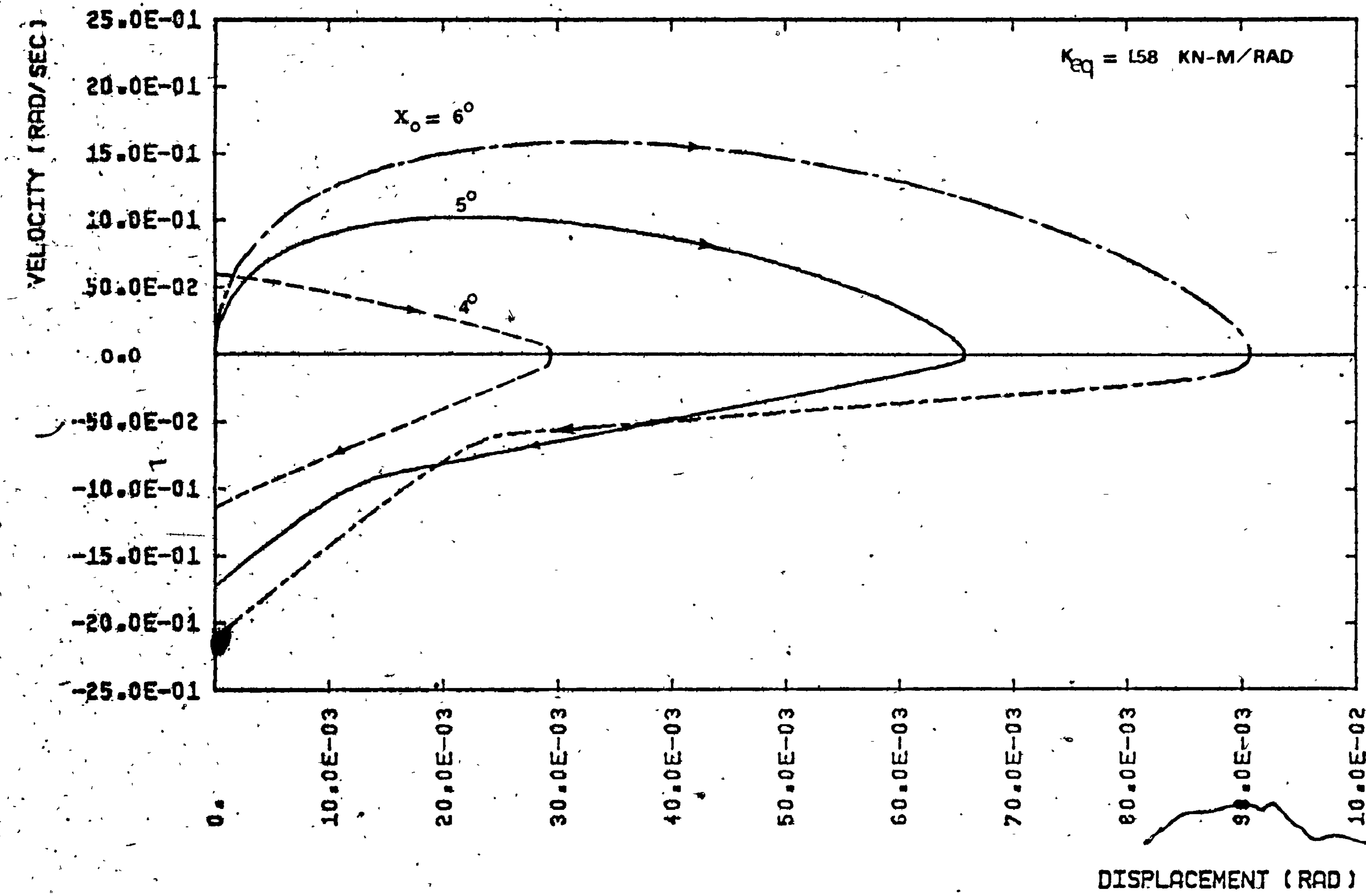

Figure 3.12(d). Phase Plane Plot of the Valve for Different Initial Setting Angles.

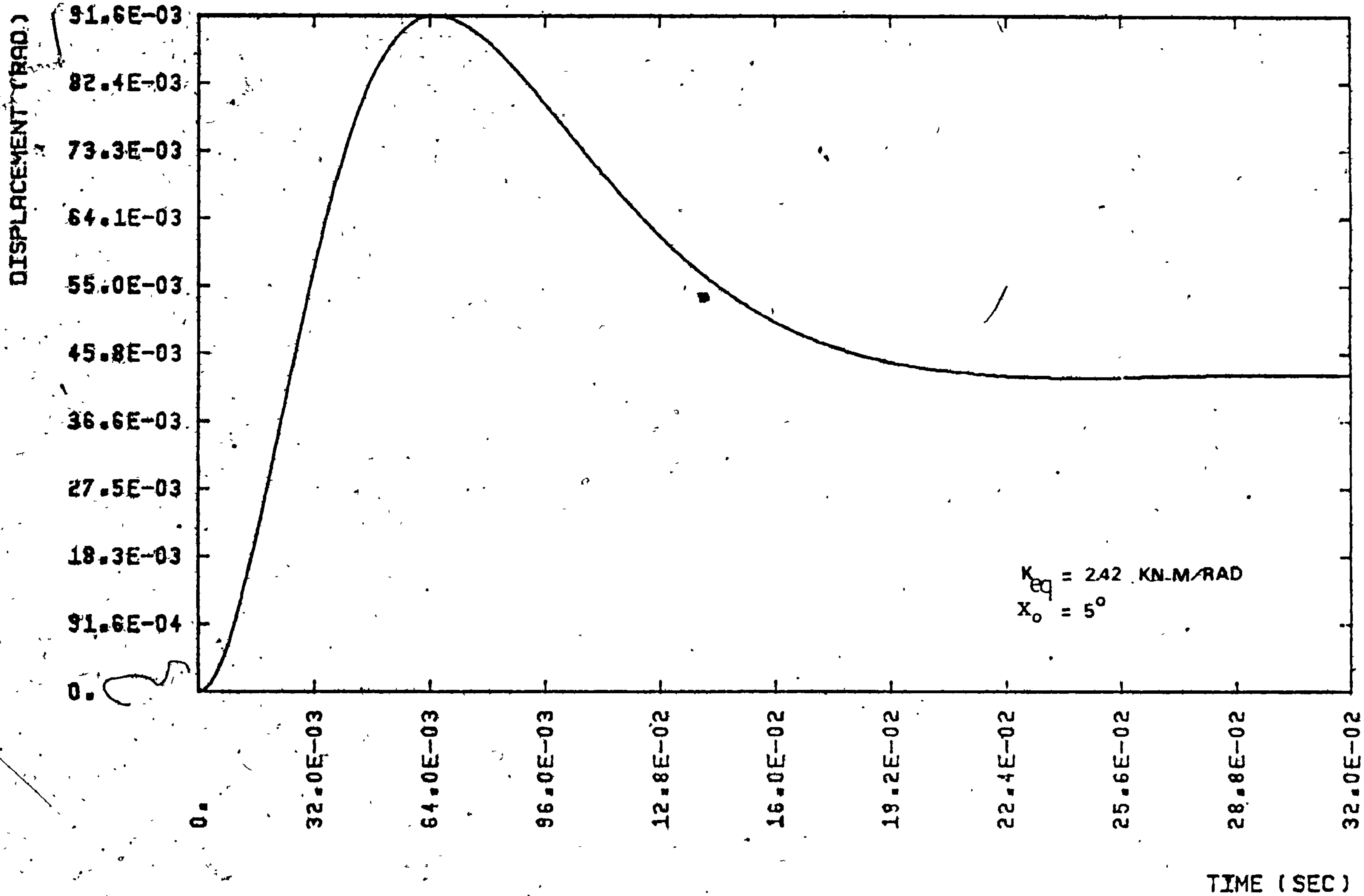

Figure 3.13(a). Transient Response; the Valve Opens and Stays Open.

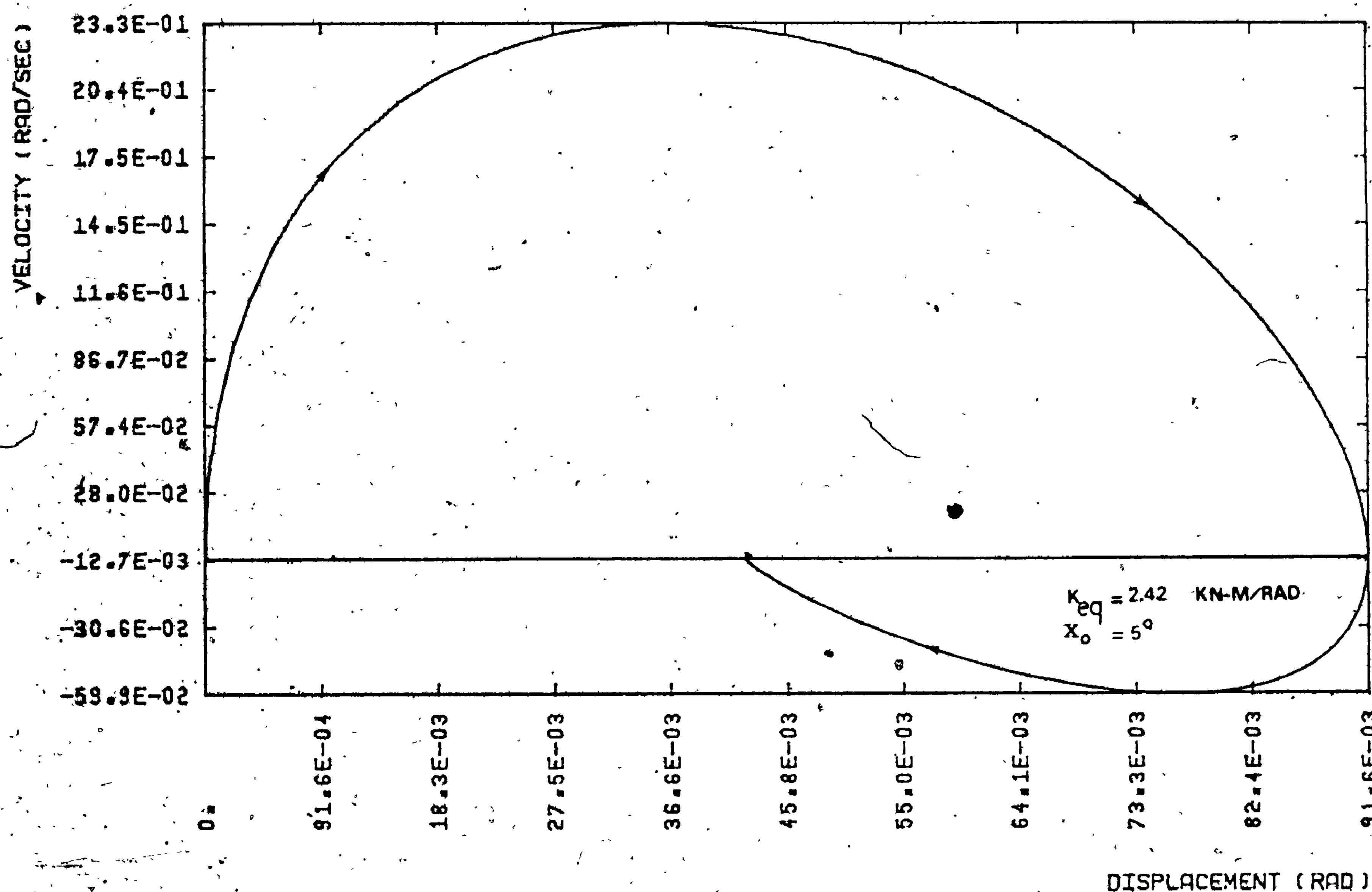

Figure 3.13(b). Phase Plane Plot; the Valve Opens and Stays Open.

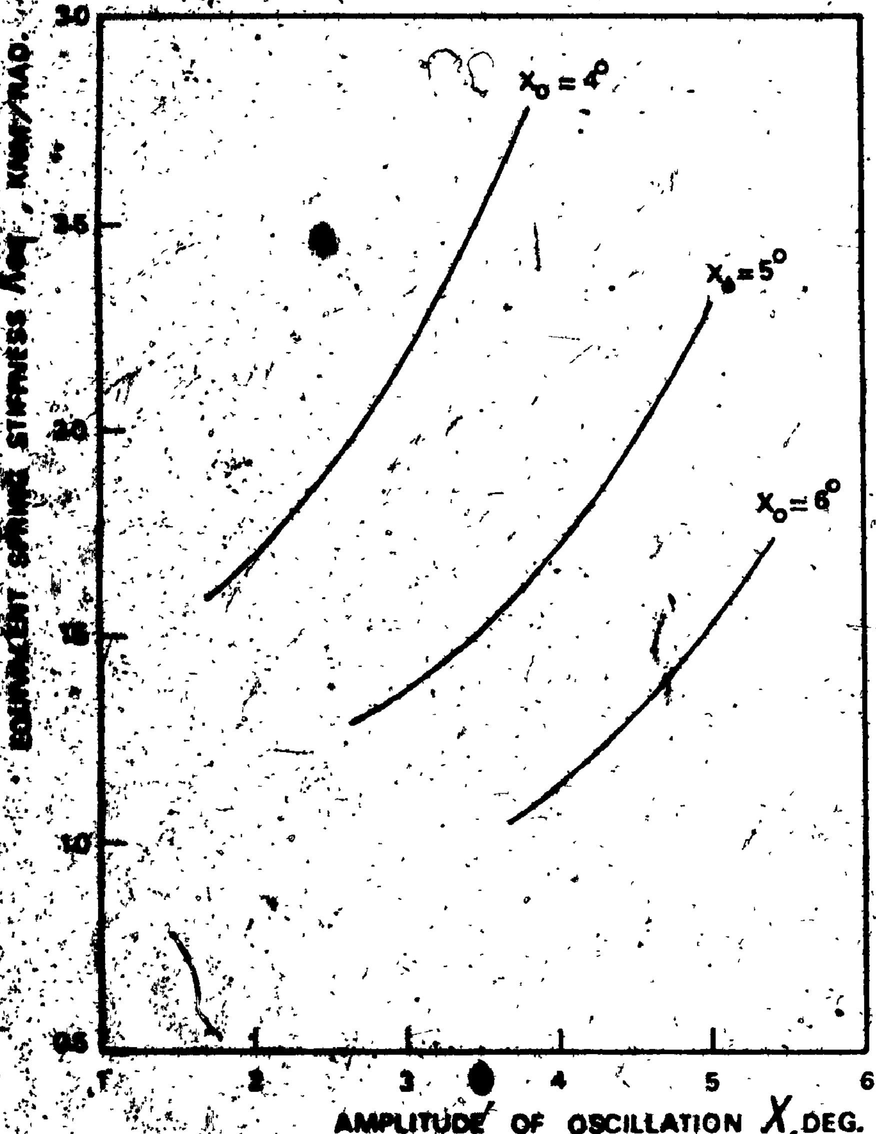

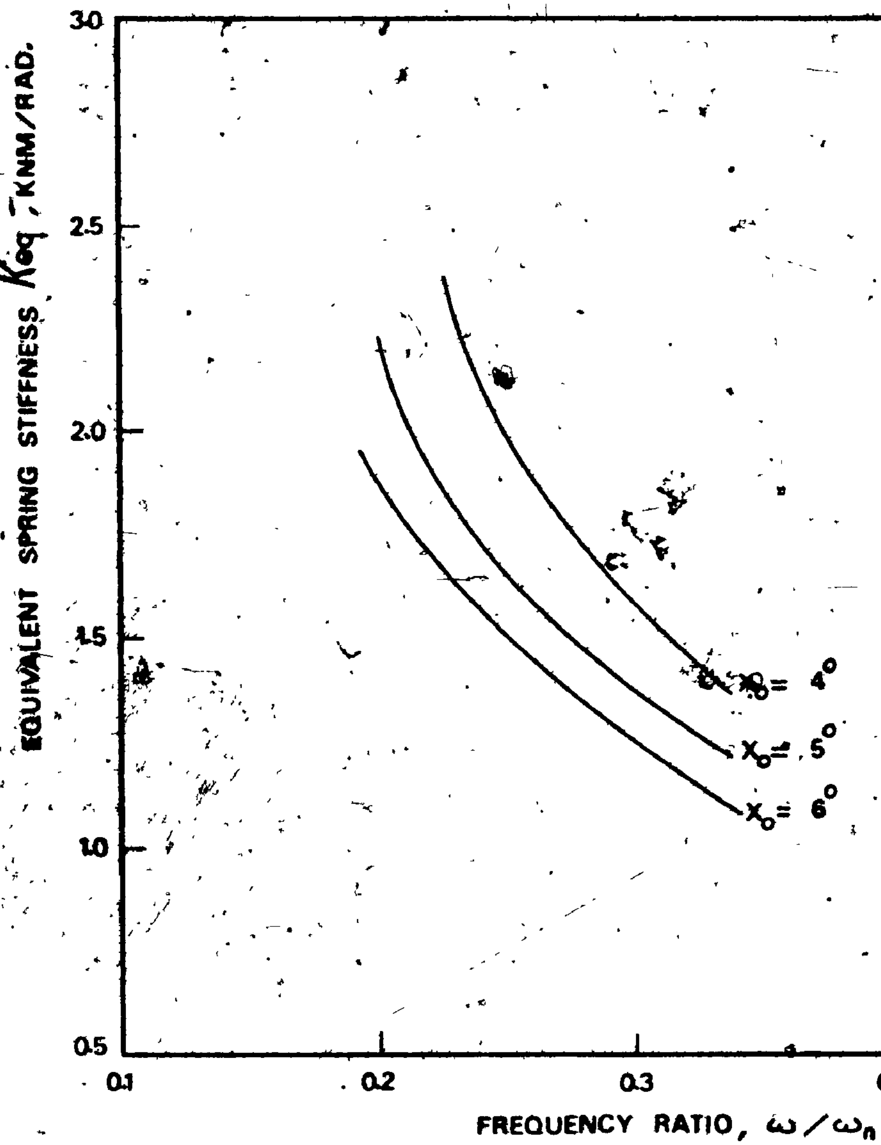

RESULTS OF SEMI-EMPIRICAL MODEL

Figure 3.14. Amplitude of Oscillation vs Equivalent Spring Stiffness.

Figure 3.15. Frequency Ratio vs Equivalent Spring Stiffness.

for a constant available hydrostatic head the amplitude of vibration of the valve increases while the frequency decreases as spring stiffness or initial setting angle increases.

The piece-wise linear approximation of the hydrodynamic load gives rise to a displacement dependent hydrodynamic force. This component of the hydrodynamic load represents the fluid-elastic interaction during the vibration cycle. From equation 3.7, the effective system stiffness, K, becomes:

$$K = K_{eq} - C_i R_o S \alpha_j , \qquad j = 1,\ 2,\ \text{and } 3 \qquad 3.8$$

Since the slope of the linear approximation of the hydrodynamic load is greater during closing than that during opening ($\alpha_1 > \alpha_3$), the effective system stiffness is greater during the opening than during the closing part of the cycle. This explains the phenomenon of rapid opening and slow closing for large amplitude valve oscillations. For small amplitudes, the flow does not have the chance to become well established. Hence, the difference in effective system stiffness between opening and closing is smaller and the limit cycle more nearly approximates a simple harmonic motion.

3.4.4 Conclusion

A semi-empirical model of check valve self-excited vibrations has been derived in order to understand the effect of a displacement dependent hydrodynamic load component. A mathematical expression for the hydrodynamic load is obtained in the form of piece-wise linear approximation which results in a displacement dependent hydrodynamic load component.

The main features of the model results are:

1) The valve motion is not of a simple harmonic nature; the opening portion of each cycle is more rapid than the closing portion.

2) The self-excited vibration frequencies are well below the natural frequencies.

3) The effect of an increase in stiffness is the opposite of that normally expected. Increasing the initial setting angle of opening (no load setting) has the same effect as increasing stiffness.

These features of the results show that the gross behaviour of the model is qualitatively the same as the experimental observations. Hence, the existence of a displacement dependent component is essential for hydrodynamic load modelling.

3.5 Derivation of the General Model

3.5.1 Introduction and Assumptions

In the previous sections it has been shown that a negatively damped simple harmonic oscillator must be ruled out as a possible mechanism, since it does not match the experimental observations. In addition, the valve motion is not of a simple harmonic nature.

On the other hand, the development of a simple semi-empirical model with a displacement dependent hydrodynamic load showed all the essential features of the observed limit cycle oscillations. This displacement dependent (or fluid-elastic) component may decrease the effective system stiffness, in particular during the closing part of the cycle. Hence, an increase in the spring stiffness results in a decrease in frequency of oscillation.

While the agreement between the above model and the experiments is encouraging, the lack of a fundamental basis for the model renders it rather unsatisfactory. Hence, further research was carried out to develop a model from first principles.

Since the model is intended to incorporate a general expression for fluid discharge in its simplest form, it is assumed that:

a) The fluid in the system is incompressible.

b) The system analysis is based on a one-dimensional flow.

c) The velocity and pressure of the fluid are uniform over a transverse cross-section of the conduit.

d) Waterhammer pressure waves and cavitation which may occur in the system have no dominant effect on the stability (11).

e) Pressure fluctuations due to vortex shedding are negligible compared with the hydrostatic and fluid inertial pressure.

f) The fluid control device (valve, seal, or gate) moves in a direction normal to the flow direction and hence, the pumping action can be neglected. For check valves which move in the direction of flow, the flow is basically around the valve plate and any pumping action which exists is neglected.

g) Although the added mass effect depends on the relative position of the moving parts with respect to the confining surfaces and perhaps on the frequency of oscillation, it is taken as a constant independent of frequency and amplitude of vibration.

h) System losses are assumed to be turbulent.

3.5.2 Fluid Discharge During Vibrations

Figure 3.16 shows a diagrammatic arrangement of a hydraulic control element (valve, gate, or seal) in a conduit of varying cross-section. Since the fluid is assumed to be incompressible, Bernoulli's equation for unsteady flow can be applied.

If Bernoulli's equation is applied at points 1 and 2, the following equation results:

$$\frac{P_1}{\sigma} + \frac{v_1^2}{2g} = \frac{P_2}{\sigma} + \frac{v_2^2}{2g} + h_{f_{12}} + I_{12}\frac{dq}{dt} \qquad 3.10$$

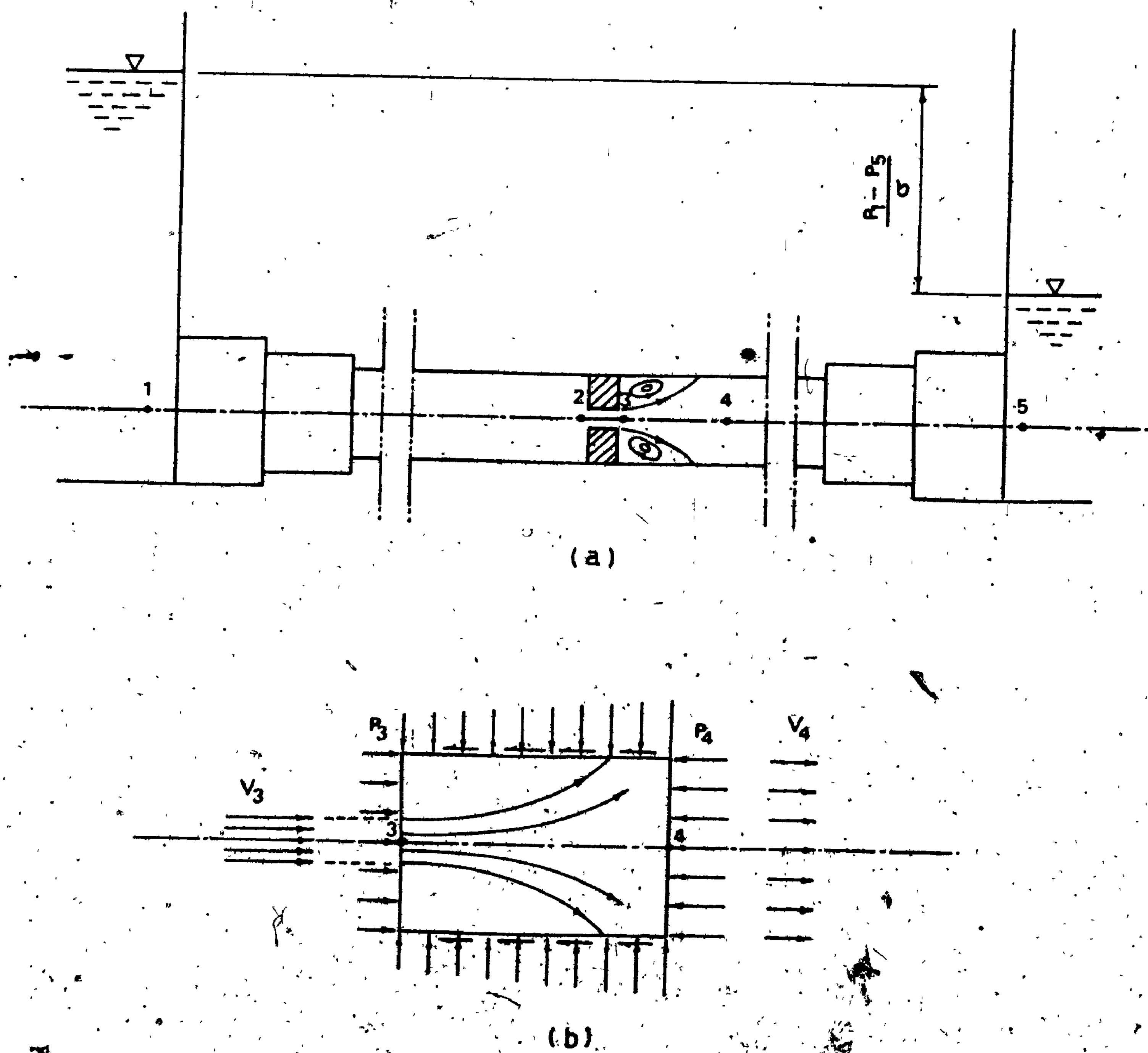

Figure 3.16. Diagrammatic Arrangement of a Hydraulic Control Device in a Conduit of Varying Cross-section.

where:

P_i is local static pressure at section i;

v_i is mean fluid velocity at section i;

h_{fij} represents the flow losses between the two sections i and j due to friction, entrance, sudden flow area changes and other minor losses;

I_{ij} is the fluid inertance between the two sections i and j; and

q is the fluid flow rate.

Also between sections 2 and 3 gives:

$$\frac{P_2}{\sigma} + \frac{v_2^2}{2g} = \frac{P_3}{\sigma} + \frac{v_c^2}{2g} + h_{f_{23}} + I_{23}\frac{dq}{dt} \qquad 3.11$$

where v_c is the velocity at the vena contracta through the control element which has flow area a_c, contraction coefficient c_c, and velocity coefficient c_v.

Between sections 3 and 4 the jet is diffused transversely until it completely fills the downstream pipe. As the flow expands in the downstream direction, the pressure increases to supply the retarding force necessary to decrease the momentum flux. Bernoulli's equation between these two sections gives:

$$\frac{P_3}{\sigma} + \frac{v_c^2}{2g} = \frac{P_4}{\sigma} + \frac{v_4^2}{2g} + h_{f_{34}} + I_{34}\frac{dq}{dt} \qquad 3.12$$

Finally between sections 4 and 5 results in:

$$\frac{P_4}{\sigma} + \frac{v_4^2}{2g} = \frac{P_5}{\sigma} + \frac{v_5^2}{2g} + h_{f_{45}} + I_{45}\frac{dq}{dt} \qquad 3.13$$

The continuity equation is

$$q = a_2 v_2 = c_c a_c v_c \quad 3.14$$

From equations 3.11 and 3.14

$$v_c^2 = c_v^2 \frac{2g}{\lambda} \left[\frac{p_2 - p_3}{\sigma} - I_{23} \frac{dq}{dt} \right] \quad 3.15.a$$

where

$$\lambda = 1 - \left(\frac{c_c a_c}{a_2} \right)^2 \quad ; \text{ and} \quad 3.15.b$$

a_i is the cross-sectional area of the conduit at section i.

Equations 3.10, 3.12, and 3.13 can be combined together in the form of:

$$\frac{p_2 - p_3}{\sigma} = \frac{p_1 - p_5}{\sigma} - (I_{12} + I_{34} + I_{45}) \frac{dq}{dt} - (h_{f_{12}} + h_{f_{34}} + h_{f_{45}}) - \frac{1}{2g}(v_2^2 - v_c^2) \quad 3.16$$

Substituting into equation 3.15 gives the following:

$$v_c^2 = c_v^2 \frac{2g}{\lambda} \left[\frac{p_1 - p_5}{\sigma} - h_f - \frac{1}{2g}(v_2^2 - v_c^2) - I \frac{dq}{dt} \right] \quad 3.17.a$$

where

$$h_f = h_{f_{12}} + h_{f_{34}} + h_{f_{45}} ; \quad 3.17.b$$

$$I = I_{12} + I_{23} + I_{34} + I_{45} ; \quad 3.17.c$$

$$v_1 = v_5 = 0$$

The head loss due to the sudden expansion can be estimated analytically by applying the momentum equation. It is useful to imagine a control volume enclosing the fluid just downstream of the control device. This control volume is shown separately in Figure 3.16(b) with one end (3) at the entrance to the large conduit and the other end (4) far enough downstream to be in a region of parallel flow. Note that two regions may be specified in the control volume – one which appears as a highly irregular flow and the other a region of reasonably smooth flow. Because of the high turbulence and mixing action in the pocket of fluid there is little recovery of pressure from the kinetic energy of the fluid entering from the main stream. Instead, the kinetic energy is dissipated into internal energy and heat transfer. The pressure in the pocket, thus tends to remain equal to the low pressure P_3 at the point of separation (33).

If shear stresses are neglected, the momentum equation for the above control volume becomes:

$$P_3a_4 - P_4a_4 = \rho a_4v_4^2 - \rho c_c a_c v_c^2 + \sigma a_4 I_{34} \frac{dq}{dt} \quad 3.18$$

Upon using the momentum equation (3.18), Bernoulli's equation (3.12), and the continuity equation (3.14), the solution for $h_{f_{34}}$ is:

$$h_{f_{34}} = \frac{v_4^2}{2g}\left(1 - \frac{a_4}{c_c a_c}\right)^2 \quad 3.19$$

Since flow losses are proportional to velocity head, the losses and velocity heads can be combined together in the form of:

$$h_f + \frac{1}{2g}(v_2^2 - v_c^2) = \frac{\psi}{a_2^2}\frac{q^2}{2g} \quad 3.20$$

where ψ is a factor which accounts for flow losses and velocity heads referring to section 2 of the conduit, i.e. the friction factor of an equivalent pipe of cross-sectional area a_2, average flow velocity v_2, and characterized by the same losses and velocity head as the actual system (31). Hence ψ can be written as:

$$\psi = 1 - \left(\frac{a_2}{c_c a_c}\right) + a_2^2 \sum_i \frac{\psi_i}{a_i^2} \qquad 3.21$$

where

ψ_i is the loss factor for conduit i whose cross-sectional area is a_i.

Similarly, the inertia head can be replaced by an equivalent term:

$$I \frac{dq}{dt} = \frac{L^*}{a_2 g} \frac{dq}{dt} \qquad 3.22$$

L^* is the length of the pipe of constant cross-sectional area a_2, that has the same inertia effect as the actual system. If the conduit consists of sections of different cross-section a_i and length L_i, then the equivalent length (19) L^* is

$$L^* = a_2 \sum_i \frac{L_i}{a_i} \qquad 3.23$$

Substituting equations 3.14, 3.20, and 3.22 into 3.17(a) gives:

$$q^2 = C_d^2 \frac{a_c^2}{\lambda} \left[2g \frac{\Delta P}{\sigma} - \frac{\psi}{a_2^2} q^2 - \frac{2L^*}{a_2} \frac{dq}{dt}\right] \qquad 3.24$$

where

c_d is the discharge coefficient ($c_c c_v$);

ΔP is the total hydrostatic pressure drop across the system.

Equation 3.24 is a nonlinear first order differential equation which represents the fluid discharge through the control element as a function of total static pressure drop across the system, loss factor, fluid inertia factor, dynamic discharge coefficient, and degree of opening of the control element.

3.5.3 Elastic Structure Modelling

The hydraulic control device is modelled as an elastic single degree of freedom system. The opening gap of the control device, being measured in the direction of opening, is taken as the generalized co-ordinate. Hence, the equation of motion of the vibrating body in a general form is:

$$M\ddot{x} + C\dot{x} + K(x - x_0) + F = 0 \qquad 3.25$$

For certain cases this equation, owing to the type of control device, may be regarded as an equation of force balance. In cases where the control element rotates, it represents an equation of moment balance. The generalized co-ordinate x may be either a translational or a rotational displacement of the system. It follows that M, C, and K may represent reduced mass*, damping force coefficient‡, and

---

* accounting for the so-called "virtual mass".

‡ accounting for the hydrodynamic damping.

linear spring stiffness or reduced moment of inertia, damping torque coefficient, and torsional stiffness depending on whether the generalized co-ordinate is a translation or a rotation respectively. This assumption helps in generalizing the present probem for further analysis.

The hydrodynamic load F in equation 3.25, not including added mass (or inertia) and damping effects, is given by the integral of the pressure difference across the control element over its area.

$$F = \int_S \Delta p \, ds$$

The pressure difference, Δp, is the result of four different components, as described in section 3.3; these components briefly are:

a) total static pressure drop across the system, $\Delta P = P_1 - P_5$;

b) inertia pressure of the fluid, $I\frac{dq}{dt}$;

c) local high flow velocity effects; and

d) system losses which are assumed to be turbulent.

For simplicity, the hydrodynamic load is replaced by an average pressure difference acting upon the control element whose area is S. Hence, the differential equation of motion, equation 3.25, becomes:

$$M\ddot{x} + C\dot{x} + K(x-x_o) + C_1S[\Delta P \pm \frac{\sigma}{2ga_2^2} q^2 - \frac{L^*\sigma}{ga_2} \frac{dq}{dt}] = 0 \qquad 3.26$$

and the fluid discharge through the control element is given by:

$$q^2 = C_d^2 \frac{a_c^2}{\lambda} [2g \frac{\Delta P}{\sigma} - \frac{\psi}{a_2^2} q^2 - \frac{2L^*}{a_2} \frac{dq}{dt}] \qquad 3.24$$

In the equation 3.26 C_i is a coefficient resulting from the integration process over the surface of the vibrating body. This coefficient depends on the type and geometry of the control element under consideration (valve, seal, or gate). For example, in the case of seals, which have a very complicated geometry, this coefficient reduces the elementary pressures to a force acting at an effective centre of effort.

The system dynamic behaviour is governed by equations 3.24 and 3.26 which are coupled, non-linear differential equations. A non-dimensional form of these equations would assist in generalizing the present problem. In addition, the results can also be presented in a more compact and meaningful way.

3.5.4 Non-Dimensional Analysis

Before non-dimensionalizing equations 3.24 and 3.26 it is necessary to introduce the reference quantities K_r, ω_r, d, Δp_r, and q_r. The reference frequency, ω_r, is related to the reference stiffness, K_r, by:

$$\omega_r^2 = K_r/M \qquad 3.27(a)$$

Any characteristic dimension of flow control device can be taken as the reference dimension, d, which should have the same units as the generalized displacement, x. It may be an angle of rotation when equation 3.26 represents a moment balance (check valves or seals); in other cases, when the governing equation is a force balance (gates), it may represent a characteristic length. The opposite is true for C_i, it may be either the moment arm for the case of moment balance or a dimensionless coefficient equal to unity for the case of force balance. According to these definitions for C_i and d, the product $(C_i d)$ is in length-units for both cases. Then, the reference pressure difference, Δp_r, is defined as:

$$\Delta p_r = \frac{1}{2} \rho (\omega_r C_i d)^2 \qquad 3.27(b)$$

and the reference flow rate, q_r, is:

$$q_r = a_2 \sqrt{2g \frac{\Delta p_r}{\sigma}}$$

$$= a_2 \omega_r C_i d \qquad 3.27(c)$$

where ρ is the fluid density.

If the width of the control device is defined by W, the flow area, a_c, becomes:

$$a_c = Wx \qquad 3.28(a)$$

when x is a linear displacement and in length-units.

If x represents an angle of rotation, equation 3.28(a) becomes:

$$a_c = Sx \qquad 3.28(b)$$

Then, the dimensionless quantities are:

discharge	$\bar{q}$	=	q/q_r	(a)	
pressure	$\Delta\bar{P}$	=	$\Delta P/\Delta P_r$	(b)	
stiffness	$\bar{K}$	=	K/K_r	(c)	3.29
displacement	$\bar{x}$	=	x/d	(d)	
time	τ	=	$\omega_r t$	(e)	

From equations 3.27, 3.28, and 3.29, the system equations 3.24 and 3.26 become:

$$\frac{d^2\bar{x}}{d\tau^2} + 2\xi\frac{d\bar{x}}{d\tau} + \bar{K}\,(\bar{x} - \beta) + \frac{1}{2}\,\mu\,[\Delta\bar{P} - \psi\bar{q}^2 - \alpha\,\frac{d\bar{q}}{d\tau}\,] = 0 \qquad 3.30$$

$$\bar{q}^2 = C_d^2\,\frac{\bar{x}^2}{\eta^2 - c_c^2\bar{x}^2}\,[\Delta\bar{P} - \psi\bar{q}^2 - \alpha\,\frac{d\bar{q}}{d\tau}\,] \qquad 3.31$$

with an inertia factor

$$\alpha = 2L^*/C_1 d \qquad 3.32(a)$$

damping factor

$$\xi = C/2M\omega_r \qquad 3.32(b)$$

initial opening factor

$$\beta = x_0/d \qquad 3.32(c)$$

and mass ratio factor

$$\mu = \frac{C_i^3\,\rho S d}{M} \qquad 3.32(d)$$

where η is either

$$\eta = a_2/Wd \qquad 3.32(e)$$

when d has the units of length, or

$$\eta = a_2/Sd \qquad 3.32(f)$$

when d is a rotation angle.

3.5.5 Parametric Studies

A simple mathematical model for hydraulic control devices has been derived from first principles. Since several parameters are introduced into the governing equations, a parametric study for these equations should be a further understanding of the different cases in which this model can be applied. These parameters are:

a) stiffness . . . . $\overline{K}$

b) initial gap opening (no load opening) . . ε

c) hydrostatic pressure difference . . . . . $\Delta\overline{P}$

d) damping . . . . ζ

e) inertia . . . . α

f) loss . . . . ψ

g) mass ratio . . . . μ

h) dynamic discharge coefficient . . . . . . C_d

Each parameter will be studied in turn while keeping the other parameters constant. The system's differential equations are solved numerically by the Runge-Kutta Method (26). The numerical values of the parameters used are noted in Appendix B.

a) Stiffness ($\overline{K}$)

The stiffness parameter is defined by the ratio of the system stiffness to the reference stiffness. The dimensionless displacement ($\overline{x}$) is plotted against the dimensionless time (τ) in Figure 3.17 (a), while the phase plane is presented in Figure 3.17 (b). Figure 3.17 (c) shows the dimensionless discharge ($\bar{q}$) against dimensionless displacement. It is clear from these figures that increasing the system stiffness causes the following:

1) The amplitude of oscillation increases while the frequency decreases. This is in contrast with the effect of increasing stiffness in free vibration and shows the same trends as observed experimentally.

2) The control device opens faster and closes slower than in cases characterized by smaller stiffness. This is attributable to the fact that the spring force is the driving force during the opening and the resisting force during the closing part of the cycle. This phenomenon is exemplified in the phase plane plot, Figure 3.17 (b), where the control device has higher velocities during opening and lower velocities during closing.

3) The area enclosed by the curve of discharge against displacement, Figure 3.17 (c), increases, and hence the energy transferred to the system per cycle increases. This results in increasing amplitude oscillations until the point at which the net energy transferred to the system is balanced by the energy dissipated by damping forces and the kinetic energy lost in slamming.

4) The maximum flow rate is increased although flow

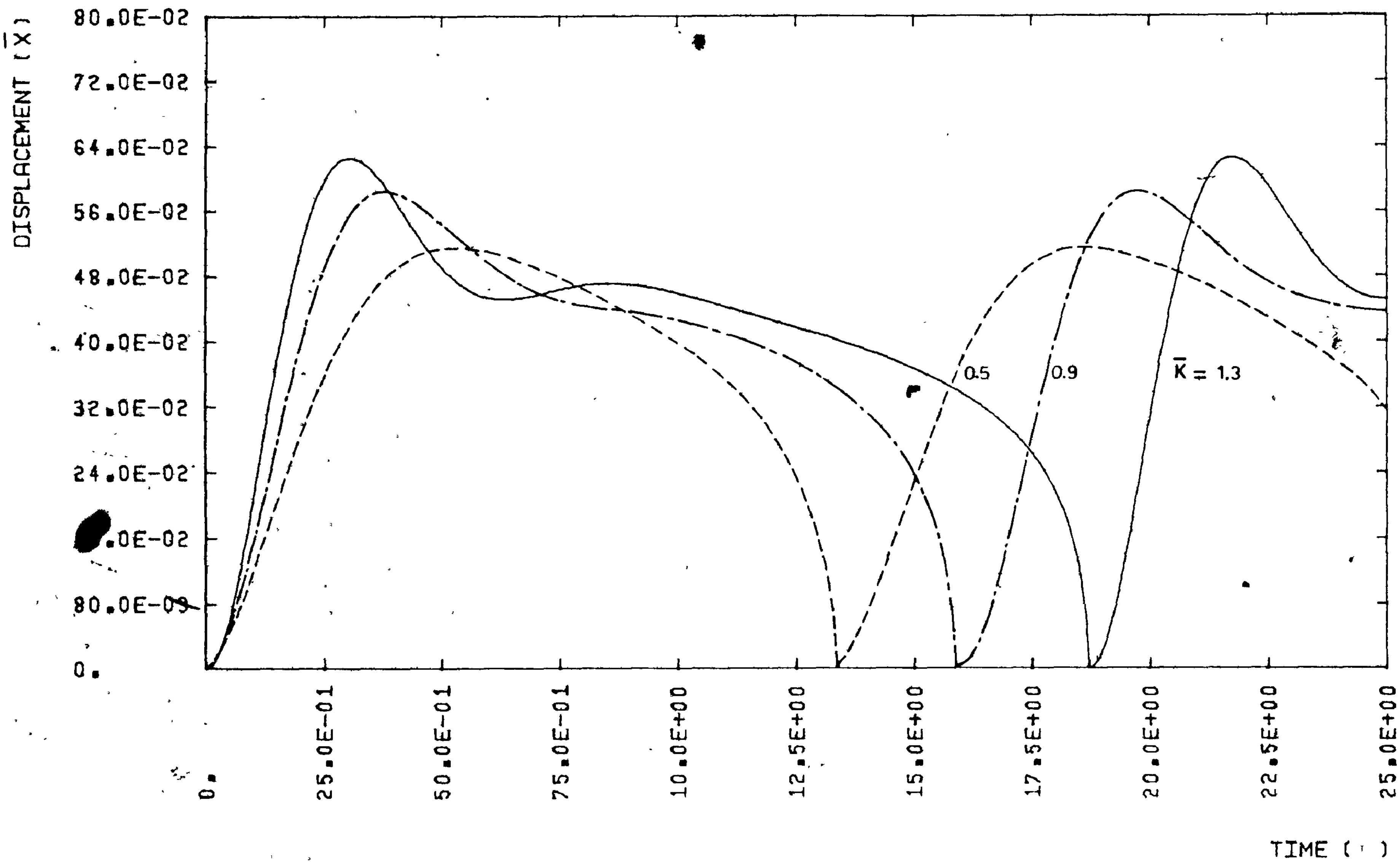

Figure 3.17(a). Parametric Results of the Model: Vibrational Response for Different Values of Stiffness Parameter.

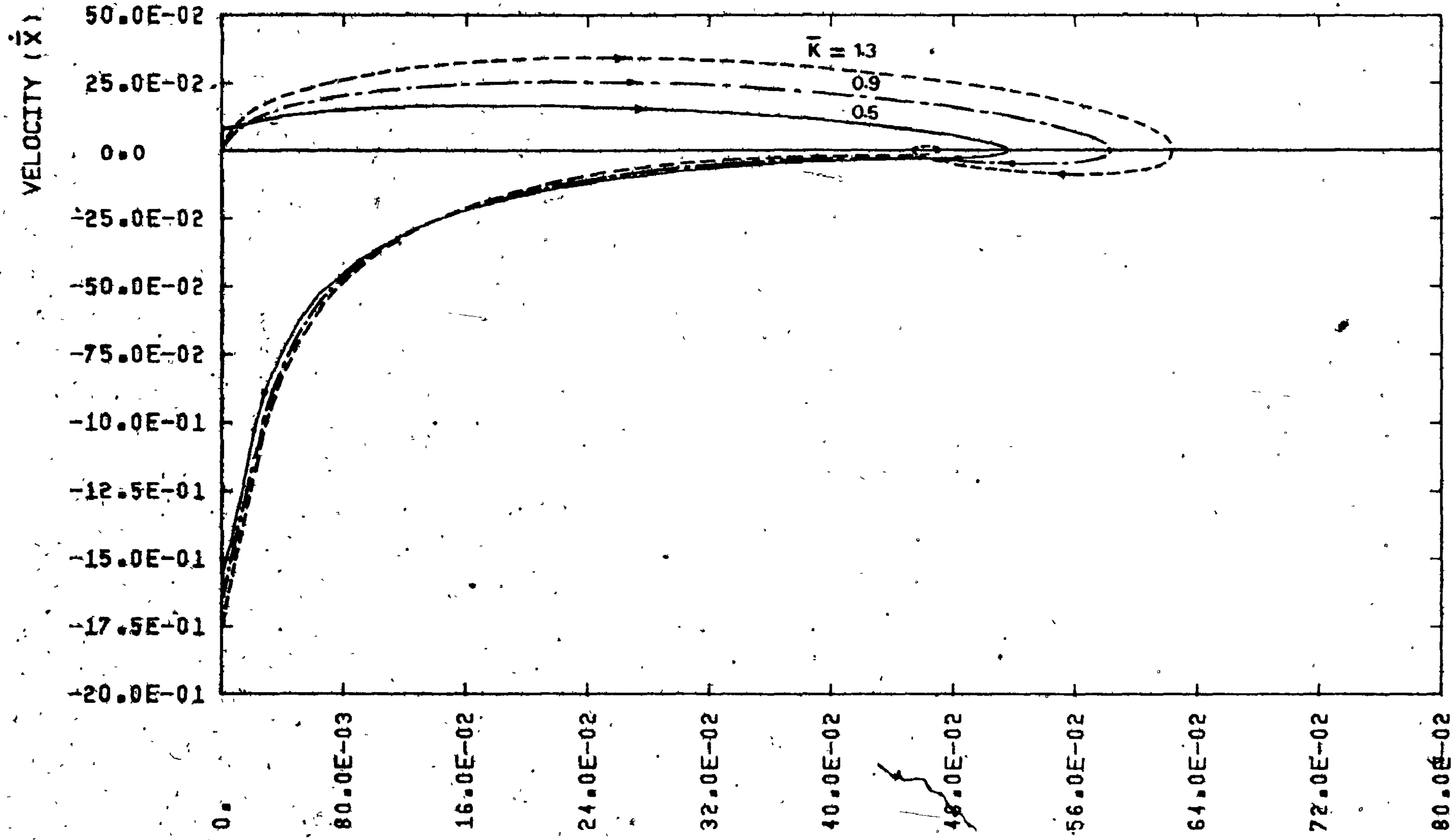

Figure 3.17(b). Parametric Results of the Model: Phase Plane Plot for Different Values of Stiffness Parameter.

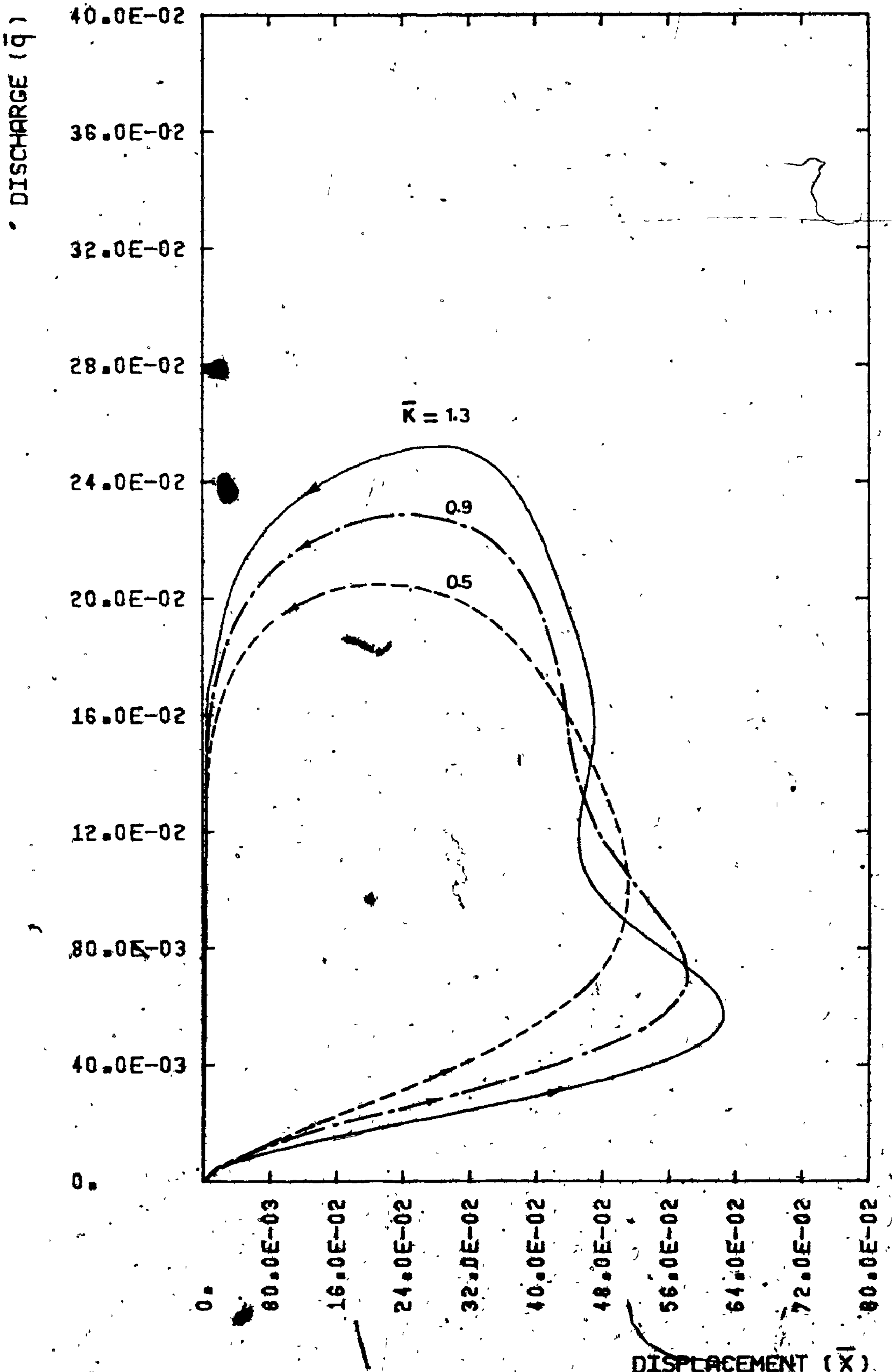

Figure 3.17(c). Parametric Results of the Model: Dimensionless Discharge vs Dimensionless Displacement for Different Values of Stiffness Parameter.

re-establishment is more delayed. This results in higher fluid inertial head in the last few degrees of the closing portion; in increased slamming velocity, and in higher values of waterhammer pressure waves subsequent to closing.

b) No Load Setting Factor (β)

Figures 3.18 show the same curves as the previous case, but the no load setting factor is taken as the variable parameter, holding the other factors constant. The effect of an increase in initial setting is similar to the effect of an increase in the system stiffness. This is illustrated by equation 3.28 where the dimensionless spring force, F_s, is:

$$F_s = \bar{K}(\bar{x} - \beta)$$
$$= -\bar{K}(\beta - \bar{x})$$

Since the dimensionless displacement, $\bar{x}$, is smaller than the parameter β over most of the cycle, an increase in the parameter β or $\bar{K}$ should have a similar effect on the results of the model.

The above figures show that the opening time of the control device is independent of the initial gap opening, Figure 3.18 (a), although an increase in the system stiffness results in a decrease in the opening time, Figure 3.17 (a). This is explained by the dependence of the natural frequency of the system on its stiffness and the fact that the control element resembles its natural response in quiescent fluid

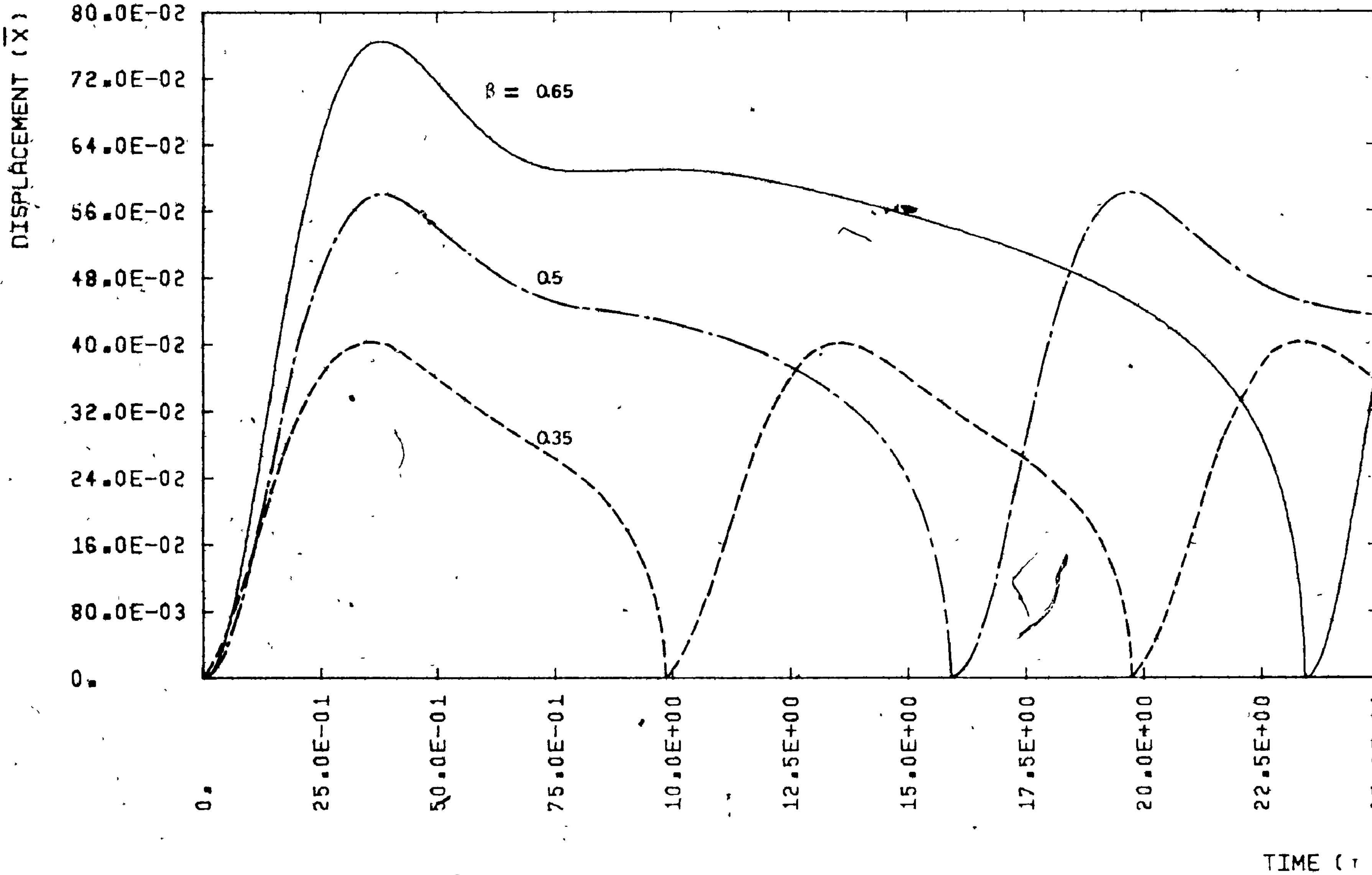

Figure 3.18(a). Parametric Results of the Model: Vibrational Response for Different Values of Initial Setting Parameter.

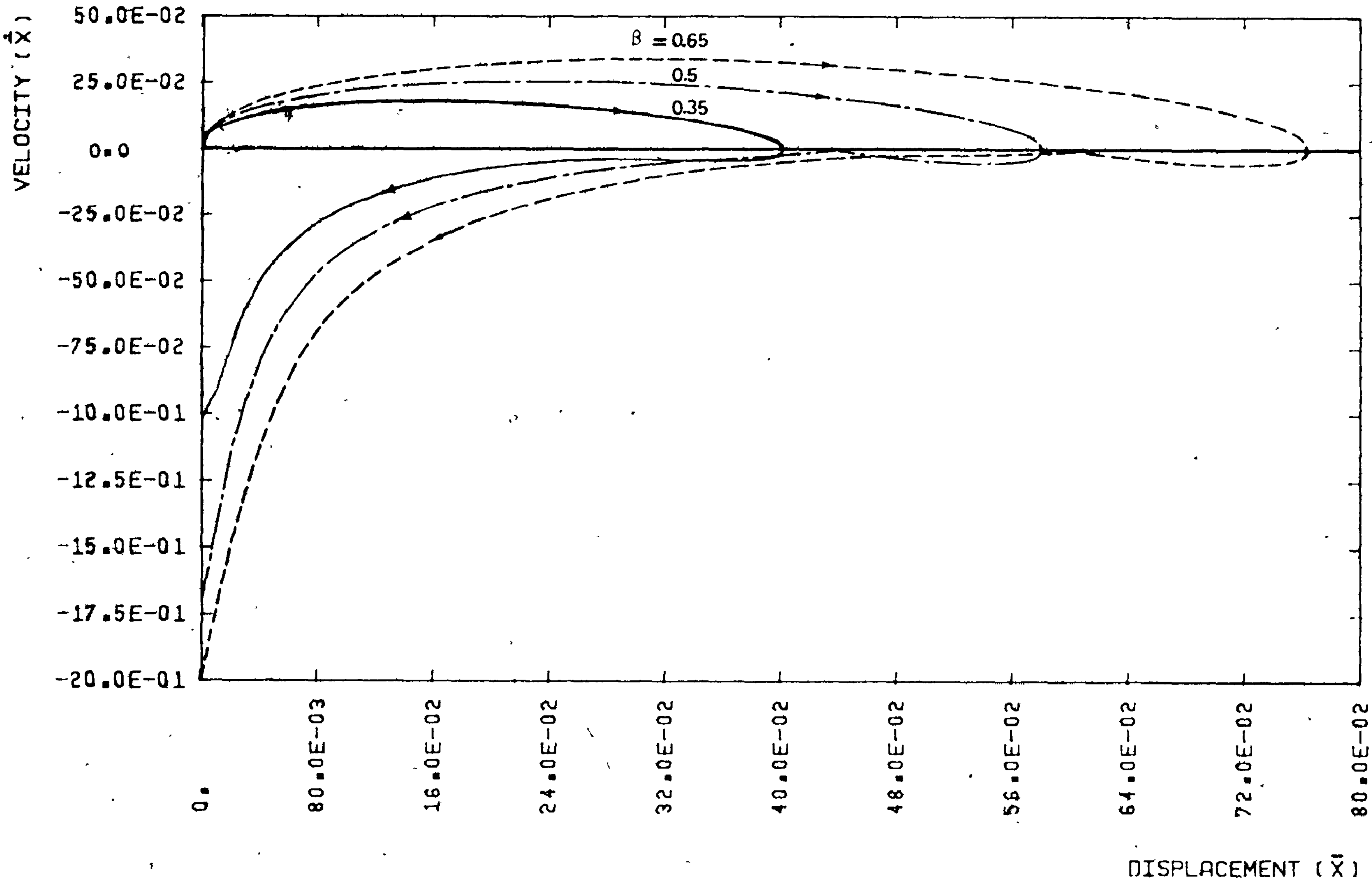

Figure 3.18(b). Parametric Results of the Model: Phase Plane Plot for Different Values of Initial Setting Parameter.

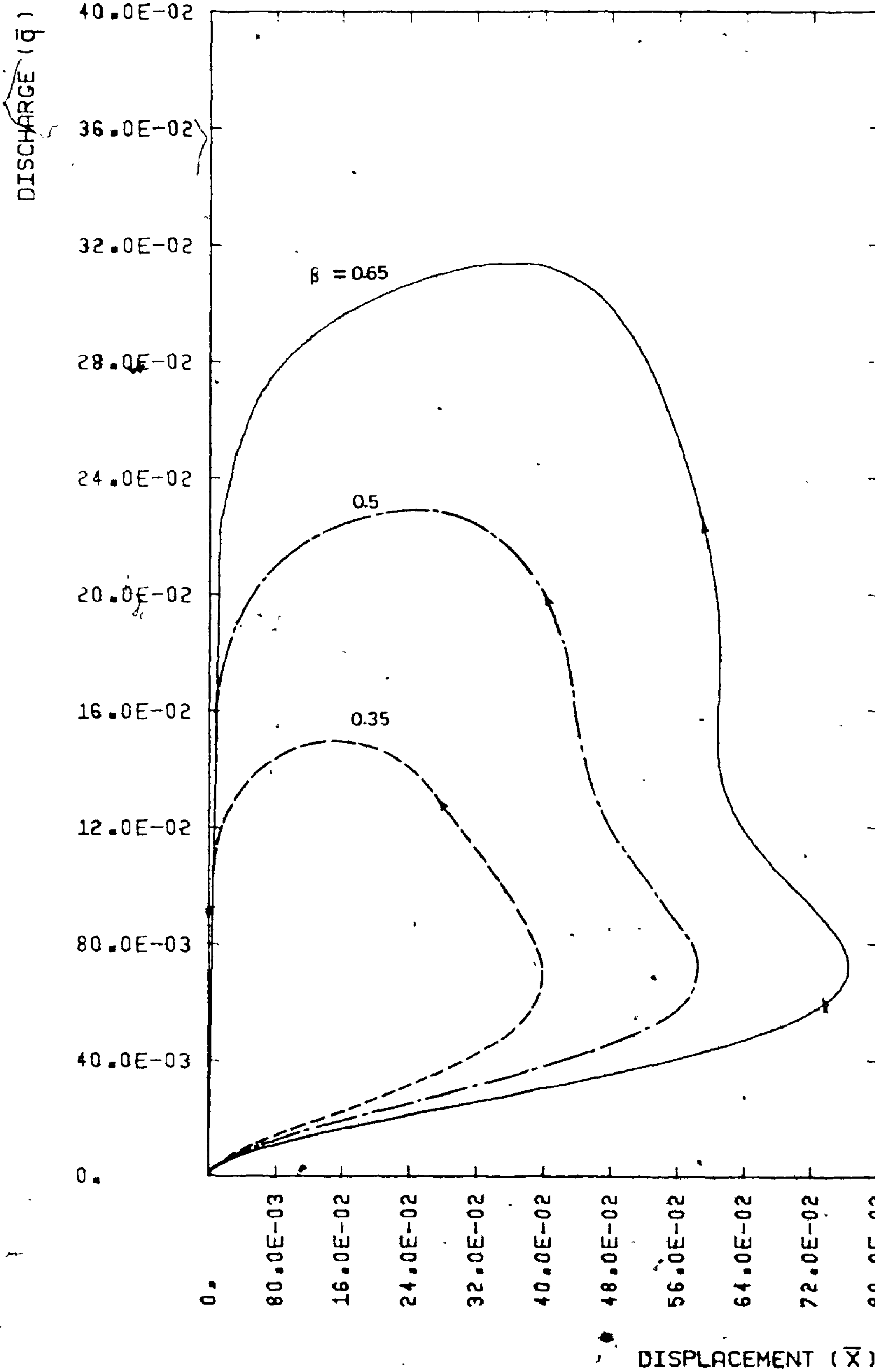

Figure 3.18(c). Parametric Results of the Model: Dimensionless Discharge vs Dimensionless Displacement for Different Values of Initial Setting Parameter.

during the opening portion of the cycle. Thus, an increase in stiffness increases the system's natural frequency, resulting in a shorter opening time. On the other hand, the system's natural frequency in quiescent fluid is independent of the initial gap opening. Hence, the opening time stays constant with different values of no load setting factor (β).

c) Hydrostatic Pressure Difference Factor ($\Delta\overline{P}$)

There is no need to carry out further parametric studies for this factor since its effect is obvious from equation 3.30. An increase in hydrostatic pressure difference should lead to a decrease in amplitude and period of oscillation, i.e. it has the opposite effect of an increase in stiffness or initial gap setting. The stability map of the check valve, Figure 3.1, shows that an increase in stiffness, initial gap setting or a decrease in hydrostatic pressure difference should have similar effect on the valve's dynamic behaviour.

d) Damping Factor (ξ)

The model's behaviour with different values of damping factor is the same as the behaviour of any mechanical system. Simply, decreasing the damping factor results in a decrease in the energy dissipated by the damping forces which in turn causes an oscillation of increasing amplitude and velocity until a balance is again achieved between energy dissipated and energy transferred to the device from the flow. Figures 3.19 show the system's behaviour for different

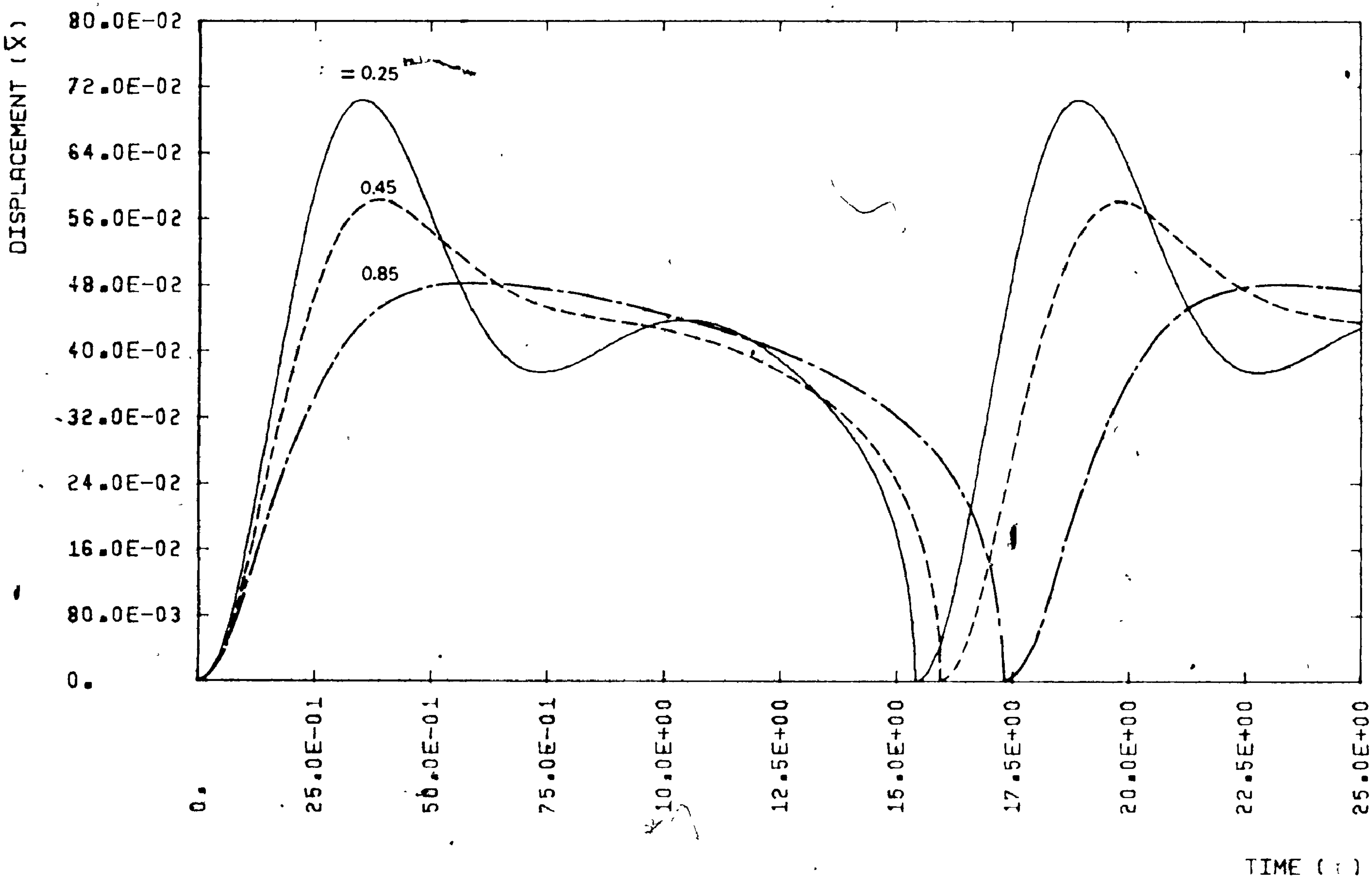

Figure 3.19(a) Parametric Results of the Model: Effect of the Damping Factor on the System's Dynamic Behaviour.

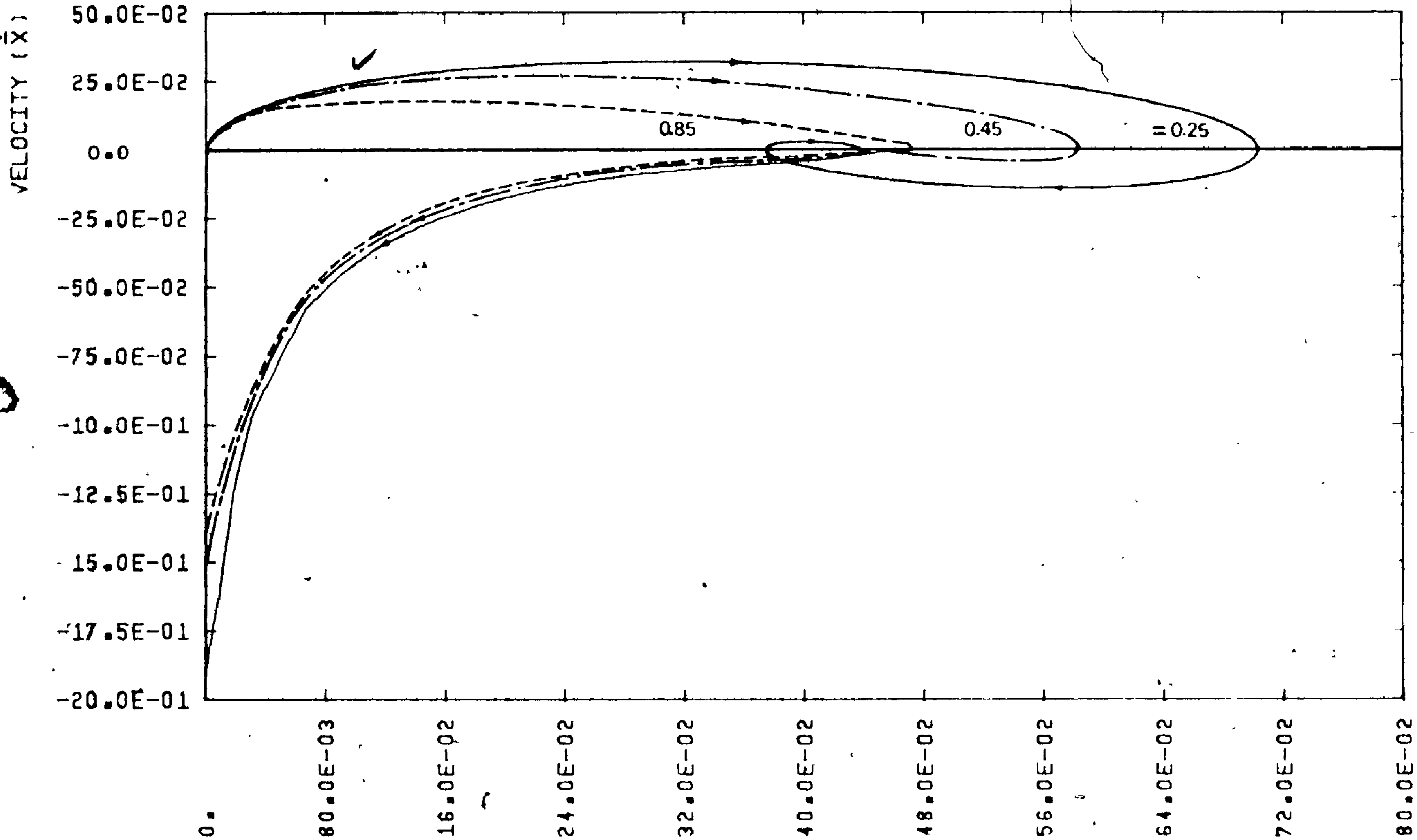

Figure 3.19(b) Parametric Results of the Model: Phase Plane Plot for Different Values of the Damping Factor.

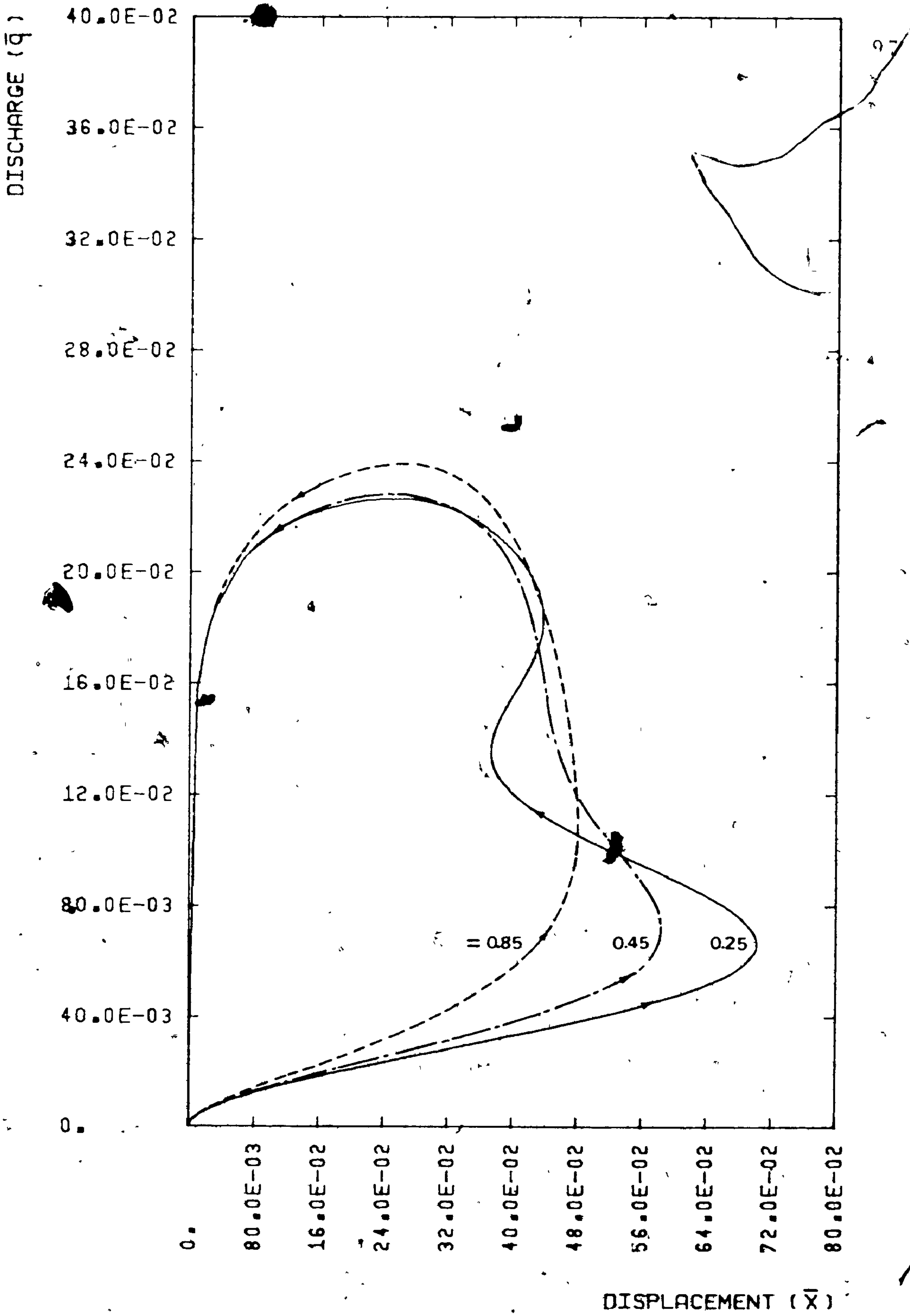

Figure 3.19(c). Parametric Results of the Model: Dimensionless Discharge vs Dimensionless Displacement for Different Values of the Damping Factor.

values of damping factor while the other factors are kept constant.

e) Inertia Factor (α)

The inertia factor has a very significant effect on the system's behaviour. As defined from equation 3.32 (a) the inertia factor is:

$$\alpha = 2L^*/C_{f1} d \qquad 3.32\ (a)$$

where

$$L^* = a_2 \sum_i \frac{L_i}{a_i}$$

The equivalent length, L*, depends on the geometric properties of the system under consideration. For a control device in a pipeline system, assuming that the upstream and downstream pipes have the same cross-sectional area, the equivalent length can be written as:

$$L^* = L_u + L_d + l_v \frac{a}{a_v}$$

where

L_u is the upstream pipe length;

L_d is the downstream pipe length;

l_v is the jet length through the control device, which has vena contracta cross-sectional area a_v; and

a is the pipe cross-sectional area.

In the case of pipelines, since the jet equivalent length is very small in comparison with total equivalent length, it can be neglected. But in the case of seal vibration, the upstream and downstream equivalent lengths are nearly zero and the jet equivalent length becomes dominant. The inertia factor in this case should be a function of displacement because the jet cross-sectional area, a_v, is a function of the gap opening and pressure difference.

For small values of inertia factor, the flow is more readily re-established. The fluid discharge becomes nearly in phase with the displacement, i.e. the maximum flow rate is reached at the maximum angle of opening, Figure 3.20 (c). At the beginning of the closing portion of the cycle, the discharge rate of change reverses rapidly. The result is an increase in the closing hydrodynamic load and hence, the closing time decreases dramatically as shown in Figure 3.20 (a).

Generally, as the inertia factor increases, a lag develops in discharge re-establishment, the vibrational wave-forms distort, and the amplitude, period of oscillations, and slamming velocity increase dramatically. The opening time of the control device remains essentially the same since the spring stiffness is unchanged. The parametric results of the model with different values of inertia factor are shown in Figure 3.20.

f) Loss Factor (ψ)

In this analysis turbulent flow is assumed to exist in the system. The loss factor includes all kinds of losses

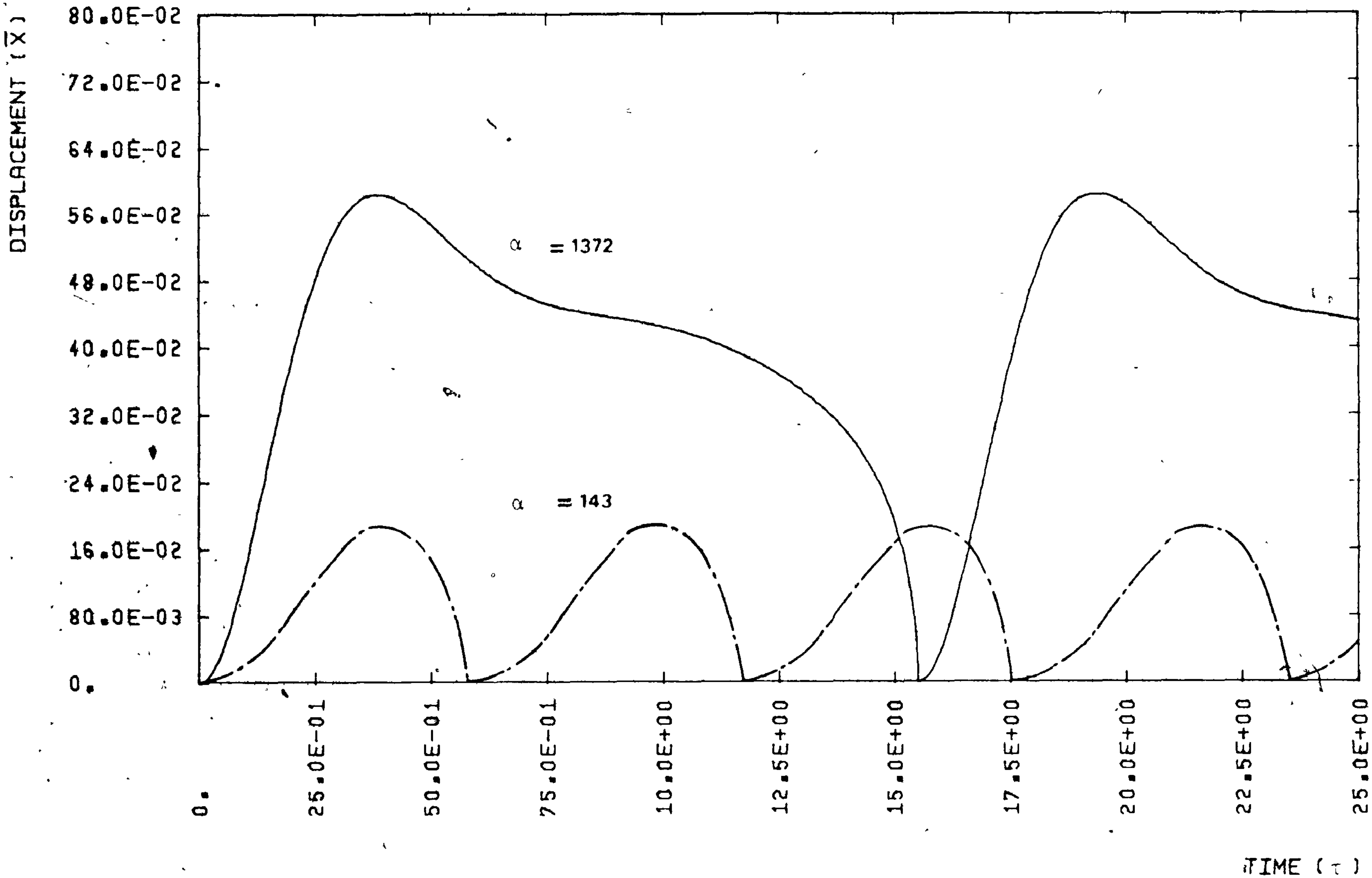

Figure 3.20(a). Parametric Results of the Model: Effect of Inertia Factor on the System's Dynamic Behaviour.

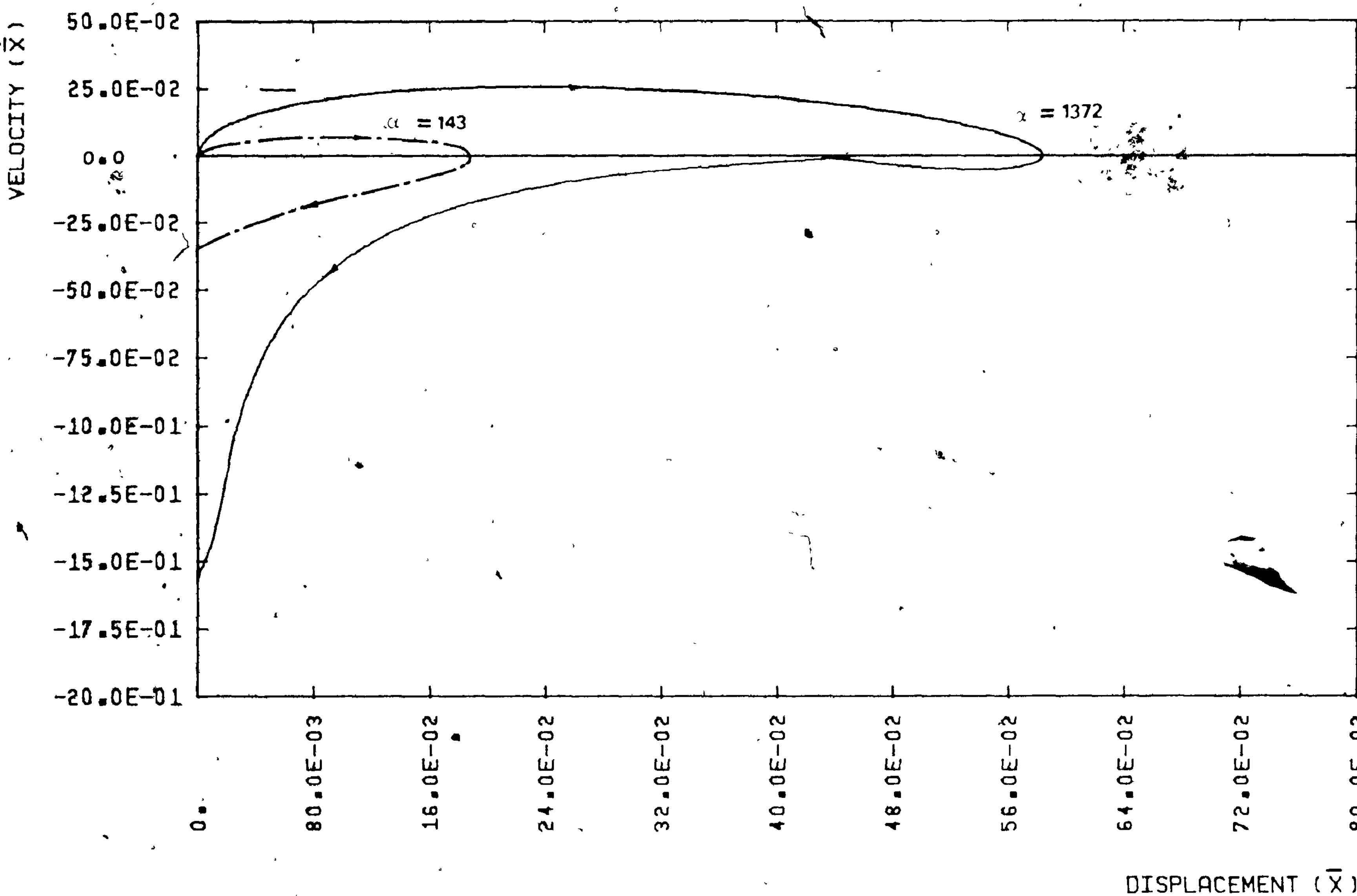

Figure 3.20(b) Parametric Results of the Model: Phase Plane Plot for Different Values of Inertia Factor.

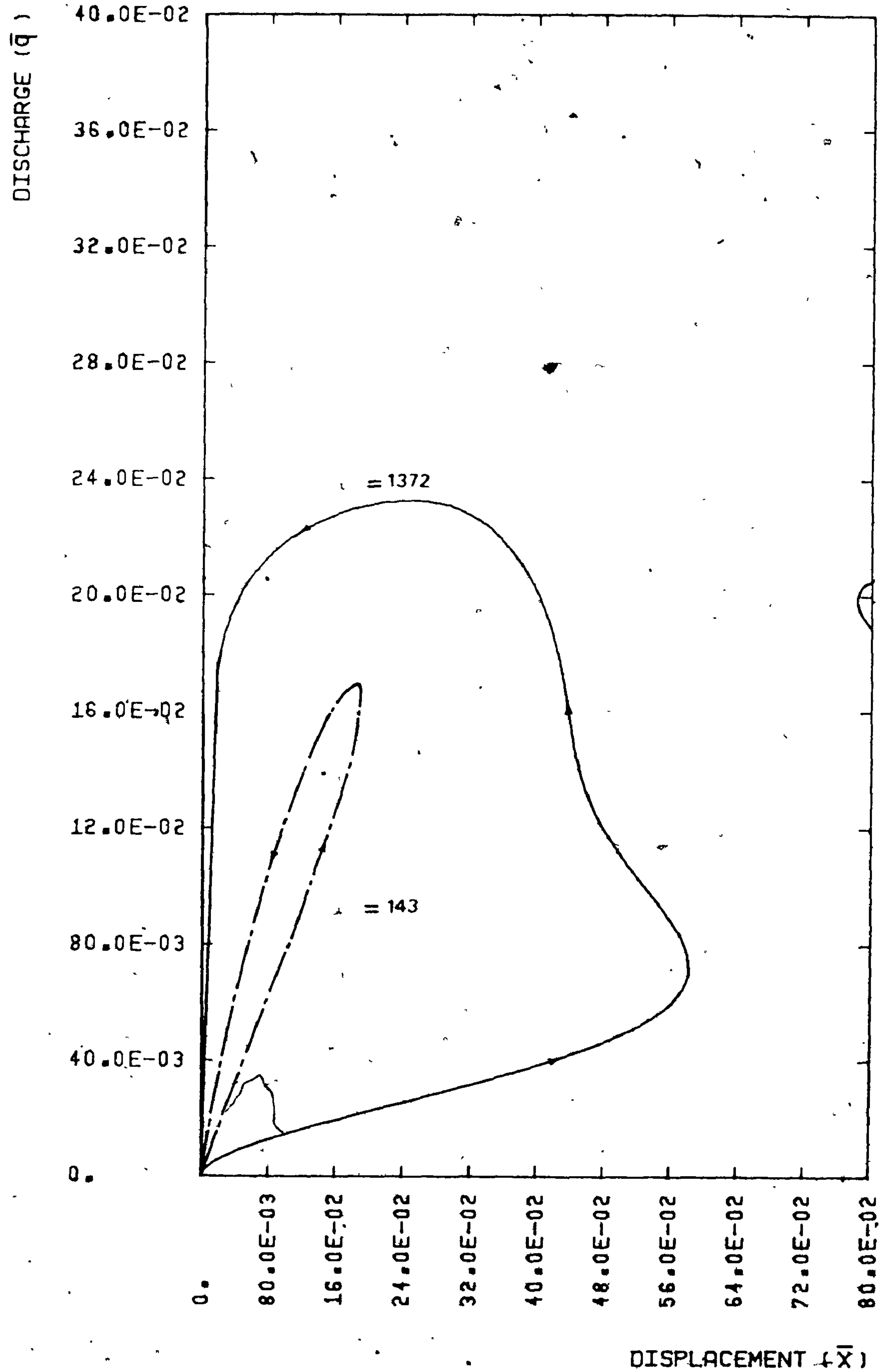

Figure 3.20(c). Parametric Results of the Model: Dimensionless Discharge vs Dimensionless Displacement for Different Values of Inertia Factor.

which may occur in the system such as friction in conduits, entrance, exit, sudden changes in cross-sectional area, valves, and elbow losses. All these losses are taken as constant since there is apparently no information concerning the variation of turbulent losses under unsteady conditions. No significant effect deriving from the loss factor has been observed on the vibrational response of the system. An increase in the loss factor results in a slight increase in the period of oscillation while the amplitude and wave-forms remain essentially the same.

g) Mass Ratio Parameter (μ)

The mass ratio parameter represents the density ratio between the working fluid and the vibrating structure material. Its value can be varied over a wide range since the working fluid may be gas or liquid, and the material of the vibrating structure can be either steel (valves and gates) or rubber (seals). Equation 3.30 shows that the exciting hydrodynamic load is a function of the mass ratio parameter and hence, it should have a significant effect on the dynamic behaviour of the hydraulic control device. Figure 3.21 shows the system's response for three different fluid media. The solid line represents the system's response under the action of water flow while the system's behaviour under the action of air flow is represented by the broken line.

For small values of the mass ratio, as in the case

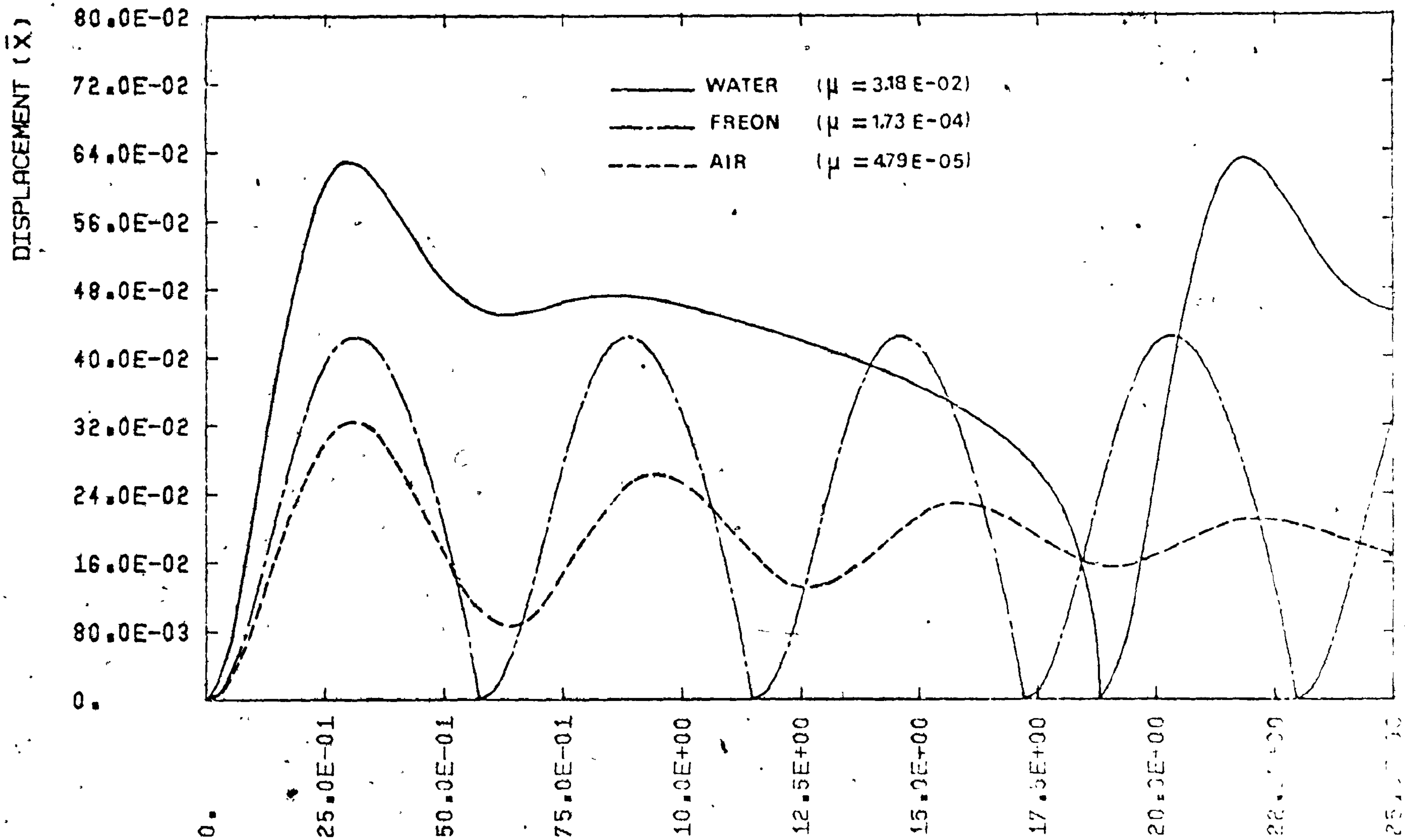

Figure 3.21. Parametric Results of the Model: Effect of the Mass Ratio on the System's Dynamic Behaviour.

of air flow, the fluid inertial head over small openings is relatively small compared with the static head. Hence, the total hydrodynamic pressure difference is not sufficient to close the control device against the elastic force. This results in damped oscillations which virtually resemble the natural response of the elastic structure in a quiescent fluid.

For the case of heavy gases, Freon for example, the fluid inertial pressure becomes more significant and provides an extra dynamic pressure which can force the control device to close against the elastic force. Since the fluid inertia is small, the maximum discharge during the cycle of oscillation occurs almost simultaneously with maximum opening. The flow and therefore the hydrodynamic closing load rapidly become re-established and accelerate the control device towards its seat.

For water flow which has relatively high mass ratio, the fluid takes longer to re-establish itself. A lag develops and the maximum discharge occurs sometime after the control device has reached its maximum opening. This results in an increase in amplitude and period of vibration. In addition, the closing portion becomes much longer than the opening portion.

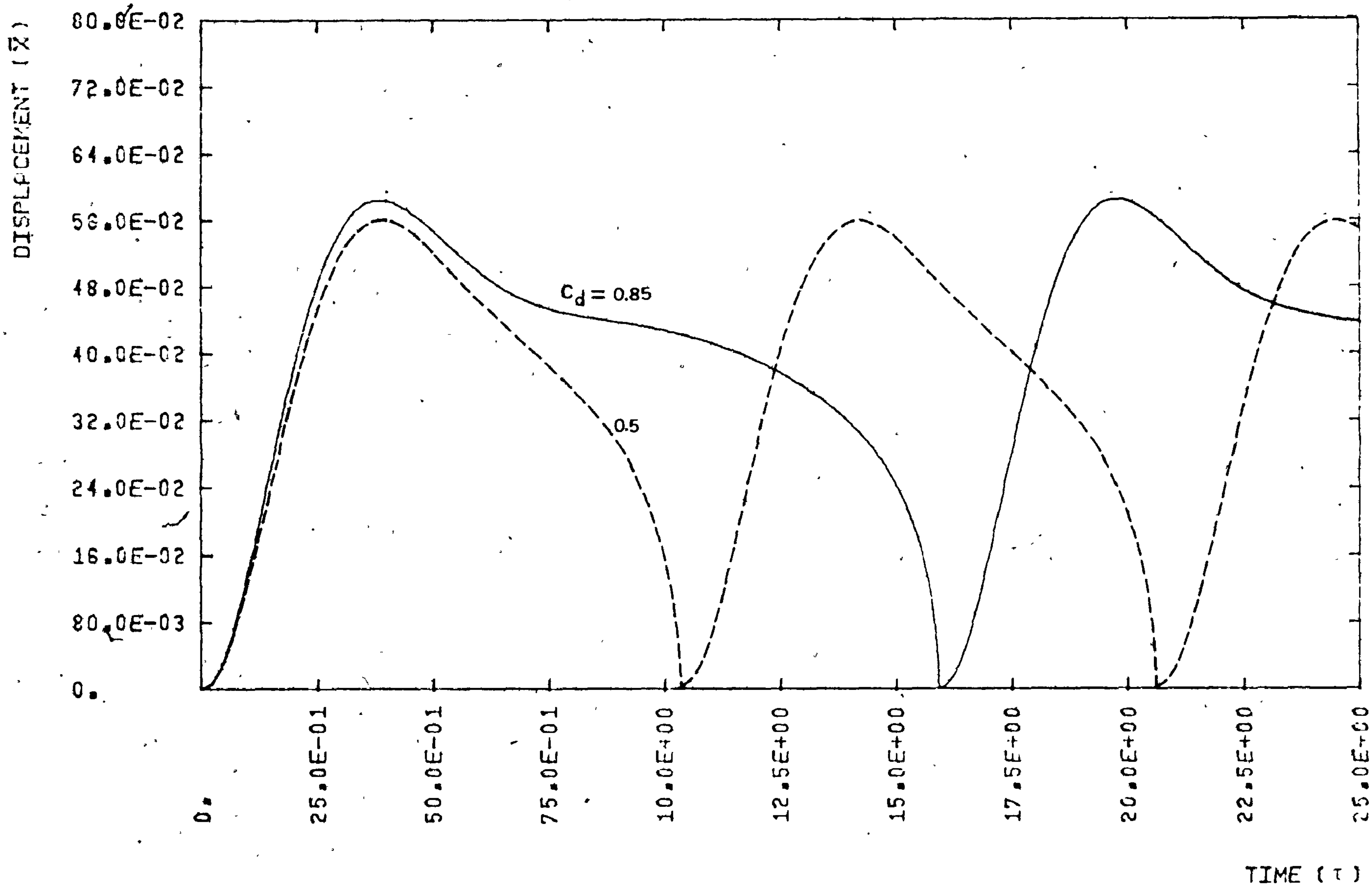

Figure 3.22(a). Parametric Results of the Model: Effect of Dynamic Discharge Coefficient on the System's Dynamic Behaviour:

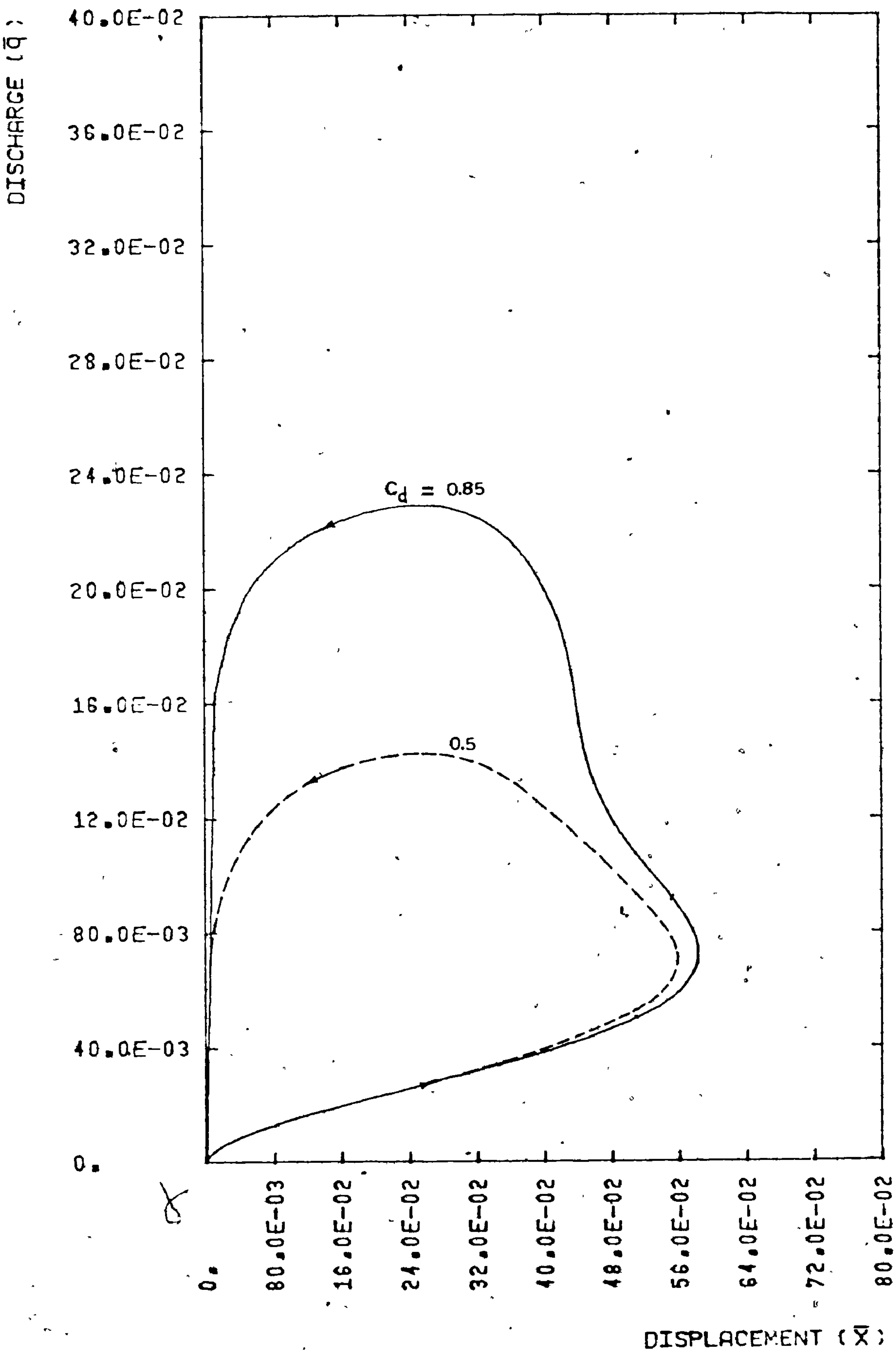

Figure 3.22(b). Parametric Results of the Model: Dimensionless Discharge vs Dimensionless Displacement for Different Values of Dynamic Discharge Coefficient.

h) Discharge Coefficient (C_d)

Experimental observations in the literature have shown that the static discharge coefficient of fluidic control elements is displacement dependent, (11) and (13), while the dynamic one is displacement and frequency dependent, (21) and (32). For the present, the dynamic discharge coefficient is taken as a constant to demonstrate that the system's instability is not necessarily attributable to the linear variation in discharge coefficient which has been assumed in recent papers (9), (14).

Since the elastic force dominates during the opening portion of the cycle, the dynamic discharge coefficient, which has been assumed to be constant here, has a slight effect on the amplitude of vibration and the opening time remains constant. As the dynamic discharge coefficient increases, the flow is more readily re-established as seen in Figure 3.22 (b), and hence, controls the closing part of the cycle. This result is shown in Figure 3.22 (a) where the closing time is much longer for the higher value of the dynamic discharge coefficient.

CHAPTER 4

MODEL APPLICATIONS AND COMPARISON WITH AVAILABLE EXPERIMENTAL DATA

Although it is impossible to establish a mathematical model which is sufficiently general to represent all types of fluid control devices, a single model can represent quite a variety of such devices appearing to have the same excitation mechanism. Accordingly, the model developed in the previous chapter is applicable for any fluid control device with a jet flow mechanism of excitation. The model has been derived in a very simple but general way; hence, the parameters appearing in the differential equations of motion can be calculated for any problem under consideration. Swing check valves, plug valves, J-bulb rubber seals, and hydraulic gates with a skimmer wall are some examples of devices having a mechanism of self-excitation which can be explained by the proposed model. Only two applications, check valve and seal vibrations, are studied and compared with the available experimental data.

4.1 Swing Check Valve Application

4.1.1 System Under Consideration

The experimental circuit used in reference (11) is shown in Figure 4.1. The required pressure was obtained by

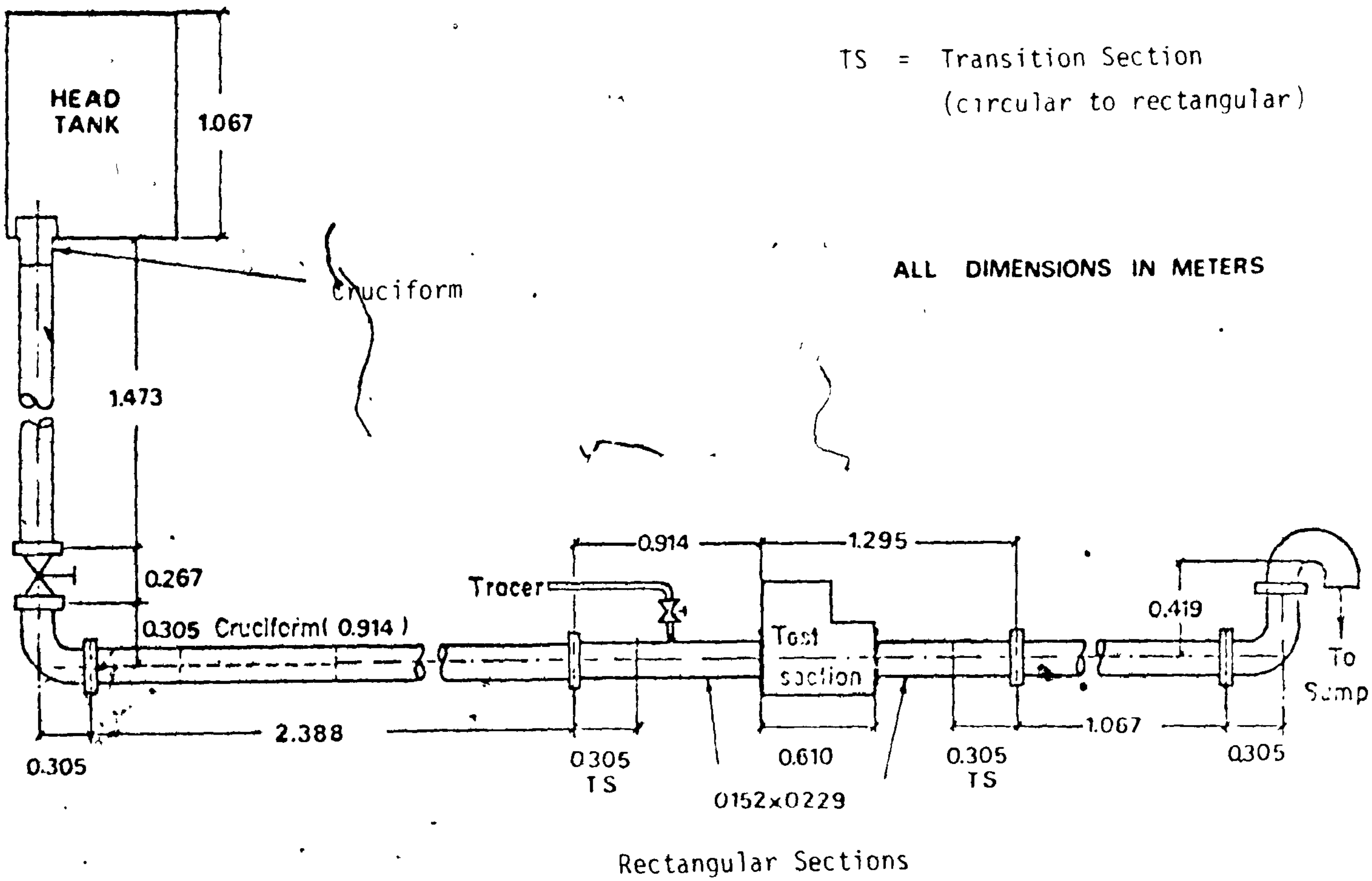

Figure 4.1. Experimental Apparatus of Check Valve's Model, Ref. (11).

using a constant-head water tank. A six-inch diameter steel pipeline was connected to the constant head reservoir and a gate valve was used to regulate discharge. At the entrance into the pipeline from the high level reservoir, a short cruciform was inserted to prevent the development of a vortex. Also downstream of the gate valve a longer cruciform was inserted into the pipeline to prevent the secondary flows in the pipeline.

Two identical transition sections were used to transform the six-inch diameter circular pipeline cross-section into the 6" x 9" rectangular cross-section of the test section. The cross-sectional geometry transformation was affected over a length of 12 inches and the flow was allowed to develop over the remaining 24 inches of rectangular pipeline. A double-screen filter was installed about 20 inches from the test section inlet. The numerical values of parameters are indicated in Appendix C.

4.1.2 Discharge Coefficient of the Valve

Adubi (11) has conducted steady state experiments in which the valve was held fixed at different angles and reverse flow through it was measured. Then he derived the reverse discharge coefficient, Figure 4.2. It is clear that the static reverse discharge coefficient does not apply quantitatively under the unsteady flow conditions of valve

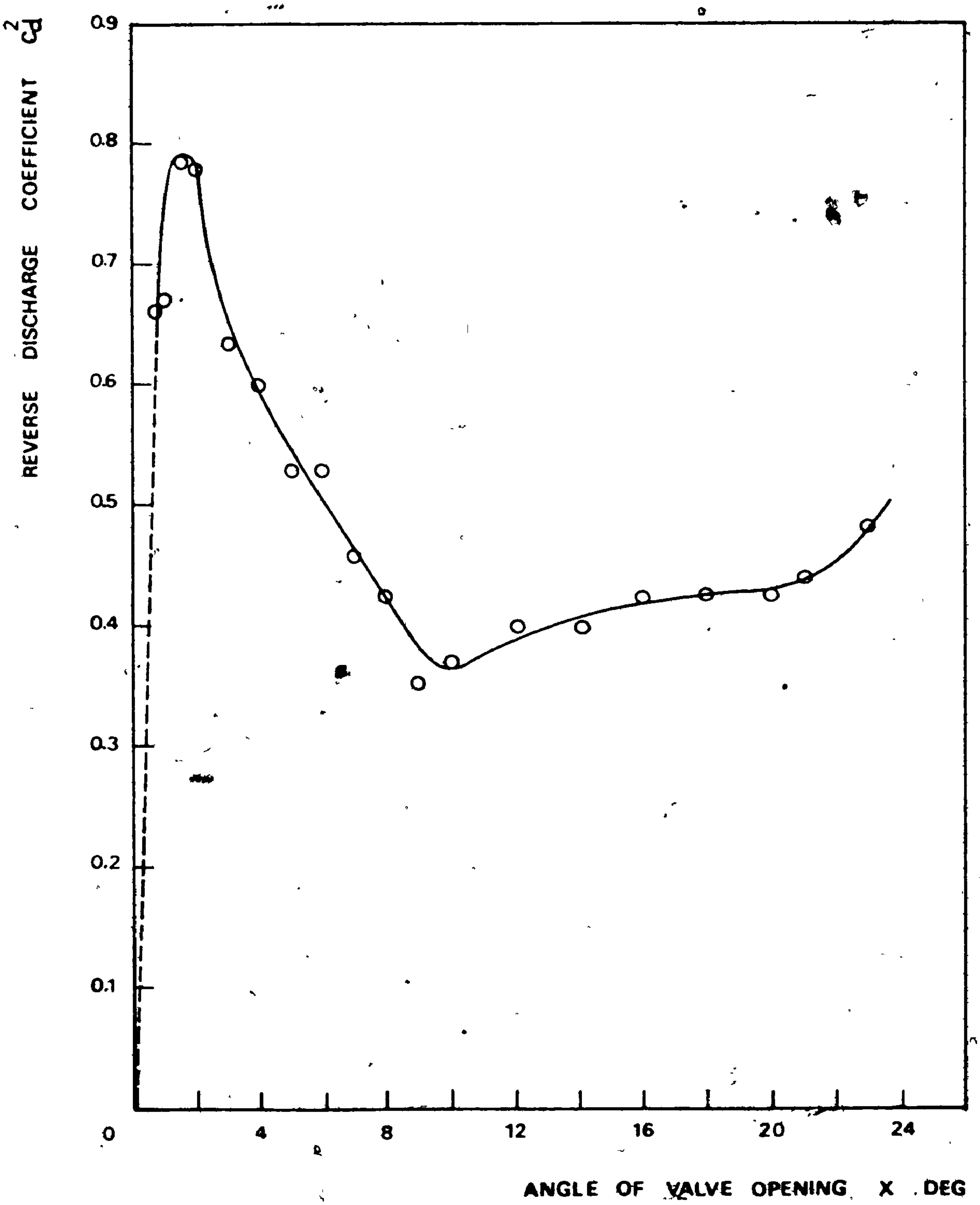

Figure 4.2. Dynamic Discharge Coefficient of the Valve vs Angle of Opening, Ref. (11).

oscillations.

Daily, Hankey, and Jordaan (21) have taken into account the effects of fluid inertia, and have shown that, for water flow through square-edged orifices in pipes, the discharge coefficient increases when the flow accelerates, and decreases when the flow decelerates. McCloy and McGuigan (32) have examined experimentally and theoretically the combined effects of time varying pressure drop and orifice area, and since in this case fluid inertia effects did not account for all the flow rate reduction, it was deduced that the orifice coefficients must be frequency dependent. At present very little is known about discharge coefficient variations in unsteady fluid flow, and the exact nature of these changes cannot be accounted for in this analysis.

4.1.3 Model Results in Comparison with Available Experimental Data

The parameters included in equations 3.30 and 3.31 have been evaluated for the system under consideration, Figure 4.1. The numerical values of parameters are given in Appendix C. The parametric results of the model and the experimental data are shown in Figure 4.3. In Figure 4.3(a) the maximum displacement of the valve is plotted against the equivalent spring stiffness. The frequency ratio is plotted

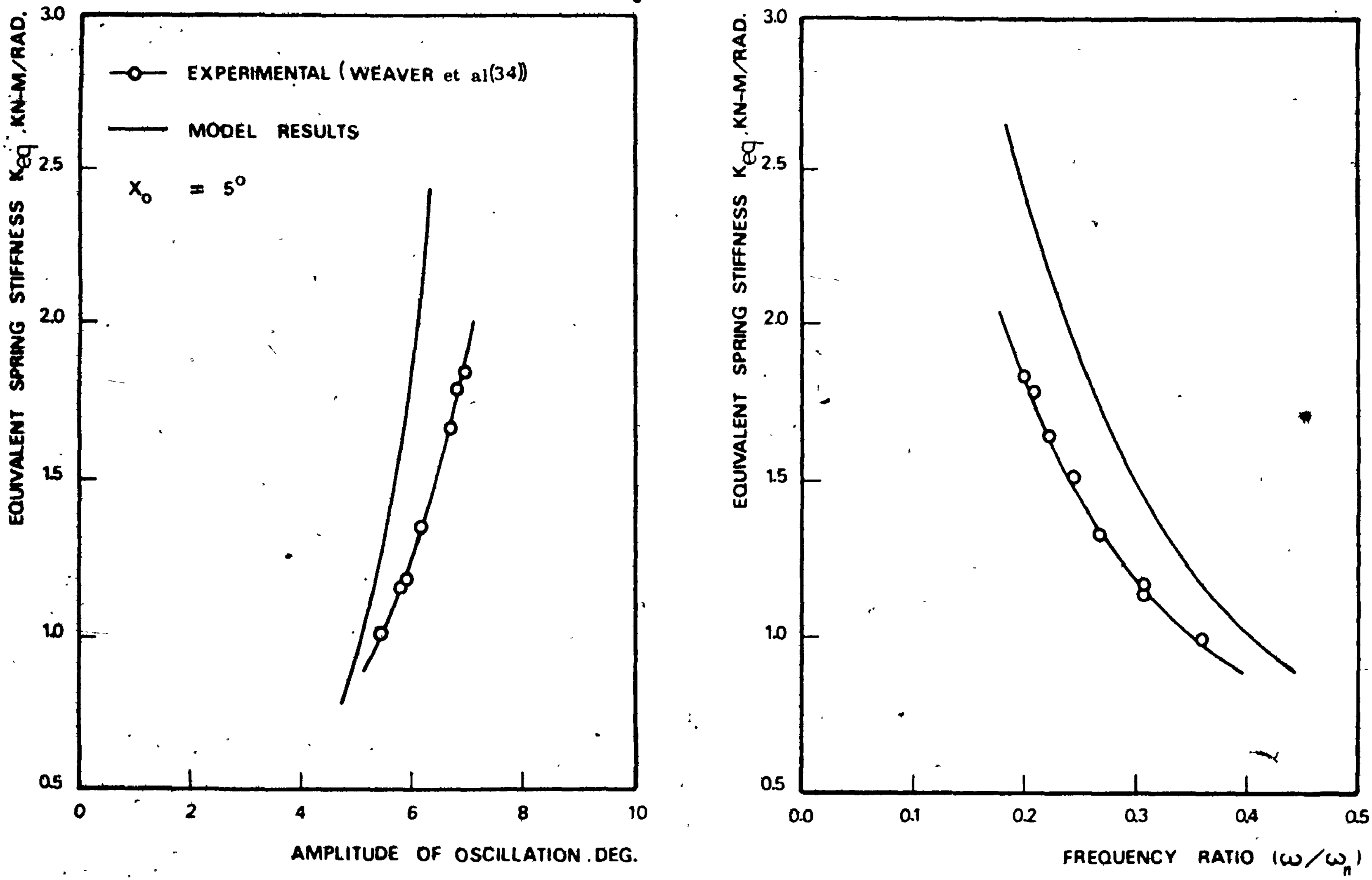

Figure 4.3. Parametric Results of Check Valve Application in Comparison with Experimental Data.

against the equivalent spring stiffness in Figure 4.3(b).

Figure 4.3 shows that the results of the model and the experimental observations behave in a qualitatively similar manner. In addition, a close prediction for amplitude and frequency of oscillation can be obtained by the model. The valve behaviour with certain parameter values can be either stable (in the sense of opening or closing) or unstable (exhibits a limit cycle oscillation).

The valve instability is due to the high rate of change of discharge over the last few degrees of the closing portion and the hysteretic hydrodynamic loading resulting from fluid inertia. These results are shown in Figure 3.17 (c) which agrees with the experimental observations reported by Weaver and Adubi (12), Figure 3.3 (a).

The model has been derived from first principles and some assumptions have been made for purposes of simplicity (see section 3.5.1). The fluid phenomena which have been neglected in comparison with static, loss, and fluid inertial heads must have a small effect on the hydrodynamic load in view of the good agreement with experimental observations. The discrepancy is undoubtedly largely due to the approximation made regarding the dynamic discharge coefficient. Hence, it is unreasonable to expect complete agreement between the model and experimental data. More research is necessary in order to develop a better understanding of discharge coefficient variation under conditions of accelerated and decelerated flow.

4.1.4 Effect of Design Changes on the Valve's Dynamic Behaviour

The theoretical model of the valve has shown that the vibration could not be eliminated by adjustments of stiffness, damping, initial setting angle or other parameters. Only a change in valve geometry which changes the discharge characteristics, may provide relief from the dynamic instability. Adubi (11) has examined the effect of various changes in the design of the valve. However, it could not be known beforehand precisely how each modification to the valve geometry would modify the flow rate to achieve the desired result. In this section the theoretical model of the valve is used to predict the effect of geometric design changes on the valve behaviour.

The discharge must be reduced more gradually over a much greater angle of closure so that there is no sudden rise in closing pressure difference across the valve. This can be achieved by designing a small flow area (a_v) with lower value of discharge coefficient over small angles of valve opening. The proposed design by Adubi (11) of a vibration-free swing check valve is shown in Figure 4.4. The flow area against the angle of valve opening of this

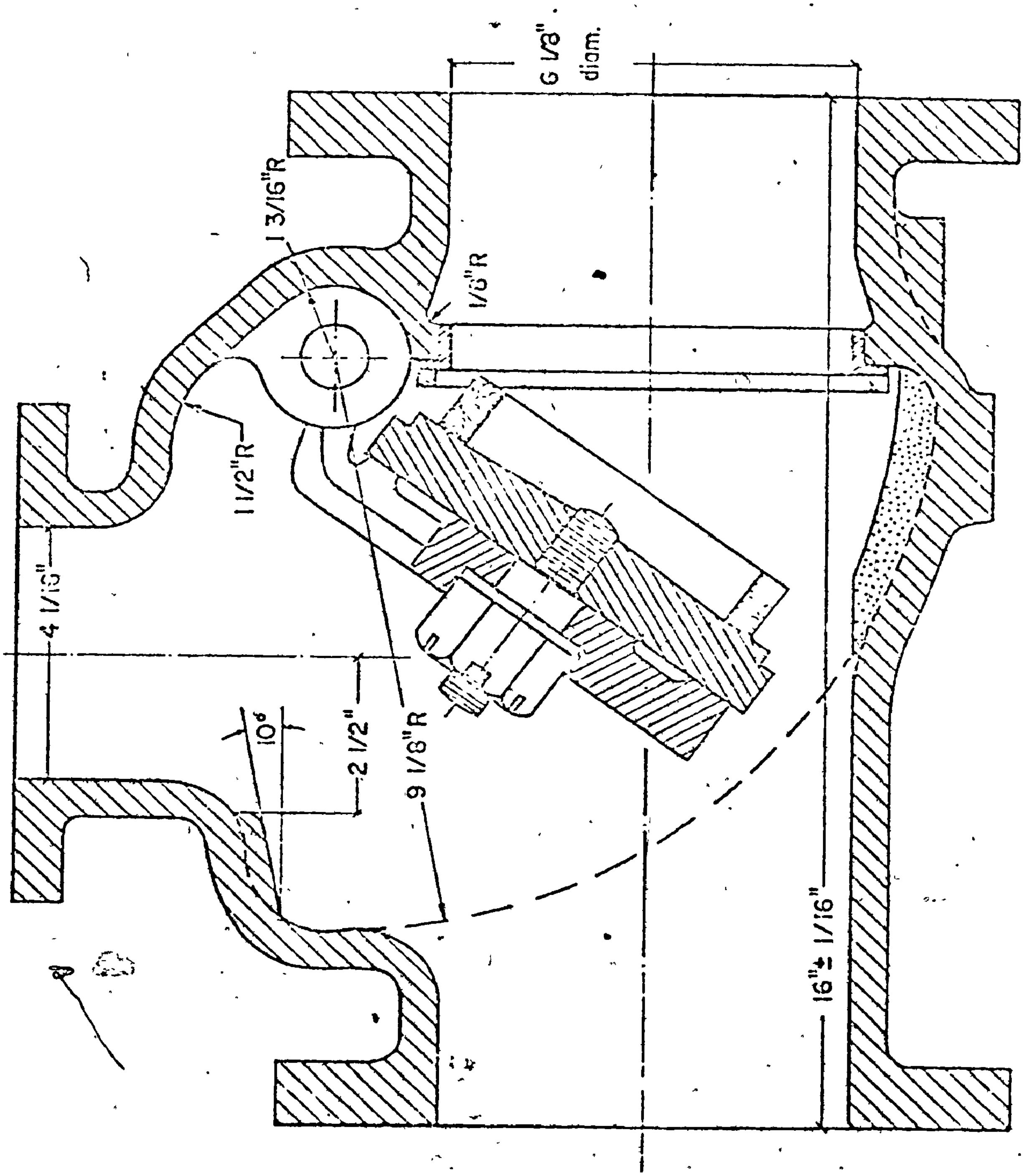

Figure 4.4. Suggested Vibration-Free Design of the Swing-Check Valve with Spring Damper, Ref. (11).

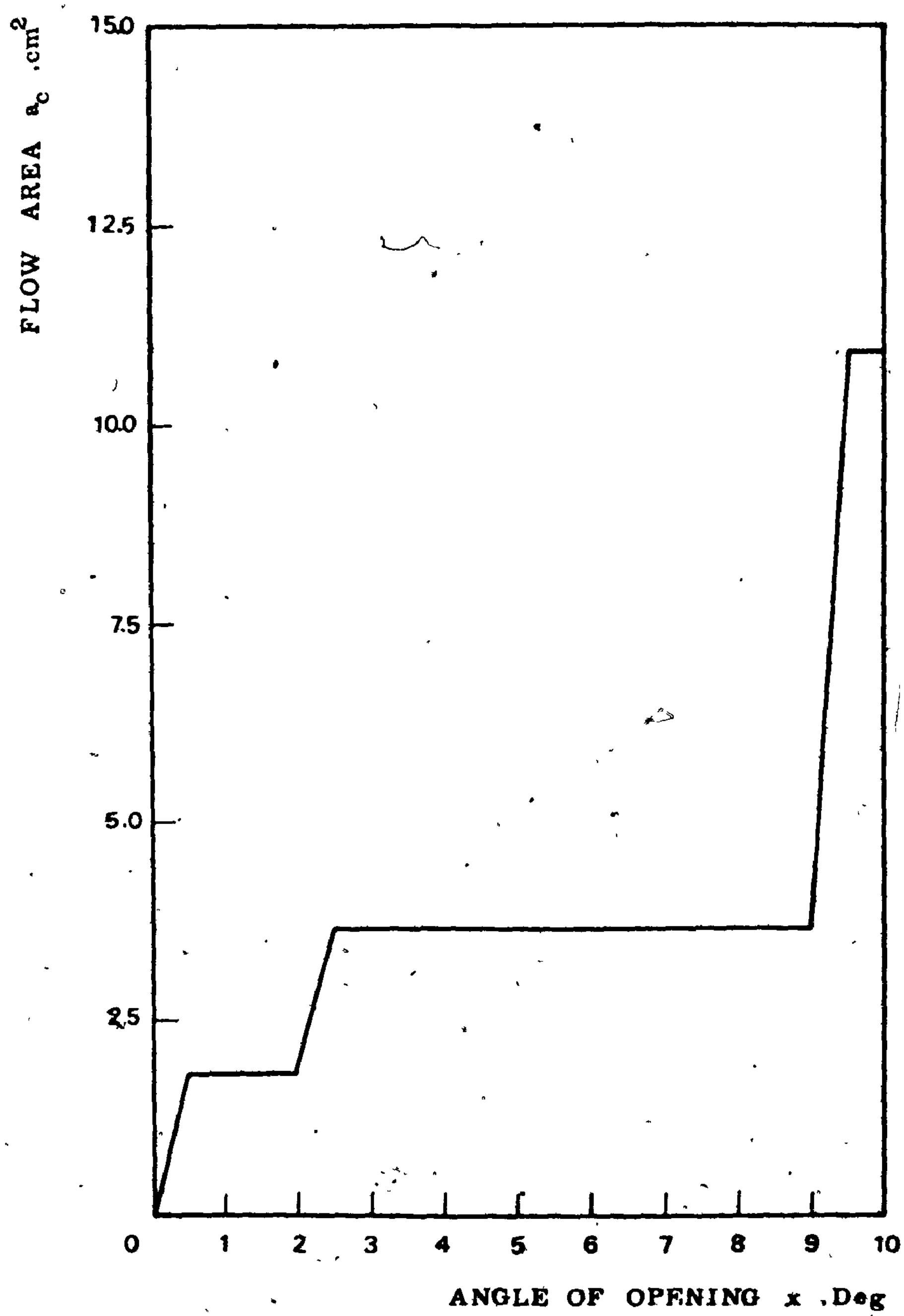

Figure 4.5. Flow Area vs Angle of Opening for the Vibration--Free Design of the Swing-Check Valve.

design is shown in Figure 4.5. Inserting the flow area during vibration into equation 3.30 and using a small value for the dynamic discharge coefficient (Cd = 0.5) results in stabilizing the valve dynamically. Figure 4.6 shows the valve reponse for the same case shown in Figure 3.17, $\overline{K}$ = 0.5. This represents a point in the lower sub-region of the stability map, i.e. the valve is statically stable in the sense that it stays closed. The modified valve slammed shut, bounced weakly once and remained shut instead of executing limit cycle oscillations. On the other hand, Figure 4.7 shows the valve's dynamic response for the case shown in Figure 3.17, $\overline{K}$ = 1.3, which is represented by a point in the upper sub-region of the stability map. Hence, the valve is statically stable in the sense that it stays open. The valve with design changes slammed shut, bounced back and remained open at a small angle instead of executing limit cycle oscillations.

The mathematical model can be used to predict how modifications to the valve geometry modify the valve's dynamic stability behaviour.

4.2 Application to Seal Vibrations

As explained in Chapter 1, many cases are known in practice where the gate seals develop self-excited vibrations over a wide range of operating heads. Seal vibrations may be due either solely to a jet-flow mechanism, Figure 1.3(a),

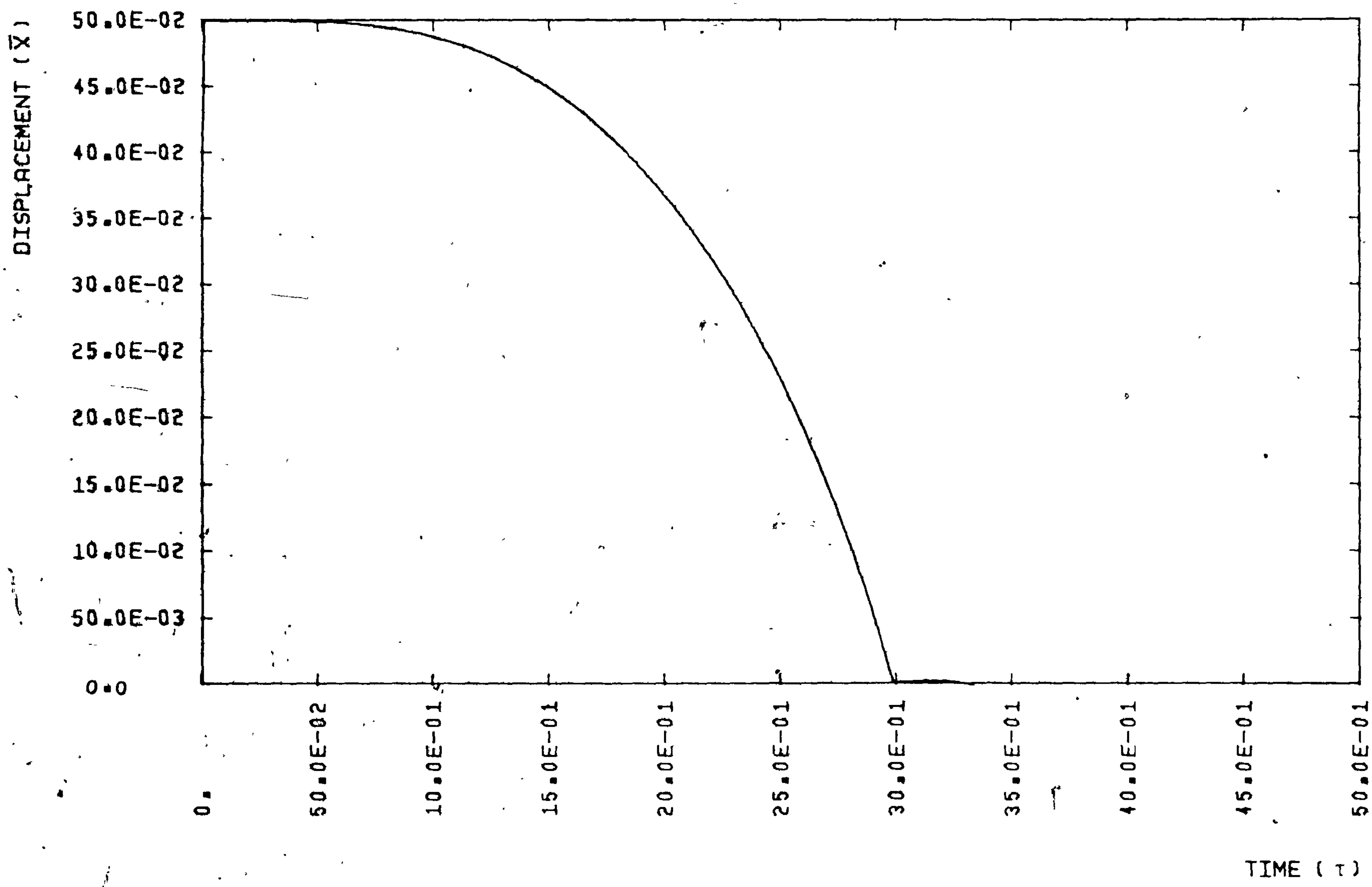

Figure 4.6. Transient Response of the Vibration-Free Design of the Swing-Check Valve, $\overline{K} = 0.5$; $\beta = 0.5$.

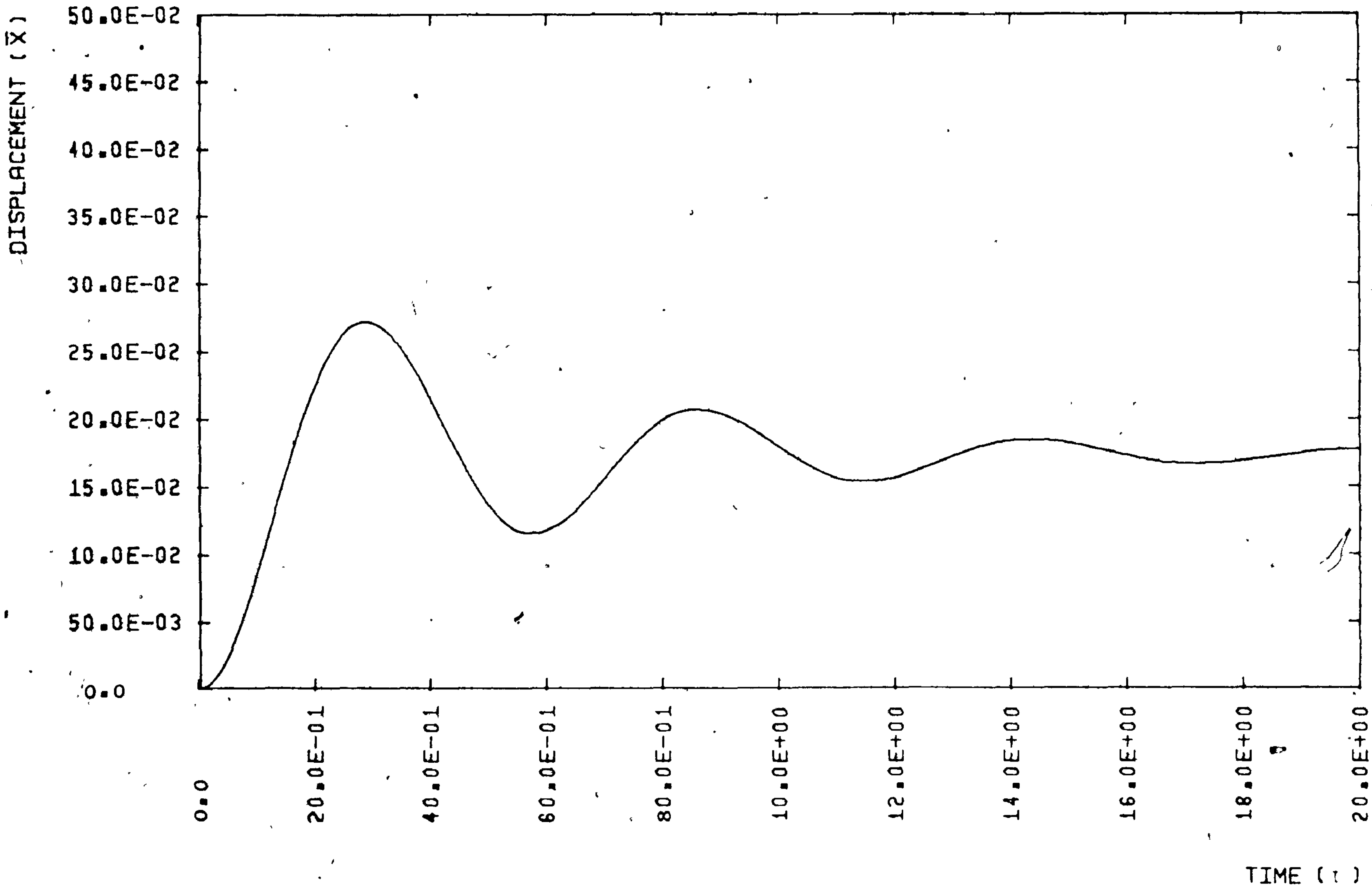

Figure 4.7. Transient Response of the Vibration-Free Design of the Swing-Check Valve, $\bar{K}$ = 1.3; β = 0.5.

(b), or to a combination of jet-flow and eddy mechanisms, Figure 1.3(c), (d), depending on the seal configuration. Seals with a jet-flow mechanism of excitation can be described mathematically by the proposed model. In this section the proposed model is used to predict the dynamic behaviour of J-bulb rubber seals. Preliminary analysis has shown that the model results are in good agreement with the experimental data given by Lyssenko and Chepajkin (14).

4.2.1 Inertia Factor

The inertia factor is one of the most important parameters to be considered in different model applications. Although it has a very high value for valves in pipeline systems, its value is relatively small for the case of seals. The inertia factor, as defined by equation 3.30, depends on the system equivalent length, L*, which was defined by:

$$L^* = L_u + L_d + a_2 \frac{l_v}{a_v}$$

In application to check valves, the upstream and downstream equivalent lengths, L_u and L_d, dominate. The jet equivalent length, $a_2 l_v/a_v$, can be neglected and hence, the system equivalent length is considered constant during the cycle of oscillation. When seals are considered, the equivalent length is mainly due to the jet of fluid through the control device. The upstream and downstream equivalent lengths are negligible in comparison. In this case, the system equivalent length becomes function of the vena contracta area, a_v, and jet length, l_v, which in turn are functions of seal displacement and frequency.

4.2.2 Model Results in Comparison with Available Experimental Data

There is little available information concerning the jet length and vena contracta area for seals especially under unsteady flow conditions. For this reason the jet equivalent length has been assumed to have a relatively small constant value over the whole cycle of oscillations. Figures 4.8(a), (b), (c), and (d) show the model's results applied to seal vibration. The numerical values for parameters are noted in Appendix D.

Figure 4.8 (a) shows that the seal oscillation is not of a simple harmonic nature, although the frequency of oscillation is close to the natural frequency of the seal. The opening time is longer than the closing time. This is undoubtedly due to the small inertia factor which results in smaller values of fluid inertial head and phase shift between displacement and discharge. The maximum discharge during the cycle of seal's oscillation occurs almost simultaneously with maximum opening, which contrasts with the

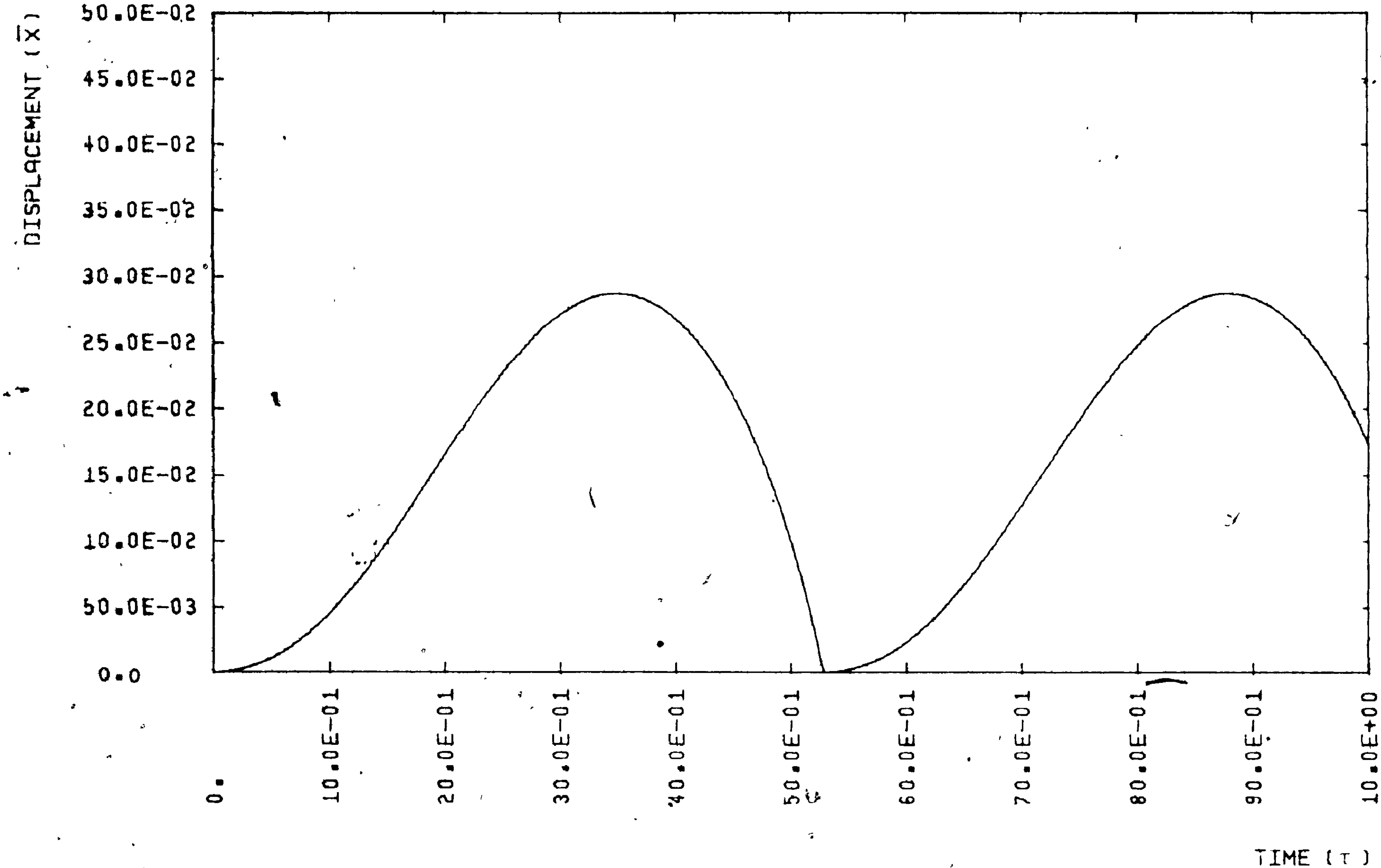

Figure 4.8(a). Application to Seal Vibrations: Vibrational Waveform.

behaviour of check valve. Both the flow rate and the hydrodynamic closing load rapidly become re-established. The closing load due to static pressure drop plus inertial head then accelerates the seal towards its seat. Hence, the seal closes rapidly executing a higher frequency of oscillation than that for valves with greater values of inertia factor. This result is shown in the phase plane plot, Figure 4.8(b), where the opening velocity is slower than the closing velocity. The small phase shift between the seal displacement and flow re-establishment is shown in Figure 4.8(c). The hydrodynamic pressure difference across the valve during a cycle of oscillation is shown in Figure 4.8(d). The area enclosed is proportional to the energy transferred to the seal per cycle. Note that the minimum pressure difference is not a great deal less than that at seal opening.

Thus, the theoretical model shows that the seal oscillates with a frequency (21.7 Hz) which is close to its natural frequency (18.7 Hz). This agrees with the experimental data given by Lyssenko and Chapaikin (14). They have reported that the J-bulb rubber seals vibrate in a periodic non-sinusoidal manner with a frequency range from 10 to 30 Hz. In addition, the oscillations are considered dangerous since the seal frequency and the natural frequency of the gate and its parts could coincide.

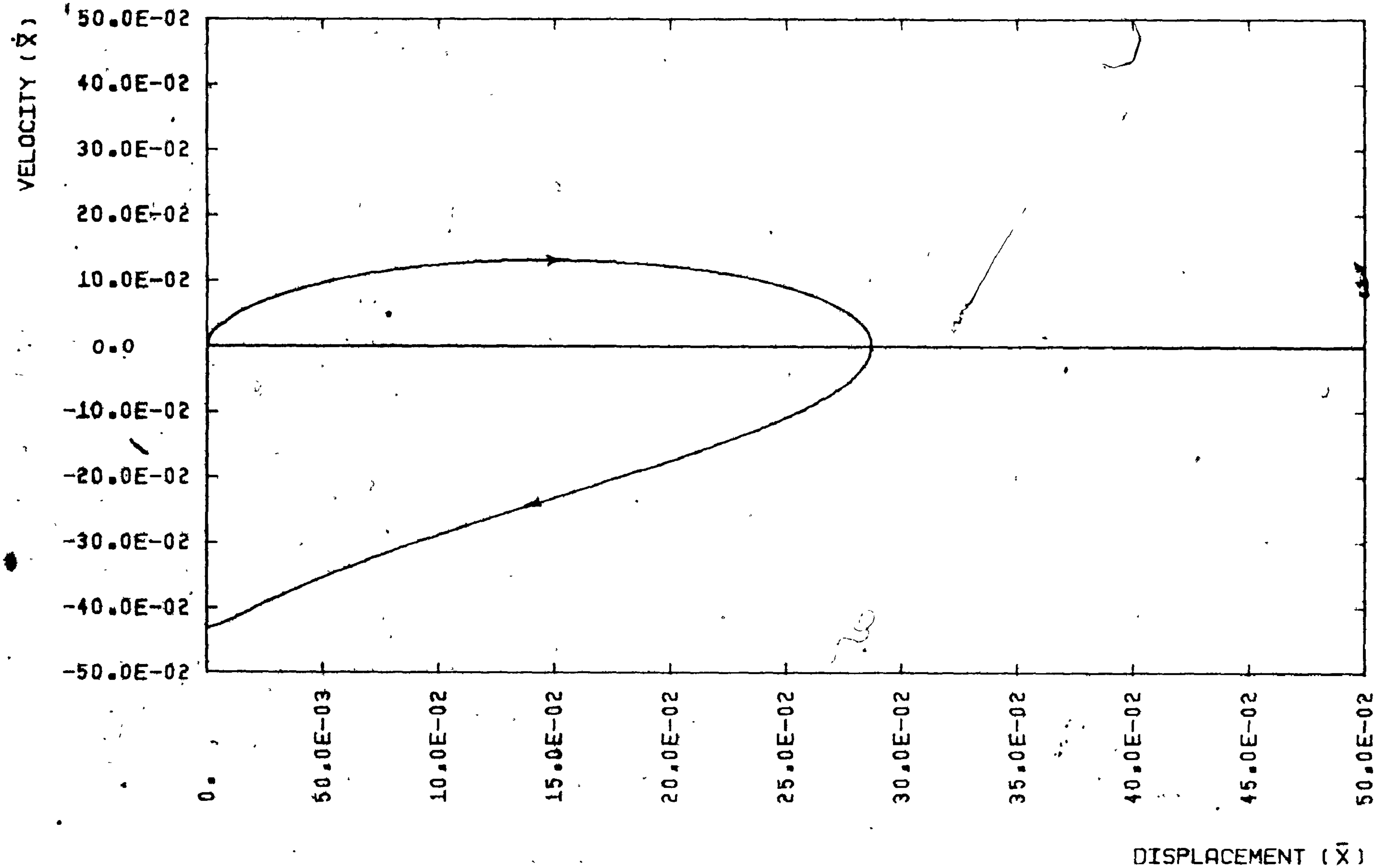

Figure 4.8(h). Application to Seal Vibrations: Phase Plane Plot.

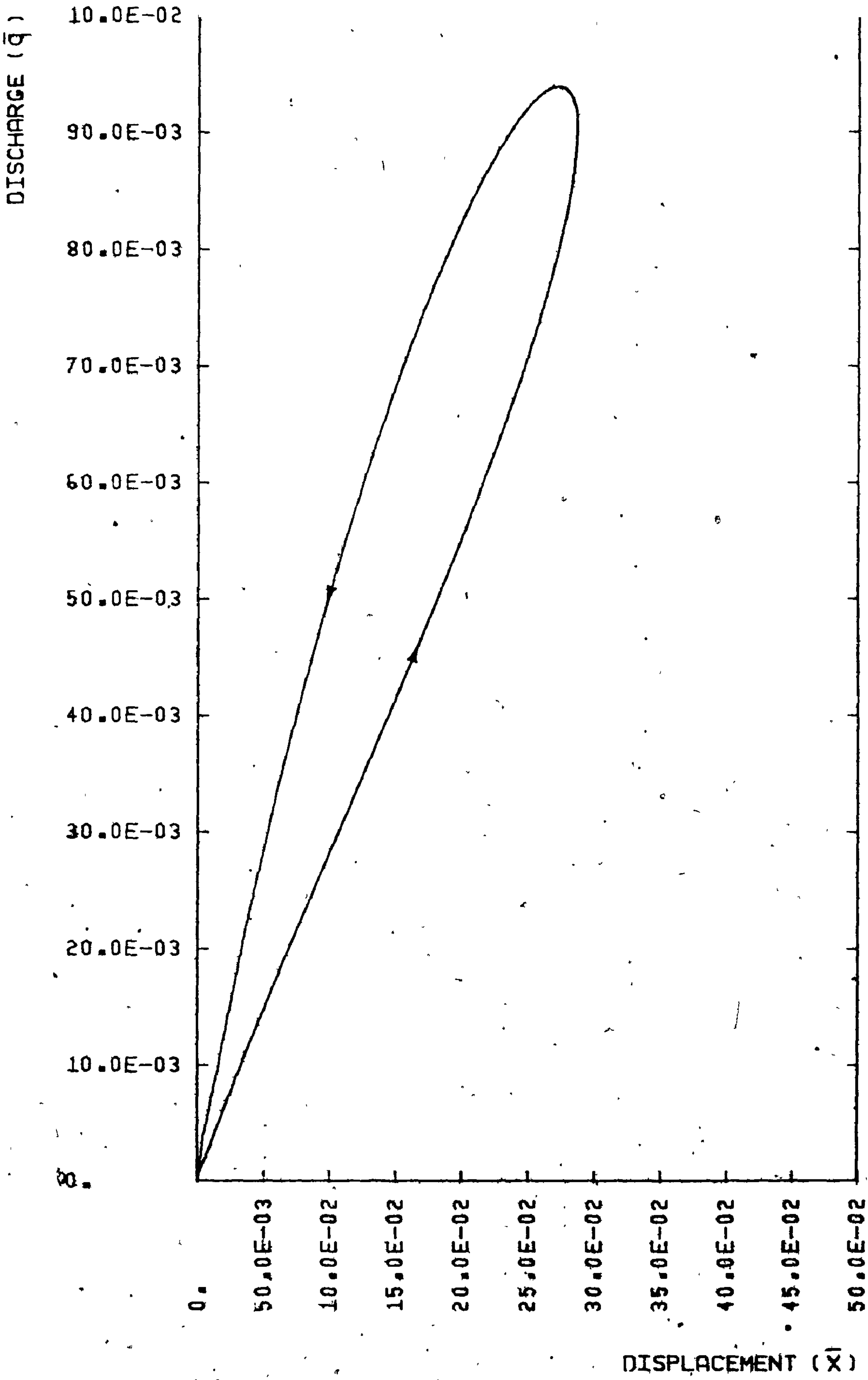

Figure 4.8(c). Application to Seal Vibrations: Dimensionless Discharge vs Dimensionless Displacement.

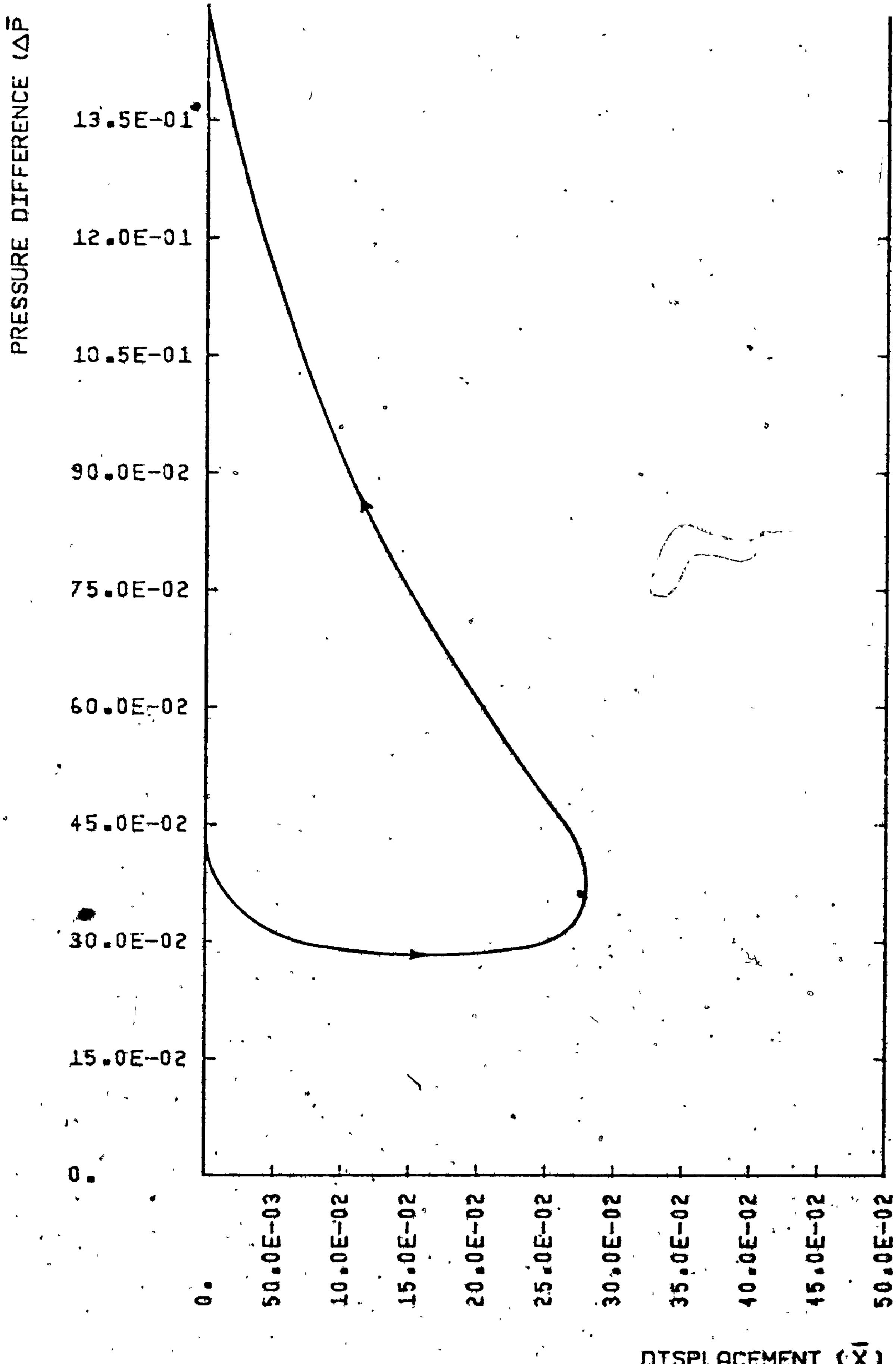

Figure 4.8(d) Application to Seal Vibrations: Dimensionless Pressure Difference vs Dimensionless Displacement.

4.3 Gate Vibrations

It is known that hydraulic leaf gates and gate valves may be subjected to various modes of self-excited vibrations differing in their physical characteristics and in the conditions under which they are generated. The jet flow mechanism as described in Chapter 2 produces the horizontal vibrations of partially opened hydraulic leaf gates with a skimmer wall. Also, if a vertical leaf gate or valve is operating under very small openings, the flow separation and reattachment to the gate bottom is prevented and hence, the eddy mechanism of excitation is no longer valid. Vertical gate vibrations under such conditions are caused essentially by the jet-flow mechanism.

The proposed model can be used to depict the stability behaviour of hydraulic gates under the action of a jet-flow mechanism of excitation. Such application is considered beyond the scope of the present research since the model must be developed using the appropriate design characteristics and experimental data.

CHAPTER 5

CONCLUSION

The negatively damped simple harmonic oscillator proposed by earlier researchers must be ruled out as possible machanism of excitation for many hydraulic control devices. Such a model is not capable of predicting certain important aspects of the observed behaviour. Thus, the hydrodynamic load cannot be expressed mathematically as a simple velocity dependent component.

A semi-empirical model for check valve vibrations has been developed which shows that the essential features of the observed behaviour can be predicted by representing the hydrodynamic load as a displacement dependent force. This displacement dependent component causes a decrease in frequency of oscillation when the spring stiffness increases. Although this phenomenon is in contrast with free vibration, it agrees with the experimental observations. While this model presents encouraging results, its general applicability is limited by its lack of a firm basis in fundamental principles.

Thus, further research was conducted to develop a general mathematical model for hydraulic control devices from first principles. This model can be applied to any control device with a jet-flow mechanism of excitation.

Unsteady flow phenomena have been taken into account in deriving the model's equations. A complete parametric study was undertaken to show the influence of each parameter on the model's behaviour. The model was then tested against available experimental data for check valves and seals. The results were found to be in good agreement quantitatively with the available experimental data reported by Weaver et al (34) and qualitatively with that of Lyssenko and Chepajkin (14). The quantitative data of the latter were insufficient for comparison.

The mechanism of instability is considered to be the same for plug valves, check valves, gate valves, hydraulic gate J-bulb rubber seals, and other flow control devices operating at small openings. Therefore, the proposed model can be used to predict the dynamic behaviour of the control devices and the effect of design changes on their dynamic stability.

An important area for further research relating to self-excited oscillations of flow control devices is in establishing dynamic discharge coefficient characteristics. Such characteristics can only be studied through difficult and tedious experiments and are expected to be dependent on total pressure difference, frequency of oscillation and specific device geometry.

Nevertheless, approximate dynamic discharge coefficients give quite reasonable agreement with experimental observations. The model is therefore, useful for both improving our understanding of the mechanism of self-excitation and obtaining stability characteristics for the design of flow control devices.

REFERENCES

1. Tobes, G., "Flow-Induced Structure Vibrations", Proc. ASCE, J. Eng. Mech. Div., EM6, 1965, pp. 39-66.

2. Weaver, D.S., "On Flow-Induced Vibrations in Hydraulic Structures and Their Alleviation", Canadian Journal of Civil Engineering, Vol. 3, No. 1, 1976, pp. 126-137.

3. Simmons, W.P., "Experiences with Flow-Induced Vibrations", Proc. ASCE, J. Hyd. Division, HY4, July 1965, pp. 185-204.

4. Campbell, F.B., "Vibration Problems in Hydraulic Structures", Proc. ASCE, J. Hyd. Division, HY2, March 1961, pp. 61-77.

5. Douma, J.H., "Field Experiences with Hydraulic Structure", IVTAM/IAHR Symposium on Flow-Induced Structural Vibrations, Karlsruhe, Germany, 1972, Springer-Verlag, 1974, pp. 223-249.

6. Simmons, W.P., "Experiences With Flow-Induced Vibrations", Proc. ASCE, J. Hyd. Div., HY2, 1966, pp. 45.

7. Schmidgall, T., "Spillway Gate Vibrations on Arkansas River Dams", Proc. ASCE, J. Hyd. Division, HY1, Jan. 1972, pp. 219-238.

8. Hardwick, J.D., "Flow'Induced Vibration of Vertical-Lift Gate", Proc. ASCE, J. Hyd. Div., Vol. 100, HY5, 1974, pp. 631-644.

9. Abelev, A.S. and Dolnikov, L.L., "Experimental Investigations of Self-Excited Vibrations of Submerged Vertical-Lift Hydraulic Gates", IUTAM, IAHR Symposium on Flow-Induced Structural Vibrations, Karlsruhe, Germany, 1972, Springer-Verlag, 1974, pp. 265-277.

10. Naudascher, E., "Vibration of Gates During Overflow and Underflow", Proc. ASCE, J. Hyd. Div., Vol. 87, Sept. 1961, pp. 63-86.

11. Adubi, F.A., "The Hydroelastic Vibration of a Hydraulic Swing Check Valve", Ph.D. Thesis, McMaster University, Hamilton, Ontario, Canada, 1975.

12. Weaver, D.S., and Adubi, F.A., "Flow Visualization Studies of Check Valve Vibrations" Proceeding of the Symposium on Turbulence in Fluids, Missouri-Rolla, 1975, Science Press, Princeton, N. J., 1977.

13. Weaver, D.S., Kouwen, N., and Mansour, W.M., "On the Hydroelastic Vibration of a Swing Check Valve" IUTAM/IAHR Symposium on Flow-Induced Structural Vibrations, Karlsruhe, Germany, 1972, Springer-Verlag, 1974, pp. 333-338.

14. Lyssenko, P.E. and Ghepajkin, G.A., "On Self-Excited Oscillations of Seals Concerning the Gates of Hydro-Technical Structures" IUTAM/IAHR Symposium on Flow-Induced Structural Vibrations, Karlsruhe, Germany, 1972, Springer-Verlag, 1974, pp. 278-296.

15. Wood, C.J., Discussion of paper by Weaver, Kouwen and Mansour, IUTAM/IAHR Symposium, Karlsruhe, Germany, 1972.

16. Wonik, G., Discussion of reference (14) above, IUTAM/IAHR Symposium, Karlsruhe, Germany, 1972.

17. Iversen, H.W., "An Analysis of the Hydraulic Ram" ASME Trans., J. of Fluids Eng., June 1975, pp. 191-196.

18. Krol, J., "The Automatic Hydraulic Ram: Its Theory and Design", ASME Paper No. 76-DE-17, 1976.

19. Parmakian, J., "Waterhammer Analysis", Dover Publications, Inc., New York, 1963.

20. McCloy, D., "Effects of Fluid Inertia and Compressibility on the Performance of Valves and Flow Meters Operating Under Unsteady Conditions", J. Mech. Eng. Science, Vol. 8, No. 1, 1966, pp. 52-61.

21. Daily, J.W., Hankey, W.L., Olive, R.W. and Jordaan, J.R., "Resistance Coefficients for Accelerated and Decelerated Flows Through Smooth Tubes and Orifices", ASME Trans., July 1956, pp. 1071-1077.

22. Chandrasekaran, A.J., Saini, S.S. and Malhotra, M.M., Virtual Mass of Submerged Structures", Proc. ASCE, J. Hyd. Division, HY5, 1972, pp. 887-896.

23. IUTAM/IAHR Symposium on Flow-Induced Structural Vibrations, Karlsruhe, Germany, 1972, (Proceeding Published by Springer-Verlag, 1974).

24. Boltin, V.V., "Nonconservative Problems of Theory of Elastic Stability", Pergamon Press, New York, 1963.

25. Fung, Y.C., "The Theory of Aeroelasticity", John Wiley & Sons, Inc., New York, N.Y. 1957.

26. Stagg and El Abiad, "Computer Methods in Power System Analysis", McGraw-Hill, 1968.

27. International Symposium on Vibration Problems in Industry, Keswick, England, 1973. (U.K. Atomic Energy Authority at Windscale, N.P.L.).

28. Naudascher, E., and Locher, F. A., "Flow-Induced Forces on Portruding Walls", ASCE Jo. Hyd. Div., Vol. 100, HY2, 1974, pp. 295-313.

29. Butenin, N.V., "Elements of the Theory of Nonlinear Oscillations", Blaisdell Publishing Company, New York, 1965.

30. Stoker, J.J., "Nonlinear Vibrations in Mechanical and Electrical Systems", Interscience Publishers, Inc., New York, 1957.

31. Albertson, M.L., Barton, J.R., and Simons, D. B., "Fluid Mechanics for Engineers", Prentice-Hall Civil Engineering and Engineering Mechanics Series, 1960.

32. McCloy, D. and McGuigan, R.H., "Some Static and Dynamic Characteristics of Poppet Valves", Proc. Convn. Advances in Automatic Control, Proc. Instn. Mech. Engrs., 1964-65, 179 (pt 8H, paper 23), pp. 199.

33. Shames, I.H., "Mechanics of Fluids", McGraw-Hill Book Company, Inc., 1962.

34. Weaver, D.S., Adubi, F.A., and Kouwen, N. "Flow-Induced Vibrations of a Hydraulic Valve and Their Elimination", ASME Paper No. 77-FE-24, 1977.

APPENDIX A

COMPUTER PROGRAM

The purpose of this program is to obtain a numerical solution of a system of first-order ordinary differential equations with given initial values. The modified Runge-Kutta method for the solution of initial-value problems is used. It is a fourth-order integration procedure which is stable and self-starting; that is, only the functional values at a single previous point are required to obtain the functional values ahead. Control of accuracy and adjustment of the step size is done by comparison of the results due to double and single step size.

Given the system of first-order ordinary differential equations:

$$y_1' = \frac{dy_1}{dx} = f_1\,(x,\ y_1,\ y_2,\ .\ .\ .\ ,\ y_n)$$

$$y_2' = \frac{dy_2}{dx} = f_2\,(x,\ y_1,\ y_2,\ .\ .\ .\ ,\ y_n)$$

. . . .

. . . .

$$y_n' = \frac{dy_n}{dx} = f_n\,(x,\ y_1,\ y_2,\ .\ .\ .\ ,\ y_n)$$

and the initial values:

$$y_1(x_0) = y_{1,0},\ y_2(x_0) = y_{2,0},\ \ldots\ldots\ldots,\ y_n(x_0) = y_{n,0}$$

and using the vector notation, the given problem appears as follows:

$$\underline{Y}' = \frac{d\underline{Y}}{dx}$$

$$= \underline{F}\ (x, \underline{Y})\ \text{with}\ \underline{Y}(x_0) = \underline{Y}_0 \quad \ldots\ldots\ldots\ldots \quad A.1$$

where $\underline{Y}$, $\underline{F}$ and $\underline{Y}_0$ are column vectors.

A.1 Semi-empirical Model of Check Valve

The equation of motion for the valve disc is

$$J_d\ddot{x} + C_d\dot{x} + (K_{eq} - C_iR_oS\alpha_j)x = K_{eq}x_o - C_iR_oSP_j \quad ..3.7$$

Substituting x for the time t, y_1 for the displacement x, and y_2 for the velocity $\dot{x}$ and rearranging the following equations are obtained:

$$y_1' = \frac{dy_1}{dx} = y_2 \quad \ldots\ldots\ldots\ldots\ldots\ldots \quad A.2(a)$$

$$y_2' = \frac{dy_2}{dx} = \frac{1}{J_d}\ [K_{eq}\,x_o - C_iR_oSP_j - C_dy_2 - (K_{eq} - C_iR_oS\alpha_j)y_1] \quad A.2(b)$$

or

$$\underline{Y}' = \frac{d\underline{Y}}{dx} = \underline{F}\ (x, \underline{Y})$$

which is the same form given by equation A.1.

At the instant of closing, the displacement y_1 continues in the negative direction which has no physical meaning. The minimum displacement of the valve disc is zero representing the closed position. Hence, the following correction should take place:

$$y_1 = o \; ; \; \dot{y}_2 = -R_c \dot{y}_2 \quad \text{at } y_1 \leq 0$$

where the coefficient of restitution R_c is equal to zero if the hydrostatic pressure force is smaller than the spring force, and is equal to a small positive fraction if the hydrostatic pressure force is greater than the spring force at the closing position. This small fraction can replace the waterhammer and bouncing effects which initiate the valve opening in the latter case.

```
      PROGRAM TST (INPUT,OUTPUT,TAPE5=INPUT,TAPE6=OUTPUT)

CXXXXXXXXXXXXXXXXXXXXXXXXXXXXXXXXXXXXXXXXXXXXXXXXXXXXXXXXXXXXXXXXXXXXXXXX
CXXXXXXXXXXXXXXXXXXXXXXXXXXXXXXXXXXXXXXXXXXXXXXXXXXXXXXXXXXXXXXXXXXXXXXXX
CX                                                                     XX
CX                                                                     XX
CX                        A SEMI-EMPIRICAL MODEL                       XX
CX                                                                     XX
CX                      FOR CHECK VALVE VIBRATIONS                     XX
CX                                                                     XX
CX                                                                     XX
CXXXXXXXXXXXXXXXXXXXXXXXXXXXXXXXXXXXXXXXXXXXXXXXXXXXXXXXXXXXXXXXXXXXXXXXX
CXXXXXXXXXXXXXXXXXXXXXXXXXXXXXXXXXXXXXXXXXXXXXXXXXXXXXXXXXXXXXXXXXXXXXXXX


C     (A) DESCRIPTION OF SUBROUTINE RKGS
C         ==============================
C
C       THIS SUBROUTINE CAN BE USED TO SOLVE A SYSTEM OF FIRST ORDER
C     ORDINARY DIFFERENTIAL EQUATIONS WITH GIVEN INITIAL VALUES
C
C     DEFINITION OF PARAMETERS
C     ------------------------
C
C     PRMT    -AN INPUT AND OUTPUT VECTOR WITH DIMENSION GREATER OR
C              EQUAL TO 5,WHICH SPECIFIES THE PARAMETERS OF THE
C              INTERVAL AND OF ACCURACY AND WHICH SERVES FOR COMMUNICA-
C              TION BETWEEN OUTPUT SUBROUTINE AND SUBROUTINE RKGS.
C              EXCEPT PRMT(5) THE COMPONENTS ARE NOT DESTROYED BY
```

```
C           SUBROUTINE RKGS AND THEY ARE
C
C     PRMT(1) -LOWER BOUND OF THE INTERVAL (INPUT),
C     PRMT(2) -UPPER BOUND OF THE INTERVAL (INPUT),
C     PRMT(3) -INITIAL INCREMENT OF THE INDEPENDENT VARIABLE (INPUT),
C     PRMT(4) -UPPER ERROR BOUND (INPUT).IF ABSOLUTE ERROR IS GREATER
C              THAN PRMT(4) INCREMENT GETS HALVED. IF INCREMENT IS LESS
C              THAN PRMT(3) AND ABSOLUTE ERROR LESS THAN PRMT(4)/50
C              INCREMENT GETS DOUBLED. PRMT(4) MAY BE CHANGED BY MEANS
C              OF SUBROUTINE OUTPUT.
C     PRMT(5) -NO INPUT PARAMETER. SUBROUTINE RKGS INITIALIZES PRMT(5)=0.
C              IF THE USER WANTS TO TERMINATE SUBROUTINE RKGS AT ANY
C              OUTPUT POINT,HE HAS TO CHANGE PRMT(5) TO NON-ZERO BY
C              MEANS OF HIS OUTPUT SUBROUTINE.
C
C     Y       -INPUT VECTOR OF INITIAL VALUES. (DESTROYED)
C              LATERON Y IS THE RESULTING VECTOR OF DEPENDENT VARIABLES
C              COMPUTED AT INTERMEDIATE POINTS X.
C
C     DERY    - INPUT VECTOR OF ERROR WEIGHTS. (DESTROYED)
C              THE SUM OF ITS COMPONENTS MUST BE EQUAL TO 1.LATERON
C              DERY IS THE VECTOR OF DERIVATIVES WHICH BELONG TO
C              FUNCTION VALUES Y AT A POINT X.
C
C     NDIM    -AN INPUT VALUE WHICH SPECIFIES THE NUMBER OF EQUATIONS IN
C              THE SYSTEM.
C
C     IHLF    -AN OUTPUT VALUE WHICH SPECIFIES THE NUMBER OF BISECTIONS
C              OF THE INITIAL INCREMENT. IF IHLF GETS GREATER THAN 10,
C              SUBROUTINE RKGS RETURNS WITH ERROR MESSAGE IHLF=11 INTO
```

```
C              MAIN PROGRAM.ERROR MESSAGE IHLF=12 OR IHLF=13 APPEARS IN
C              CASE PRMT(3)=0 OR IN CASE SIGN(PRMT(3)).NE.SIGN(PRMT(2)
C              -PRMT(1)) RESPECTIVELY.
C
C     FCT      -THE NAME OF AN EXTERNAL SUBROUTINE. THIS SUBROUTINE COMP-
C              UTES THE RIGHT HAND SIDES DERY OF THE SYSTEM TO GIVEN
C              VALUES OF X AND Y. ITS PARAMETER LIST MUST BE X,Y,DERY.
C
C     OUTP     -THE NAME OF AN EXTERNAL OUTPUT SUBROUTINE. ITS PARAMETER
C              LIST MUST BE IHLF,NDIM,PRMT. IF PRMT(5) IS CHANGED TO
C              NON-ZERO,SUBROUTINE RKGS IS TERMINATED.
C
C     AUX      -AN AUXILIARY STORAGE ARRAY WITH 8 ROWS AND NDIM COLUMNS.
C
C
C     REMARKS
C     -------
C
C     THE PROCEDURE TERMINATES AND RETURNS TO CALLING PROGRAM,IF
C     (1) MORE THAN 10 BISECTIONS OF THE INITIAL INCREMENT ARE NECESSARY
C         TO GET SATISFACTORY ACCURACY (ERROR MESSAGE IHLF = 11),
C     (2) INITIAL INCREMENT IS EQUAL TO 0 OR HAS WRONG SIGN (ERROR
C         MESSAGE IHLF = 12 OR IHLF = 13),
C     (3) THE WHOLE INTEGRATION INTERVAL IS WORKED THROUGH,
C     (4) SUBROUTINE OUTP HAS CHANGED PRMT(5) TO NON-ZERO.
C
C
C     (B) PHYSICAL DIMENSIONS OF THE SYSTEM
C         =================================
```

```
C     SK          IS THE SPRING STIFFNESS
C     THO         IS THE INITIAL SETTING ANGLE
C     ZETA        IS THE DAMPING FACTOR
C     A           IS THE CROSS-SECTIONAL AREA OF THE PIPE JUST UPSTREAM
C                 OF THE VALVE
C     RC          MOMENT ARM OF CENTRE OF PRESSURE
C     CM          IS THE REDUCED MASS OF THE VALVE DISC
C     XY          IS THE ANGLE ALONG WHICH THE INERTIAL PRESSURE DOMINATES
C
C     P1,P2,      PRESSURE DIFFERENCES AT INSTANTS OF CLOSING
C     AND P3      AND OPENING
C
C     ALFA1,
C     ALFA2,      SLOPES OF THE BILINEAR APPROXIMATION  OF THE
C     ALFA3       PRESSURE DIFFERENCE
C
C     CPMIN       MINIMUM PRESSURE DIFFERENCE DURING THE CYCLE
C
C     RC          IS THE COEFFICIENT OF RESTITUTION.
C                 AT INSTANT OF OPENING,IF THE HYDROSTATIC PRESSURE
C                 FORCE IS GREATER THAN THE SPRING FORCE TAKE RC=0.5.
C                 IF THE SPRING FORCE IS GREATER THAN THE HYDROSTATIC
C                 PRESSURE FORCE PUT RC=0.0
C
C
      COMMON/A/YY1,YY2,XX,HH,P1,P2,P3,YMAX,CPMIN,CM,A,RC,C,ALFA1,
     1ALFA2,ALFA3,SK,THO,XC,RC,KKK,XY,SL
      COMMON/B/T(500),S(500),V(500),SD(500)
      COMMON/CC/X,Y,CEPY,AUX
```

```
DIMENSION Y(2),DERY(2),PRMT(5),HY(2),HZ(2),HYC(2),AUX(8,2)
EXTERNAL FCT,OUTP


SK       = 68.520528*17.0
THO      = 0.017453*5.0
F1       = 20.869565*34.0
F2       = 20.869565*47.2
F3       = 20.869565*19.75
CFMIN    = 20.975208*2.5


ZEATA    = 0.45
A        = 0.463
FC       = 0.4009
CM       = 0.31767
PH       = 0.025
PRMT(2)  = 0.6
RC       = 0.0
NDIM     = 2


XC       = 0.0
Y(1)     = 0.0
Y(2)     = 0.0
XX       = 0.0
YMAX     = THO
YY1      = Y(1)
YY2      = Y(2)
DERY(1)  = 0.4
```

```
CERY(2) = 0.6

SL      = 0.41304

C       = 35.0*ZEATA
ALFA1   = (P1-DPMIN)/YMAX
ALFA3   = (P3-DPMIN)/YMAX
XY      = (YMAX-0.0283616)*SL
DPMIN2  = P1-ALFA1*XY
ALFA2   = (P2-DPMIN2)/XY

FRMT(1) = 0.0
FRMT(3) = HM/10.0
FRMT(4) = 0.5E-03

KKK     = 1
T(1)    = FRMT(1)
S(1)    = YY1
V(1)    = YY2
SC(1)   = S(1)/0.017453

DATA HX/10HTIME (SEC)/
DATA HY/10HDISPLACEME,8HNT (RAD)/
DATA HZ/10HVELOCITY (,8HRAD/SEC)/
DATA HYC/10HDISPLACEME,8HNT (DEG)/
```

```
      WRITE(6,20)
   20 FORMAT(1H1,2X,*PT.NO.*,11X,*TIME*,13X,*DISPLACEMENT*,
     111X,*VELOCITY*,30X,*ACCELERATION*,7X,*IHLF*,/)

      WRITE(6,40)
   40 FORMAT(19X,*(SEC.)*,15X,*(RAD.)*,13X,
     1*(RAD/SEC)*,30X,*(RAD/SC.SEC)*,////)


      CALL  RKGS(PRMT,NDIM,IHLF,FCT,OUTP)

  300 WRITE(6,310) IHLF
  310 FORMAT(1H1,5X,I4)


      AB(1)   = 0.0
      AB(2)   = 0.5

      BC(1)   = 0.0
      BC(2)   = 0.1

      CC(1)   = -2.5
      CC(2)   = 2.5


      CALL MAP(AB,BC,2,HX,HY,10,18)
      CALL PLTMPL(T,S,KKK)
      CALL PLOT(12.,0.0,-3)

      CALL MAP(BC,CC,2,HY,HZ,18,18)
```

```
      CALL PLTMPL(S,V,KKK)
      CALL PLOT(0.0,0.0,999)


      STOP
      END
      SUBROUTINE OUTP(IHLF,NDIM,PRMT)
      COMMON/A/YY1,YY2,XX,HH,P1,P2,P3,YMAX,DPMIN,DM,A,BC,C,ALFA1,
     1ALFA2,ALFA3,SK,THO,XC,RC,KKK,XY,SL
      COMMON/B/T(500),S(500),V(500),SD(500)
      COMMON/CC/X,Y,DERY,AUX
      DIMENSION Y(2),DERY(2),AUX(8,2),PRMT(5)


      IF(IHLF.GT.10)   GO TO 300
      IF(Y(1).LT.0.0)   GO TO 70
      IF(YY2.EQ.0.0) GO TO 100


      IF(Y(2)*YY2)   60,60,100
   60 IF(YY2.LT.0.0) GO TO 100

      IF(ABS(YMAX-YY1).LE.0.0005)   GO TO 50

      YMAX     = Y(1)

      DPMIN    = P3-ALFA3*YMAX
      ALFA1    = (P1-DPMIN)/YMAX
      XY       = (YMAX-0.0293616)*SL
      IF(XY.LT.0.0) GO TO 100
```

```
      CFMIN2   = P1-ALFA1*XY
      ALFA2    = (F2-DFMIN2)/XY
      GC TC 100

   70 CCNTINUE
      X     = XX+YY1*(X-XX)/(YY1-Y(1))
      Y(2)     = YY2+YY1*(Y(2)-YY2)/(YY1-Y(1))
      Y(1)     = 0.0

      WRITE(6,200) KKK,X,(Y(I),I=1,2),(CERY(I),I=1,2),IHLF

      T(KKK)   = X
      S(KKK)   = Y(1)
      V(KKK)   = Y(2)
      SD(KKK)  = S(KKK)/0.017453

      KKK      = KKK+1

      Y(2)     = -FC*Y(2)
      CERY(1)  = Y(2)
      CI       = 1.0
      Z        = CI*PO*A
      CERY(2)  = (SK*THO-Z*P3-C*Y(2)-(SK-Z*ALF13)*Y(1))/CM

      CC 3 I=1,NCIM
      AUX(1,I) = Y(I)
      ALX(2,I) = CERY(I)
```

```
      ALX(3,I) = 0.0
    3 ALX(6,I) = 0.0
      GC TC 100


   30 WRITE(6,40)
   40 FCRMAT(1H1,5X,*STEADY STATE SOLUTICN IS CBTAINED*
     1,/,10X,*MAX. ERROR 1.05 PERCENT*)
      FRNT(5) = 5.0

  100 CONTINUE

      IF(Y(1).EC.YY1.ANC.Y(2).EC.YY2)   X=XX

   10 WRITE(6,200) KKK,X,(Y(I),I=1,2),(DERY(I),I=1,2),IHLF
  200 FCRMAT(3X,I5,5(5X,E16.9),5X,I3,//)


      T(KKK) = X
      S(KKK) = Y(1)
      V(KKK) = Y(2)
      SD(KKK) = S(KKK)/0.317493


      IF(KKK.GT.300) GO TO 300
      KKK = KKK+1

  110 YY1 = Y(1)
      YY2 = Y(2)
      XX  = X
```

```
      GO TO 320
  300 WRITE(6,310) IHLF
  310 FORMAT(1H1,5X,I4)
      PRMT(5) = 5.0
      KKK = KKK-1

  320 CONTINUE

      RETURN
      END
      SUBROUTINE FCT(X,Y,DERY)
      COMMON/A/YY1,YY2,XX,HF,P1,P2,P3,YMAX,CFMIN,CM,A,RC,C,ALFA1,
     1ALFA2,ALFA3,SK,THO,XC,RC,KKK,XY,SL
      DIMENSION Y(2),DERY(2)


      CI       = 1.0


      DERY(1) = Y(2)
      Z        = CI*RO*A


      IF(Y(2)) 10,5,20
    5 IF(YY2.GT.0.0) GO TO 10

   20 DERY(2) = (SK*THO-Z*P3-C*Y(2)-(SK-Z*ALFA3)*Y(1))/CM
```

```
      GO TO 30
   10 IF(Y(1).LT.XY) GO TO 40
      DERY(2) = (SK*THO-Z*P1-C*Y(2)-(SK-Z*ALFA1)*Y(1))/CM
      GO TO 30
   40 DERY(2) = (SK*THO-Z*P2-C*Y(2)-(SK-Z*ALFA2)*Y(1))/CM
   30 CONTINUE
      RETURN
      END
      SUBROUTINE  RKGS(PRMT,NDIM,IHLF,FCT,OUTP)
C
C
      COMMON/CC/X,Y,DERY,AUX
      DIMENSION Y(2),DERY(2),AUX(8,2),A(4),B(4),C(4),PRMT(5)
      DO 1 I=1,NDIM
    1 AUX(8,I)=.06666667*DERY(I)
      X=PRMT(1)
      XEND=PRMT(2)
      H=PRMT(3)
      PRMT(5)=0.
      CALL FCT(X,Y,DERY)
C
C     ERROR TEST
      IF(H*(XEND-X))38,37,2
C
```

```
C     PREPARATIONS FOR RUNGE-KUTTA METHOD
    2 A(1)=.5
      A(2)=.2928932
      A(3)=1.707107
      A(4)=.1666667
      B(1)=2.
      B(2)=1.
      B(3)=1.
      B(4)=2.
      C(1)=.5
      C(2)=.2928932
      C(3)=1.707107
      C(4)=.5
C
C     PREPARATIONS OF FIRST RUNGE-KUTTA STEP.
      DO 3 I=1,NDIM
      AUX(1,I)=Y(I)
      AUX(2,I)=DERY(I)
      AUX(3,I)=0.
    3 AUX(6,I)=0.
      IREC=0
      H=H+H
      IHLF=-1
      ISTEP=0
      IEND=0
C
C
C     START OF A RUNGE-KUTTA STEP
    4 IF((X+H-XEND)*H)7,6,5
    5 H=XEND-X
```

```
    6 IEND=1
C
C      RECORDING OF INITIAL VALUES OF THIS STEP
    7 CALL OUTP(IREC,NDIM,PRMT)
      IF(PRMT(5))40,8,40
    8 ITEST=0
    9 ISTEP=ISTEP+1
C
C
C      START OF INNERMOST RUNGE-KUTTA LOOP
      J=1
   10 AJ=A(J)
      BJ=B(J)
      CJ=C(J)
      DO 11 I=1,NDIM
      R1=H*DERY(I)
      R2=AJ*(R1-BJ*AUX(6,I))
      Y(I)=Y(I)+R2
      R2=R2+R2+R2
   11 AUX(6,I)=AUX(6,I)+R2-CJ*R1
      IF(J-4)12,15,15
   12 J=J+1
      IF(J-3)13,14,13
   13 X=X+.5*H
   14 CALL FCT(X,Y,DERY)
      GOTO 10
C      END OF INNERMOST RUNGE-KUTTA LOOP
C
C
C      TEST OF ACCURACY
```

```
   15 IF(ITEST)16,16,20
C
C      IN CASE ITEST=0 THERE IS NO POSSIBILITY FOR TESTING OF ACCURACY
   16 DO 17 I=1,NDIM
   17 AUX(4,I)=Y(I)
      ITEST=1
      ISTEP=ISTEP+ISTEP-2
   18 IHLF=IHLF+1
      X=X-H
      H=.5*H
      DO 19 I=1,NDIM
      Y(I)=AUX(1,I)
      DERY(I)=AUX(2,I)
   19 AUX(6,I)=AUX(3,I)
      GOTO 9
C
C      IN CASE ITEST=1 TESTING OF ACCURACY IS POSSIBLE
   20 IMOD=ISTEP/2
      IF(ISTEP-IMOD-IMOD)21,23,21
   21 CALL FCT(X,Y,DERY)
      DO 22 I=1,NDIM
      AUX(5,I)=Y(I)
   22 AUX(7,I)=DERY(I)
      GOTO 9
C
C      COMPUTATION OF TEST VALUE DELT
   23 DELT=0.
      DO 24 I=1,NDIM
   24 DELT=DELT+AUX(8,I)*ABS(AUX(4,I)-Y(I))
      IF(DELT-PRMT(4))28,28,25
```

```
C
C     ERROR IS TOO GREAT
   25 IF(IHLF-10)26,36,36
   26 DO 27 I=1,NDIM
   27 AUX(4,I)=AUX(5,I)
      ISTEP=ISTEP+ISTEP-4
      X=X-H
      IEND=0
      GOTO 19
C
C     RESULT VALUES ARE GOOD
   28 CALL FCT(X,Y,DERY)
      DO 29 I=1,NDIM
      AUX(1,I)=Y(I)
      AUX(2,I)=DERY(I)
      AUX(3,I)=AUX(6,I)
      Y(I)=AUX(5,I)
   29 DERY(I)=AUX(7,I)
      X  = X-H
      CALL OUTP(IHLF,NDIM,PRMT)
      X  = X+H
      IF(PRMT(5))40,30,40
   30 DO 31 I=1,NDIM
      Y(I)=AUX(1,I)
   31 DERY(I)=AUX(2,I)
      IREC=IHLF
      IF(IEND)32,32,39
C
C     INCREMENT GETS DOUBLED
   32 IHLF=IHLF-1
```

```
      ISTEP=ISTEP/2
      H=H+H
      IF(IHLF)4,33,33
   33 IMOD=ISTEP/2
      IF(ISTEP-IMOD-IMOD)4,34,4
   34 IF(DELT-.02*PRMT(4))35,35,4
   35 IHLF=IHLF-1
      ISTEP=ISTEP/2
      H=H+H
      GOTO 4
C
C
C     RETURNS TO CALLING PROGRAM
   36 IHLF=11
      CALL FCT(X,Y,DERY)
      GOTO 39
   37 IHLF=12
      GOTO 39
   38 IHLF=13
   39 CALL OUTP(IHLF,NDIM,PRMT)
   40 RETURN
      END
      SUBROUTINE MAP(X,Y,M,HX,HY,NHX,NHY)
      DIMENSION X(1),Y(1),HX(1),HY(1)
      NX=10
      NY=10
      XL=10.0
      YL=6.5
      XM=2.0
      YM=2.0
```

```
      XY=XL-FLCAT(NHX)*0.1
      YY=YL-FLCAT(NHY)*0.1
      CALL FLCT(0.0,0.0,-3)
      CALL CATE(C1)
      CALL LETTER(10,0.2,30.0,1.,3.,10H*MODEL 1 *)
      CALL LETTER(10,0.1,30.C,1.3,2.5,C1)
      CALL FLCT(2.,0.0,-3)
      CALL LETTER(NHX,0.1,0.C,XY,0.7,HX)
      CALL LETTER(NHY,0.1,90.C,0.8,YY,HY)
      CALL FACTCR (M ,X,Y,XL,YL,XM,YM)
      CALL FLCT(XM,YM,3)
      CALL FLCT(XL,YM,2)
      CALL FLCT(XL,YL,1)
      CALL FLCT(XM,YL,1)
      CALL FLCT(XM,YM,1)
      YS=(YL-YM)/FLOAT(NY)
      XH=XM
      YH=YM
   20 CALL FLCT(XH,YH,3)
      CALL FLCT(XH+.07,YH,2)
      CALL FLCT(XL-.07,YH,3)
      CALL FLCT(XL,YH,2)
      CALL INCHTC(XM,YH,XP,YP)
      ENCCDE(10,30,YD) YP
      CALL LETTER(10,0.1, 0.0,0.9,YH-.05,YD)
      YH=YH+YS
      IF(YH.LE.YL) GO TC 20
      XS=(XL-XM)/FLOAT(NX)
   22 CALL FLCT(XH,YM,3)
      CALL FLCT(XH,YM+.07,2)
```

```
      CALL PLOT(XH,YL-.07,3)
      CALL PLOT(XH,YL,2)
      CALL INCHTC(XH,YM,XW,YW)
      ENCODE(10,30,XD) XW
      CALL LETTER(10,0.1,90.,XH+.05,0.9,XD)
      XH=XH+XS
      IF(XH.LE.XL) GO TO 22
   30 FORMAT(2PE10.2)
      RETURN
      END
```

A.2. General Model of Hydraulic Control Devices

Substituting in the model equations (equations 3.30 and 3.31) x for the time t, y_1 for the discharge $\bar{q}$, y_2 for the displacement $\bar{x}$, and y_3 for the velocity $\dot{\bar{x}}$ and rearranging get the following equations:

$$y_1' = \frac{1}{\alpha}[\Delta\bar{P} - \psi y_1^2 - \frac{n^2 - C_c^2 y_2^2}{C_d^2} (\frac{y_1}{y_2})^2] \quad \ldots\ldots \quad A.3(a)$$

$$y_2' = y_3 \quad \ldots\ldots\ldots\ldots\ldots \quad A.3(b)$$

$$y_3' = \bar{K}(\beta - y_2) - 2\xi y_3 - \frac{1}{2}\mu(\Delta\bar{P} - \psi y_1^2 - \alpha y_1') \quad \ldots \quad A.3(c)$$

or

$$\underline{Y}' = \frac{d\underline{Y}}{dx} = \underline{F}(x, \underline{Y})$$

which is the same form given by equation A.1.

It is important to note that equation A.3(a) is a singular equation, i.e. at the closed position, both the discharge y_1 and the displacement y_2 are equal to zero. Physically, the rate of change of discharge with time y_1' should be equal to zero when the control device is closed. The following substitution was used to this mathematical singularity over a very small opening.

$$y_1' = 0 \qquad \text{at } y_2 = 0$$

$$y_1' = k \qquad \text{at } y_2 < r, \text{ and } y_2 > 0$$

where k is a small positive constant. The approximate value of k is determined by the valve which gives a smooth curve of discharge against displacement at $y_2 = r$.

```
C      RM         MASS RATIO
C      CPR        DIMENSIONLESS PRESSURE DIFFERENCE
C      PSI        LOSS FACTOR
C      ALFA       INERTIA FACTOR
C      CD         DYNAMIC DISCHARGE COEFFICIENT

C      RC         IS THE COEFFICIENT OF RESTITUTION.
C                 AT INSTANT OF OPENING,IF THE HYDROSTATIC PRESSURE
C                 FORCE IS GREATER THAN THE SPRING FORCE TAKE RC=0.05.
C                 IF THE SPRING FORCE IS GREATER THAN THE HYDROSTATIC
C                 PRESSURE FORCE PUT RC=0.0

      COMMON/A/ZEATA,CPR,SK3,BEATA,EATA,ALFA,RM,PSI,CD,CC,
     1YY1,YY2,YY3,XX,HH,YMAX,YC,RC,KKK,DERY1,DDER,Q
      COMMON/B/T(700),S(700),V(700),U(700),Z(700)
      COMMON/C/FAC5
      COMMON/GG/X,Y,DERY,AUX

      DIMENSION Y(3),DERY(3),PRMT(5),HY(2),HZ(2),HW(2),AUX(8,3)
      DIMENSION AB(2),BC(2),CD1(2),DE(2)
      DIMENSION HP(3),FG(2)
      EXTERNAL FCT,OUTP

      S       =  0.463
      A       =  0.375
      DJ      =  0.31767
```

```
      PROGRAM TST (INPUT,OUTPUT,TAPE5=INPUT,TAPE6=OUTPUT)

CXXXXXXXXXXXXXXXXXXXXXXXXXXXXXXXXXXXXXXXXXXXXXXXXXXXXXXXXXXXXXX
CXXXXXXXXXXXXXXXXXXXXXXXXXXXXXXXXXXXXXXXXXXXXXXXXXXXXXXXXXXXXXX
CX                                                           XX
CX                                                           XX
CX                                                           XX
CX                 A MECHANISM FOR SELF EXCITATION           XX
CX                                                           XX
CX                  IN HYDRAULIC-CONTROL DEVICES             XX
CX                                                           XX
CX                                                           XX
CX                                                           XX
CXXXXXXXXXXXXXXXXXXXXXXXXXXXXXXXXXXXXXXXXXXXXXXXXXXXXXXXXXXXXXX
CXXXXXXXXXXXXXXXXXXXXXXXXXXXXXXXXXXXXXXXXXXXXXXXXXXXXXXXXXXXXXX

C     (A) DESCRIPTION OF SUBROUTINE RKGS
C         ============================

C       THIS SUBROUTINE CAN BE USED TO SOLVE A SYSTEM OF FIRST ORDER
C     ORDINARY DIFFERENTIAL EQUATIONS WITH GIVEN INITIAL VALUES

C     DEFINITION OF PARAMETERS
C     ------------------------

C     PRMT     -AN INPUT AND OUTPUT VECTOR WITH DIMENSION GREATER OR
C               EQUAL TO 5,WHICH SPESIFIES THE PARAMETERS OF THE
C               INTERVAL AND OF ACCURACY AND WHICH SERVES FOR COMMUNICA-
```

```
C                 TION BETWEEN OUTPUT SUBROUTINE AND SUBROUTINE RKGS.
C                 EXCEPT PRMT(5) THE COMPONENTS ARE NOT DESTROYED BY
C                 SUBROUTINE RKGS AND THEY ARE

C        PRMT(1) -LOWER BOUND OF THE INTERVAL (INPUT),
C        PRMT(2) -UPPER BOUND OF THE INTERVAL (INPUT),
C        PRMT(3) -INITIAL INCREMENT OF THE INDEPENDENT VARIABLE (INPUT),
C        PRMT(4) -UPPER ERROR BOUND (INPUT).IF ABSOLUTE ERROR IS GREATER
C                 THAN PRMT(4) INCREMENT GETS HALVED. IF INCREMENT IS LESS
C                 THAN PRMT(3) AND ABSOLUTE ERROR LESS THAN PRMT(4)/50
C                 INCREMENT GETS DOUBLED. PRMT(4) MAY BE CHANGED BY MEANS
C                 OF SUBROUTINE OUTPUT.
C        PRMT(5) -NO INPUT PARAMETER. SUBROUTINE RKGS INIALIZES PRMT(5)=0.
C                 IF THE USER WANTS TO TERMINATE SUBROUTINE RKGS AT ANY
C                 OUTPUT POINT,HE HAS TO CHANGE PRMT(5) TO NON-ZERO BY
C                 MEANS OF HIS OUTPUT SUBROUTINE.

C        Y       -INPUT VECTOR OF INITIAL VALUES. (DESTROYED)
C                 LATERON Y IS THE RESULTING VECTOR OF DEPENDENT VARIABLES
C                 COMPUTED AT INTERMEDIATE POINTS X.

C        DERY    - INPUT VECTOR OF ERROR WEIGHTS. (DESTROYED)
C                 THE SUM OF ITS COMPONENTS MUST BE EQUAL TO 1.LATERON
C                 DERY IS THE VECTOR OF DERIVATIVES WHICH BELONG TO
C                 FUNCTION VALUES Y AT A POINT X.

C        NDIM    -AN INPUT VALUE WHICH SPECIFIES THE NUMBER OF EQUATIONS IN
C                 THE SYSTEM.

C        IHLF    -AN OUTPUT VALUE WHICH SPECIFIES THE NUMBER OF BISECTIONS
```

```
C               OF THE INITIAL INCREMENT. IF IHLF GETS GREATER THAN 10,
C               SUBROUTINE RKGS RETURNS WITH ERROR MESSAGE IHLF=11 INTO
C               MAIN PROGRAM.ERROR MESSAGE IHLF=12 OR IHLF=13 APPEARS IN
C               CASE PRMT(3)=0 OR IN CASE SIGN(PRMT(3)).NE.SIGN(PRMT(2)
C               -PRMT(1)) RESPECTIVELY.
C
C        FCT    -THE NAME OF AN EXTERNAL SUBROUTINE. THIS SUBROUTINE COMP-
C               UTES THE RIGHT HAND SIDES DERY OF THE SYSTEM TO GIVEN
C               VALUES OF X AND Y. ITS PARAMETER LIST MUST BE X,Y,DERY.
C
C        OUTP   -THE NAME OF AN EXTERNAL OUTPUT SUBROUTINE. ITS PARAMETER
C               LIST MUST BE IHLF,NDIM,PRMT. IF PRMT(5) IS CHANGED TO
C               NON-ZERO,SUBROUTINE RKGS IS TERMINATED.
C
C        AUX    -AN AUXILIARY STORAGE ARRAY WITH 8 ROWS AND NDIM COLUMNS.
C
C
C        REMARKS
C        -------
C
C        THE PROCEDURE TERMINATES AND RETURNS TO CALLING PROGRAM,IF
C        (1) MORE THAN 10 BISECTIONS OF THE INITIAL INCREMENT ARE NECESSARY
C            TO GET SATISFACTORY ACCURACY (ERROR MESSAGE IHLF = 11),
C        (2) INITIAL INCREMENT IS EQUAL TO 0 OR HAS WRONG SIGN (ERROR
C            MESSAGE IHLF = 12 OR IHLF = 13),
C        (3) THE WHOLE INTEGRATION INTERVAL IS WORKED THROUGH,
C        (4) SUBROUTINE OUTP HAS CHANGED PRMT(5) TO NON-ZERO.
C
C
C        (E) PHYSICAL DIMENSIONS OF THE SYSTEM
```

```
C          ==================================

C    S      IS THE CONTROL ELEMENT AREA WHICH IS SUBJECTED TO THE
C           PRESSURE DIFFERENCE,
C    A      IS THE CROSS-SECTIONAL AREA OF THE CONDUIT JUST UPSTREAM
C           OF THE CONTROL DEVICE,
C    CJ     IS THE REDUCED MASS (OR MOMENT OF INERTIA) OF THE MOVING
C           PARTS,
C    CI     IS THE MOMENT ARM OF THE CENTRE OF PRESSURE,
C    G      IS THE ACCELERATION OF GRAVITY,
C    GAMA   IS THE SPECIFIC WEIGHT OF THE FLOWING FLUID,
C    ROW    IS THE FLUID DENSITY,.
C    STL    IS THE EQUIVALENT LENGTH OF THE SYSTEM.

C    (C) REFERENCE QUANTITIES
C        ====================

C    D          REFERENCE DIMENSION
C    SKR        REFERENCE STIFFNESS
C    WR         REFERENCE FREQUENCY
C    DPR        REFERENCE PRESSURE DIFFERENCE

C    (D) DESIGN PARAMETERS
C        =================

C    ZEATA      DAMPING FACTOR
C    SK?        DIMENSIONLESS STIFFNESS
C    BEATA      INITIAL SETTING PARAMETER
```

```
C      RM          MASS RATIO
C      DPR         DIMENSIONLESS PRESSURE DIFFERENCE
C      PSI         LOSS FACTOR
C      ALFA        INERTIA FACTOR
C      CD          DYNAMIC DISCHARGE COEFFICIENT

C      RC          IS THE COEFFICIENT OF RESTITUTION.
C                  AT INSTANT OF OPENING,IF THE HYDROSTATIC PRESSURE
C                  FORCE IS GREATER THAN THE SPRING FORCE TAKE RC=0.05.
C                  IF THE SPRING FORCE IS GREATER THAN THE HYDROSTATIC
C                  PRESSURE FORCE PUT RC=0.0

       COMMON/A/ZEATA,DPR,SK3,BEATA,EATA,ALFA,RM,PSI,CD,CG,
      1YY1,YY2,YY3,XX,HH,YMAX,XC,RC,KKK,DERY1,DDER,Q
       COMMON/B/T(700),S(700),V(700),U(700),Z(700)
       COMMON/C/FAC5
       COMMON/GG/X,Y,DERY,AUX

       DIMENSION Y(3),DERY(3),PRMT(5),HY(2),HZ(2),HW(2),AUX(8,3)
       DIMENSION AB(2),BC(2),CD1(2),DE(2)
       DIMENSION HP(3),FG(2)
       EXTERNAL FCT,OUTP

       S        =  0.463
       A        = 0.375
       CJ       = 0.31767
```

```
      CI     = 0.4009
      GAMA   = 62.4
      G      = 32.12
      RCH    = GAMA/G
      STL    = 55.0

      D      = 0.017453*10.0
      SKR    = 68.520528*20.0
      WR     = SQRT(SKR/DJ)
      DPR    = 0.5*RCH*(CI*WR*D)**2.0
      EATA   = A/(S*D)

C     DESIGN PARAMETERS
C     =================

      ZEATA  = 0.45
      SKB    = 1.0
      BEATA  = 0.4
      RM     = RCH*S*D*(CI**2.0)/CJ
      CFB    = 547.638/DPR
      PSI    = 50.0
      ALFA   = 2.0*STL/(CI*D)
      CC     = 0.95
      CD     = 0.95

      WRITE(6,3) EATA,DPR,RM,ALFA,WR
```

```
3 FORMAT(1H1,5X,*RATA   = *,E16.9,//,
 15X,*RRR     = *,E16.9,//,
 35X,*RM      = *,E16.9,//,
 35X,*ALFA    = *,E16.9,//,
 45X,*WR      = *,E16.9,//)


  HH       = 0.5
  PRMT(2)  = 25.0
  RC       = 0.05
  YMAX     = 1.0
  XC       = 0.0
  Y(1)     = 0.0
  Y(2)     = 0.0
  Y(3)     = 0.05


  XX       = 0.5
  YY1      = Y(1)
  YY2      = Y(2)
  YY3      = Y(3)
  DERY1    = 0.0


  DERY(1)  = 0.4
  DERY(2)  = 0.5
  DERY(3)  = 0.1

  NDIM     = 3
```

```
      PRNT(1) = 0.0
      PRNT(3) = HH/10.0
      PRNT(4) = 5.5E-03
      KKK     = 1

      FAC5    = 0.5*FM*DP9
      T(1)    = PRNT(1)
      S(1)    = YY1
      V(1)    = YY2
      L(1)    = YY3
      Z(1)    = FAC5

      DATA HX/8HTIME ( )/
      DATA HY/10HDISPLACEME,6HNT ()/
      DATA HZ/10HVELOCITY (,2HX)/
      DATA HW/10HDISCHARGE ,3H( )/
      DATA HP/10HPRESSURE D,10HIFFERENCE ,4H( F)/

      WRITE(6,20)
   20 FORMAT(1H1,2X,*RT.NO.*,11X,*TIME*,13X,*DISCHARGE(Q)*,
     115X,*DISPLACEMENT*,13X,*VELOCITY*,10X,*ACCELERATION*,12X,
     2*DQ/DT*,///)

      CALL  RKGS(PRMT,Y,DERY,NDIM,IHLF,FCT,OUTP,AUX)
      KKK     = KKK-1
```

```
300 WRITE(6,310) IHLF
310 FORMAT(1H1,5X,I4)

    AE(1)    = 0.0
    AE(2)    = 10.0

    BC(1)    = 0.0
    BC(2)    = 0.5

    CC1(1)   = -0.5
    CC1(2)   = 0.5

    CALL MAP(AE,BC,2,HX,HY,8,16)
    CALL PLTPFL(T,V,KKK)
    CALL PLOT(12.0,0.0,-3)

    CALL MAP(BC,CD1,2,HY,HZ,16,12)
    CALL PLTPFL(V,U,KKK)
    CALL PLOT(0.0,0.0,999)

    STOP
    END
    SUBROUTINE OUTP(IHLF,NDIM,PRMT)
    COMMON/A/ZEATA,CPE,SKE,BEATA,EATA,ALFA,PM,PSI,CS,CC,
   1YY1,YY2,YY3,XX,HH,YY4),YC,FC,KKK,CEPY1,CCEP,G
```

```
      COMMON/B/T(700),S(700),V(700),U(700),Z(700)
      COMMON/C/FAC5

      COMMON/GG/X,Y,DERY,AUX

      DIMENSION DERY(3),Y(3),AUX(8,3),PRMT(5)

      IF(IHLF.GT.10) GO TO 200
      IF(Y(2).LT.0.0) GO TO70

      IF(YY3.EQ.0.0) GO TO 100
      IF(Y(3)*YY3) 60,60,100


   60 IF(YY3.LT.0.0) GO TO 100
      YMAX    = YY2
      IF(Y(2).GT.YY2)    YMAX = Y(2)

      GO TO 100
   70 CONTINUE

      X       = XX+YY2*(X-XX)/(YY2-Y(2))
      Y(3)    = YY3+YY2*(Y(3)-YY3)/(YY2-Y(2))
      Y(1)    = 0.0
      Y(2)    = 0.0

      WRITE(6,200) KKK,X,(Y(I),I=1,3),FAC5,DERY(1)
      T(KKK)  = X
      S(KKK)  = Y(1)
      V(KKK) = Y(2)
```

```
      U(KKK)  = Y(3)
      Z(KKK)  = FAC5
      KKK     = KKK+1
      Y(3)    = -RC*Y(3)


      DERY(1) = 0.0
      DERY(2) = Y(3)
      FAC3    = SKB*(BEATA-Y(2))
      FAC4    = 2.0*ZEATA*Y(3)
      FAC5    = 0.5*RH*(DPB-PSI*Y(1)**2.0-ALFA*DERY(1))
      DERY(3) = FAC3-FAC4-FAC5


      DO 3 I=1,NDIM
      ALX(1,I) = Y(I)
      ALX(2,I) = DERY(I)
      ALX(3,I) = 0.0
    3 ALX(6,I) = 0.0


  100 CONTINUE


      IF(Y(2).EQ.YY2.AND.Y(3).EQ.YY3)   X=RX
   10 WRITE(6,200) KKK,X,(Y(I),I=1,3),FAC5,DERY(1)
  200 FORMAT(3X,I5,6(5X,E16.9),//)


      T(KKK)  = X
```

```
      S(KKK)   = Y(1)
      V(KKK)   = Y(2)
      C(KKK)   = Y(3)
      Z(KKK)   = FAC5

      IF(KKK.GT.700) GO TO 300
      KKK      = KKK+1


  110 YY1      = Y(1)
      YY2      = Y(2)
      YY3      = Y(3)
      XX       = X
      DDER     = DERY(1)-DERY1
      DERY1    = DERY(1)

      GO TO 320


  300 WRITE(6,310) IHLF
  310 FORMAT(1H1,5X,I4)
      PRMT(5) = 5.0
      KKK      = KKK-1
  320 CONTINUE


      RETURN
      END
      SUBROUTINE FCT(X,Y,DERY)
      COMMON/A/ZEATA,DPR,SKE,BEATA,EATA,ALFA,FM,PSI,CD,CC,
```

```
 1YY1,YY2,YY3,XX,HH,YMAX,XC,FC,KKK,DERY1,DCER,D
  COMMON/C/FACE
  DIMENSION Y(3),DERY(3)

  EF       = D*Y(2)
  IF(Y(2).EQ.0.0) GO TO 10
  IF(EF.LT.0.003.AND.Y(3).LT.0.0) GO TO 15
  IF(EF.LT.0.0015.AND.Y(3).GT.0.0) GO TO 30

  FAC1     = EATA**2.0-(CC*Y(2))**2.0
  FAC2     = (Y(1)/(CC*Y(2)))**2.0
  DERY(1) = (DPB-PSI*Y(1)**2.0-FAC1*FAC2)/ALFA

  GO TO 20
10 DERY(1) = 0.0
  GO TO 20
30 DERY(1) = 0.015
  GO TO 20

15 DERY(1) = DERY1+DCER

20 DERY(2) = Y(3)

  FAC3     = SKB*(BEAT1-Y(2))
  FAC4     = 2.0*ZEATA*Y(3)
```

```
      FAC5    = 0.5*PM*(CPB-FSI*Y(1)**2.0-ALFA*CERY(1))
      CERY(3) = FAC3-FAC4-FAC5


      RETURN
      END
      SUBROUTINE  RKGS(PRMT,NDIM,IHLF,FCT,OUTP)
C
C
      COMMON/GG/X,Y,DERY,AUX
      DIMENSION Y(3),DERY(3),AUX(8,3),A(4),B(4),C(4),PRMT(5)
      DO 1 I=1,NDIM
    1 AUX(8,I)=.06666667*DERY(I)
      X=PRMT(1)
      XEND=PRMT(2)
      H=PRMT(3)
      PRMT(5)=0.
      CALL FCT(X,Y,DERY)
C
C     ERROR TEST
      IF(H*(XEND-X))38,37,2
C
C     PREPARATIONS FOR RUNGE-KUTTA METHOD
    2 A(1)=.5
      A(2)=.2928932
      A(3)=1.707107
      A(4)=.1666667
      B(1)=2.
      B(2)=1.
      B(3)=1.
```

```
      B(4)=2.
      C(1)=.5
      C(2)=.2928932
      C(3)=1.707107
      C(4)=.5
C
C     PREPARATIONS OF FIRST RUNGE-KUTTA STEP
      DO 3 I=1,NDIM
      AUX(1,I)=Y(I)
      AUX(2,I)=DERY(I)
      AUX(3,I)=0.
    3 AUX(6,I)=0.
      IREC=0
      H=H+H
      IHLF=-1
      ISTEP=0
      IEND=0
C
C
C     START OF A RUNGE-KUTTA STEP
    4 IF((X+H-XEND)*H)7,6,5
    5 H=XEND-X
    6 IEND=1
C
C     RECORDING OF INITIAL VALUES OF THIS STEP
    7 CALL OUTP(IREC,NDIM,PRMT)
      IF(PRMT(5))40,8,40
    8 ITEST=0
    9 ISTEP=ISTEP+1
C
```

```
C
C     START OF INNERMOST RUNGE-KUTTA LOOP
      J=1
   10 AJ=A(J)
      BJ=B(J)
      CJ=C(J)
      DO 11 I=1,NDIM
      R1=H*DERY(I)
      R2=AJ*(R1-BJ*AUX(6,I))
      Y(I)=Y(I)+R2
      R2=R2+R2+R2
   11 AUX(6,I)=AUX(6,I)+R2-CJ*R1
      IF(J-4)12,15,15
   12 J=J+1
      IF(J-3)13,14,13
   13 X=X+.5*H
   14 CALL FCT(X,Y,DERY)
      GOTO 10
C     END OF INNERMOST RUNGE-KUTTA LOOP
C
C
C     TEST OF ACCURACY
   15 IF(ITEST)16,16,20
C
C     IN CASE ITEST=0 THERE IS NO POSSIBILITY FOR TESTING OF ACCURACY
   16 DO 17 I=1,NDIM
   17 AUX(4,I)=Y(I)
      ITEST=1
      ISTEP=ISTEP+ISTEP-2
   18 IHLF=IHLF+1
```

```
      X=X-H
      H=.5*H
      DO 19 I=1,NDIM
      Y(I)=AUX(1,I)
      DERY(I)=AUX(2,I)
   19 AUX(6,I)=AUX(3,I)
      GOTO 9
C
C     IN CASE ITEST=1 TESTING OF ACCURACY IS POSSIBLE
   20 IMOD=ISTEP/2
      IF(ISTEP-IMOD-IMOD)21,23,21
   21 CALL FCT(X,Y,DERY)
      DO 22 I=1,NDIM
      AUX(5,I)=Y(I)
   22 AUX(7,I)=DERY(I)
      GOTO 9
C
C     COMPUTATION OF TEST VALUE DELT
   23 DELT=0.
      DO 24 I=1,NDIM
   24 DELT=DELT+AUX(8,I)*ABS(AUX(4,I)-Y(I))
      IF(DELT-PRMT(4))28,28,25
C
C     ERROR IS TOO GREAT
   25 IF(IHLF-10)26,36,36
   26 DO 27 I=1,NDIM
   27 AUX(4,I)=AUX(5,I)
      ISTEP=ISTEP+ISTEP-4
      X=X-H
      IEND=0
```

```
      GOTO 18
C
C     RESULT VALUES ARE GOOD
   28 CALL FCT(X,Y,DERY)
      DO 29 I=1,NDIM
      AUX(1,I)=Y(I)
      AUX(2,I)=DERY(I)
      AUX(3,I)=AUX(6,I)
      Y(I)=AUX(5,I)
   29 DERY(I)=AUX(7,I)
      X  = X-H
      CALL OUTP(IHLF,NDIM,PRMT)
      X  = X+H
      IF(PRMT(5))40,30,40
   30 DO 31 I=1,NDIM
      Y(I)=AUX(1,I)
   31 DERY(I)=AUX(2,I)
      IREC=IHLF
      IF(IEND)32,32,39
C
C     INCREMENT GETS DOUBLED
   32 IHLF=IHLF-1
      ISTEP=ISTEP/2
      H=H+H
      IF(IHLF)4,33,33
   33 IMOD=ISTEP/2
      IF(ISTEP-IMOD-IMOD)4,34,4
   34 IF(DELT-.02*PRMT(4))35,35,4
   35 IHLF=IHLF-1
      ISTEP=ISTEP/2
```

```
      H=H+H
      GOTO 4
C
C
C     RETURNS TO CALLING PROGRAM
   36 IHLF=11
      CALL FCT(X,Y,DERY)
      GOTO 39
   37 IHLF=12
      GOTO 39
   38 IHLF=13
   39 CALL OUTP(IHLF,NDIM,PRMT)
   40 RETURN
      END
      SUBROUTINE MAP(X,Y,M,HX,HY,NHX,NHY)
      DIMENSION X(1),Y(1),HX(1),HY(1)
      NX=10
      NY=10
      XL = 10.0
      YL  = 7.0
      XM=2.0
      YM = 2.5
      XX=XL-FLOAT(NHX)*0.1
      YY=YL-FLOAT(NHY)*0.1
      CALL PLOT(0.0,0.0,-3)
      CALL DATE(D1)
      CALL LETTER(10,0.2,30.0,1.,7.,10H*MODEL 2 *)
      CALL LETTER(10,0.1,30.0,1.3,3.5,D1)
      CALL PLOT(2.,0.0,-3)
      CALL LETTER(NHX,0.1,0.0,XX,1.2,HX)
```

```
      CALL LETTER(NHY,0.1,90.0,0.8,YY,HY)
      CALL FACTOR(M,X,Y,XL,YL,XM,YM)
      CALL PLOT(XM,YM,3)
      CALL PLOT(XL,YM,2)
      CALL PLOT(XL,YL,1)
      CALL PLOT(XM,YL,1)
      CALL PLOT(XM,YM,1)
      YS=(YL-YM)/FLOAT(NY)
      XH=XM
      YH=YM
   20 CALL PLOT(XH,YH,3)
      CALL PLOT(XH+.07,YH,2)
      CALL PLOT(XL-.07,YH,3)
      CALL PLOT(XL,YH,2)
      CALL INCHTC(XM,YH,XP,YP)
      ENCODE(10,30,YD) YP
      CALL LETTER(10,0.1, 0.0,0.9,YH-.05,YD)
      YH=YH+YS
      IF(YH.LE.YL) GO TO 20
      XS=(XL-XM)/FLOAT(NX)
   22 CALL PLOT(XH,YM,3)
      CALL PLOT(XH,YM+.07,2)
      CALL PLOT(XH,YL-.07,3)
      CALL PLOT(XH,YL,2)
      CALL INCHTC(XH,YM,XN,YN)
      ENCODE(10,30,XD) XN
      CALL LETTER(10,0.1,90.,XH+.05,1.4,XD)
      XH=XH+XS
      IF(XH.LE.XL) GO TO 22
   30 FORMAT(2PE10.2)
      RETURN
      END
```

APPENDIX B

NUMERICAL VALUES OF PARAMETERS USED IN PARAMETRIC STUDIES

Stiffness parameter	$\overline{K}$	= 0.9
Initial setting parameter	β	= 0.5
Hydrostatic pressure difference parameter	$\Delta\overline{P}$	= 26.6946
Damping factor	ξ	= 0.45
Inertia factor	α	= 1372
Loss factor	ψ	= 40
Mass ratio	μ	= 0.03184
Discharge coefficient	C_d	= 0.85
Area ratio	η	= 4.64

APPENDIX C

NUMERICAL VALUES OF PARAMETERS USED IN VALVE APPLICATION

Pipe cross-sectional area just upstream of the valve	$A = 0.03484\ m^2$
Area of valve plate	$S = 0.043\ m^2$
Moment of inertia of the valve system (including added mass)	$J = 0.431$ N-ms^2
Moment arm of centre of pressure on valve about pivot	$C_i = 0.1222$ m
Equivalent length of the valve system	$L^* = 16.764$ m
Damping factor (including hydro-dynamic damping)	[illegible] = 0.45
Loss Factor	[illegible] = 40.0
Maximum hydrostatic pressure difference	$\Delta P = 26.3$ KPa
Dynamic discharge coefficient	$C_d = 0.85$
Torsional spring stiffness K variable	from 0.5 KN-m/rad to 2.5 KN-m/rad
Initial setting angle x_o variable	from 2 deg. to 6 deg.

APPENDIX D

NUMERICAL VALUES OF PARAMETERS USED IN SEAL APPLICATION

Moment of inertia of the seal moving parts (including added mass)	$J = 0.1357$ N-ms^2
Equivalent length of the jet through the seal element	$L^* = 0.9144$ m
Loss factor	$\psi = 5.0$
Hydrostatic pressure difference	$\Delta P = 26.3$ KP_a
Dynamic discharge coefficient	$C_d = 0.65$
Stiffness of the seal	$K = 1.8857$ KN-m/rad
Initial setting angle	$x_o = 5.0$ deg.